UNIVERSIDAD AUTÓNOMA DE NUEVO LEÓN

FACULTAD DE CIENCIAS QUÍMICAS

"METABOLOMIC PROFILE AND BIOASSAY-GUIDED PHYTOCHEMICAL ANALYSIS OF THE STEMS FROM *CISSUS TRIFOLIATA*, EVALUATION OF THEIR ANTIBACTERIAL AND CYTOTOXIC ACTIVITY, AND DETERMINATION OF THE MECHANISM OF ACTION OF ONE ACTIVE COMPOUND"

Por

LUIS FERNANDO MÉNDEZ LÓPEZ

Como requisito parcial para obtener el grado de

DOCTORADO EN CIENCIAS CON ORIENTACIÓN EN FARMACIA

SAN NICOLÁS DE LOS GARZA, N.L., MAYO DE 2020

AUTONOMOUS UNIVERSITY OF NUEVO LEON

SCHOOL OF CHEMICAL SCIENCES

GRADUATE STUDIES

Metabolomic profile and Bioassay-guided Phytochemical analysis of the Stems from *Cissus trifoliata*, evaluation of their Antibacterial and Cytotoxic activity, and determination of the Mechanism of Action of one active compound.

Dissertation in partial fulfillment of the requirements for the degree of

Doctor of Science (Pharmacy)

Luis Fernando Méndez López, M.Sc.

Pharmaceutical Chemistry Laboratory

Autonomous University of Nuevo Leon, Mexico, May 2020

VoBo

Metabolomic profile and Bioassay-guided Phytochemical analysis of the Stems from *Cissus trifoliata*, evaluation of their Antibacterial and Cytotoxic activity, and determination of the Mechanism of Action of one active compound.

Thesis approval

_____
María del Rayo Camacho Corona, Ph.D.
Thesis Director

_____
Edgar Abraham García Zepeda, Ph.D.
Committee Member

_____
María del Rosario González González, Ph.D.
Committee Member

_____
Omar González Santiago, Ph.D.
Committee Member

_____
María Elena Cantú Cárdenas, Ph.D.
Subdirector, Postgraduate Studies Division

Metabolomic profile and Bioassay-guided Phytochemical analysis of the Stems from *Cissus trifoliata*, evaluation of their Antibacterial and Cytotoxic activity, and determination of the Mechanism of Action of one active compound.

Thesis revision

_____
María del Rayo Camacho Corona, Ph.D.
President

_____
Edgar Abraham García Zepeda, Ph.D.
Secretary

_____
María del Rosario González González, Ph.D.
First vocal

_____
Omar González Santiago, Ph.D.
Second vocal

_____
José Rodríguez Rodríguez, Ph.D.
Third vocal

_____
Leticia González Maya, Ph.D.
Substitute

Dedication

In memory of my Father

Luis Fernando Méndez Borges

1955-2016

ACKNOWLEDGMENTS

María del Rayo Camacho Corona. Pharmaceutical Chemistry Laboratory. School of Chemical Sciences, UANL. My deepest gratitude to my advisor, for giving me the honor to work on this fascinating project. I gratefully thank her supervision, patience, advice, and guidance. I am also would like to thank the advice and support provided for many professors from different fields that make it possible to accomplish the objectives of the study.

Elvira Garza-González. Gastroenterology Services. Hospital Universitario Dr. José Eleuterio González, UANL. I would like to thank for the training and infrastructure that made possible the antibacterial evaluation of the plant extracts.

Verónica Mayela Rivas Galindo. Department of Analytical Chemistry. School of Medicine. UANL. I would like to thank for the realization of the NMR experiments to elucidate the structure of the compounds.

María Yolanda Ríos, Ángeles Ramírez-Cisneros, Laura Álvarez. The Chemical Research Center from the Universidad Autónoma del Estado de Morelos (UAEM). For the UPLC-QTOF-MS experiments to identify the chemical composition of the extracts.

Leticia González-Maya, Jessica N. Sánchez-Carranza. School of Pharmacy, UAEM. I would like to thank their advice and expertise in the realization of the cytotoxic activity of the plant extracts against the panel of cancer cell lines.

Isaías Balderas Rentería and Eder Arredondo Espinoza. Genomic and Genetic Engineer Laboratory. School of Chemical Sciences. UANL. For their guidance and support for the realization of the bioassay-guided evaluation of the plant extracts, that include the WST1 assays, the IC_{50} determination, the RNA isolation and the bioinformatic analysis of the microarray results.

Prof. Pierluigi Caboni. Laboratory of Food Chemistry. University of Cagliari, Italy. For hosting me in his city and laboratory. The lab staff trains me in the use of high-resolution mass spectrometry equipment and software for the characterization of samples using high throughput techniques.

Jorge Ramirez Salcedo. Microarray Unit. Institute of Cellular Physiology. Universidad Nacional Autónoma de México. For the design and analysis of the microarray experiments that allowed the evaluation of the transcriptomic effects of the isolated compound.

Thesis committee. I'm pleased to thank my committee members, the professors María del Rosario González González, Omar González Santiago, and Patricia Cristina Esquivel Ferriño, which guidance helped me to improve my formation and the quality of my thesis.

Mauricio Gonzalez-Ferrara. I would like to thank the Biologist, MCs, and Director of Pacalli R.L. of C.V. for the identification and collection of the plant under study.

I would like to thank my fellow graduate students Tommaso Stefani, Bryan Espinoza, Reyna Gallegos, Juan Carrizales, and Rodrigo Vázquez. Their expertise in technical or theoretical skills helped me to improve the results presented in this thesis. It's been great to study and work with all of you.

I would like to thank CONACYT for the scholarship (210600) to carry out my Ph.D. studies.

And finally, I would like to thank the Honorable University Council of the UANL to support my decision of pursuing a doctoral degree. My deepest gratitude to the university and its people, particularly with the School of Public Health and Nutrition. I would like to thank especially its former Director Hilda Novelo Huerta and its Subdirector Alpha Berenice Medellin, that made possible this achievement and for encouraged me to pursue my professional goals.

ABSTRACT

Luis Fernando Méndez López Graduation date: June 2019

Universidad Autónoma De Nuevo León

Facultad De Ciencias Químicas

Title of the study: Metabolomic profile and Bioassay-guided Phytochemical analysis of the Stems from *Cissus trifoliata*, evaluation of their Antibacterial and Cytotoxic activity, and determination of the Mechanism of Action of one active compound.

Number of pages: 150

Dissertation in partial fulfillment of the requirements for the degree of Doctor of Science in Pharmacy

Area of study: Natural product chemistry

Objectives and methods: Bioprospecting the metabolic profile of medicinal plants has provided a reliable resource for drug discovery and advancements in biomedical research. *Cissus trifoliata* (L.) L belongs to the Vitaceae family and is an important medicinal plant used in Mexico for the management of infectious diseases and tumors. The present study aimed to identify the metabolic profile of the extracts from the stems of *C. trifoliata* and evaluate their antibacterial and cytotoxic activities. Additionally, to identify the molecules that contribute to their biological activity and to explore the mechanism of action of one active compound. The hexane, $CHCl_3$-MeOH, and aqueous extracts were prepared from the stems of *C. trifoliata* and their metabolic profile was investigated by column

chromatography, NMR, GC-MS, and LC-MS. The antibacterial activity was determined by the broth microdilution method and the cytotoxicity against cancer cell lines using the MTS proliferation assay. A bioassay-guided study of the $CHCl_3$-MeOH extract was performed using WST-1 to identify the active constituents responsible for the antiproliferative effects against cancer cells. Additionally, microarrays were used to identify the mechanism of action of one active compound against prostate cancer cells.

Contribution and conclusions: The metabolic profile of *C. trifoliata* stems was constituted of polyphenols (36%), terpenes (28%), fatty acids (18%), simple phenols (9%) and alkanes (9%). The pathway analysis indicated the high production of stilbenes, flavonoids, and sterols. The extracts showed no antibacterial activity (MIC > 500 µg/ml), but high cytotoxic effects against cancer cells ($IC_{50} \leq 30$ µg/ml). The hexane and aqueous extracts showed high antiproliferative activity against cancer cells from the liver (Hep3B, HepG2) and breast (MCF7). The bioactivity of these extracts was related to the synergistic effect of the triterpenes, sterols, flavonols, and stilbenes with cytotoxic, antiproliferative, and antiestrogenic activities. The bioassay-guided study of the $CHCl_3$-MeOH extract allowed the identification of two active fractions. Both showed significative reduction ($p > 0.05$) of cell viability on PC3 and MCF7 cancer cells at a concentration of 100 µg/ml. The cytotoxic activity was related to the synergistic anticancer effects of the mixture of coumaric acid, kaempferol, apigenin, hydroxyursolic, ursolic, and betulinic acid plus the stilbenes resveratrol, piceatannol, and viniferin. The stilbene that characterizes the Vitaceae plants is the resveratrol, thus was selected for the study of the mechanism of action. To carry out the microarray assay, PC3 cells were exposed to a non-cytotoxic inhibitory concentration (IC_{25}) of resveratrol. Results showed that this phenolic compound induced significative transcriptional changes (2-fold) in 847 genes. The functional analysis

suggested that resveratrol influences differentiation and impair cancer stemness by induction of the transcription factors POU4F2, KLF14, Hox-A3, and repression of Nanog. Resveratrol also affected cellular metabolism by upregulation of SIRT5 and repressed genes of the cancer pathways of TGF-β, Notch, PI3K/Akt, insulin/IGF-1, and MDM4/p53. Overall, the metabolic profile and biological evaluation of the stems from *C. trifoliata* correlate with high anticancer activity and together with the molecular mechanism of the identified bioactive constituents explain its traditional use in the management of tumors.

_____

María del Rayo Camacho Corona, Ph.D.
Thesis Director

TABLE OF CONTENTS

CHAPTER I……1
1. INTRODUCTION……...1
1.1. Cancer……...1
1.1.1. Cancer Drug Resistance……..2
1.2. Bacterial infections……..5
1.2.1. Mechanisms of Antibiotic Resistance……6
1.3. Antibiotic resistance in cancer patients……..7
1.4. Plants as a potential source of new drugs……8
1.4.1. Drugs derived from plants to treat cancer and bacterial infections……10
1.4.2. Targeting drug-resistance with phytochemicals……..11
1.4.3. Cell differentiation by phytochemicals for cancer treatment……..13
1.5. Plant metabolomics……15
1.5.1. Mass spectrometry-based plant metabolomics platforms……16
1.5.2. Data analysis and compound identification……..19
1.5.3. Data mining and data processing……..21
1.6. Bioassay-guided study of medicinal plants……..23
CHAPTER II……25
2. BACKGROUND……25
2.1. *Cissus trifoliata*……25
2.2. Medicinal properties of plants from the genus *Cissus*……26
2.2.1. Antibacterial and cytotoxic activity of *Cissus* extracts……28
2.2.2. Bioactive compounds isolated from *Cissus* plants……30
2.2.3. Compounds isolated and evaluated from *Cissus* plants……32
CHAPTER III……33
3. HYPOTHESIS AND OBJETIVES……33
3.1. HYPOTHESIS……33
3.2. General Objective……33
3.2.1. Specific Objectives……33
CHAPTER IV……34
4. MATERIALS AND METHODS……34

4.1. Phytochemistry……..……34
4.1.1. Plant material ……..……..34
4.1.2. Fractionation of the extracts and obtention of solids……..……..34
4.1.2.1. Fractionation of hexane extract……..……..34
4.1.2.2. Fractionation of the $CHCl_3$-MeOH extract……..……34
4.1.3. Solids obtained in the fractionation of the hexane extract……..……34
4.1.3.1. Solid one (CIR1)……..……..……..……35
4.1.3.2. Solid two (CIR2)……..……..……35
4.1.3.3. Solid three (CIR3)……..……..……..36
4.1.3.4. Solid four (CIR4)……..……..37
4.1.3.5. Solid five (CIR5)……..……...37
4.1.4. Nuclear magnetic resonance……..……..……..37
4.1.5. Gas Chromatography-Mass Spectrometry……..……....38
4.1.6. High-Performance Liquid Chromatography-Mass Spectrometry……..…..38
4.1.7. Identification of plant metabolites and data analysis……..……..40
4.1.8. Antibacterial activity……..……41
4.1.8.1. Bacterial strains……..……..41
4.1.8.2. Microdilution method……..……....42
4.1.9. Cytotoxic activity……..……...43
4.1.9.1. Cell culture and MTS assay……..……..…..43
4.1.10. Bioassay-guided cytotoxicity of the $CHCl_3$-MeOH extract by WST-1……..……...44
4.1.10.1 Determination of the IC_{50} of pure compounds……..……..……45
4.1.11. Microarrays……..……46
4.1.11.1. RNA isolation…..……..……46
4.1.11.2. RNA tagging……..……..……47
4.1.11.3. Microarray hybridization……..……48
4.1.11.4. Bioinformatic analysis of Microarrays……..……49
4.1.12. Statistical analysis……..……49
4.1.12. Waste disposal……..…..49
CHAPTER V……..……..……...50
5.1. RESULTS AND DISCUSSION……..……50
5.1.1. Plant material and extraction……..…..50
5.1.2. Structural elucidation of solids from hexane extract…..……..……..……..50
5.1.2.1. Physic and spectral data of solid 1 (CIR1)……..……..……..……50

5.1.2.2. Physic and spectral data of solid 2 (CIR2)……..…….53
5.1.2.3. Physic and spectral data of solid 3 (CIR3)…….....56
5.1.2.4. Physic and spectral data of solid 4 (CIR4)……..……..…58
5.1.2.5. Physic and spectral data of solid 5 (CIR5)…….……....62
5.1.2.6. Isolation of compounds from hexane extracts of *Cissus* plants……..……..…64
5.1.3. GC-MS analysis of hexane extract ……..……..…….65
5.1.4. UPLC-QTOF-MS analysis……..……..68
5.1.4.1. UPLC-QTOF-MS characterization of the $CHCl_3$-MeOH extract…….……..68
5.1.4.2. UPLC-QTOF-MS characterization of the aqueous extract…….……..……71
5.1.5. Metabolomic profile of the stems from *C. trifoliata*……..……73
5.1.5.1. Principal Component Analysis…….……...……73
5.1.5.2. Pathway Analysis……..……..…74
5.1.6. Biological evaluation of the extracts……..……..…75
5.1.6.1. Antibacterial activity……...……....75
5.1.6.2. Cytotoxic activity……..……...77
5.1.7. Cytotoxicity of compounds identified in the stems of *C. trifoliata*……..…..……79
5.2. Bioassay-guided study *C. trifoliata* stems……..……..…..81
5.2.1. UPLC-QTOF-MS analysis of the active fractions……...……....83
5.3. Determination of the IC_{50} of stilbenes…….……88
5.4. Mechanisms of resveratrol on PC3 cells…….……...90
5.4.1. Resveratrol influences gene expression in PC3 cells…..……..……90
5.4.2. Resveratrol influences cell differentiation……..……..…93
5.4.3. Resveratrol impair cancer stemness……..……95
5.4.4. Resveratrol reduces metastatic potential…….……..……95
5.4.5. Resveratrol reprogram cell metabolism…….……..96
5.4.6 Resveratrol abrogates cancer pathways……..……..…….97
5.4.7. Resveratrol sensitizes to apoptosis……..……...99
CHAPTER VI.……..……101
6. CONCLUSION…….……..…101
CHAPTER VII……..…...102
7. PERSPECTIVES..……..……..102
CHAPTER VIII…….....103
8. REFERENCES……..……..103

LIST OF TABLES

Table 1. Medicinal properties of plants from the genus *Cissus* by country……..……...27

Table 2. Bioactive compounds isolated from the stems of *Cissus* plants……..……..…31

Table 3. Fractionation of the hexane extract…….……..….35

Table 4. Fractionation of the $CHCl_3$-MeOH extract.…….……36

Table 5. Conditions of GC-MS analysis for the hexane extract……..…..38

Table 6. UPLC Parameters..……..…39

Table 7. Q-TOF/MS Parameters……..……..…40

Table 8. GC-MS analysis of solid 1 (CIR1)……..…....52

Table 9. GC-MS analysis of solid 2 (CIR2)……..…55

Table 10. GC-MS analysis of solid 3 (CIR3)……..……..….58

Table 11. GC-MS analysis of solid 4 (CIR4)……..……..….61

Table 12. GC-MS analysis of solid 5 (CIR5)……..……..…….64

Table 13. GC-MS analysis of hexane extract from the stems of *C. trifoliata* …….....….67

Table 14. UPLC-QTOF-MS analysis of the $CHCl_3$-MeOH stem extract of *C. trifoliata*.....70

Table 15. UPLC-QTOF-MS analysis of the aqueous stem extract of *C. trifoliata*……..…….72

Table 16. The activity of the extracts against bacteria ……..……76

Table 17. Effect of the extracts of *C. trifoliata* against cancer cells.....78

Table 18. Effect of the fractions from the $CHCl_3$-MeOH extract against cancer cells…….82

Table 19. UPLC-QTOF-MS analysis of F1 from the $CHCl_3$-MeOH extract……..84

Table 20. UPLC-QTOF-MS analysis of F2 from the $CHCl_3$-MeOH extract……..85

Table 21. The Activity of stilbenes against cancer cell lines……..89

Table 22. Functional Annotation Chart of upregulated genes…….91

Table 23. Functional Annotation Chart of downregulated genes……..……92

Table 24. List of functional annotation of upregulated genes……..117

Table 25. List of functional annotation of downregulated genes……..…..124

LIST OF FIGURES

Figure 1. ^{1}H NMR (400 MHz, $CDCl_3$) spectra of solid 1 (CIR1)……..…….51
Figure 2. ^{13}C NMR (100 MHz, $CDCl_3$) spectra of CIR1……..……..……..……..51
Figure 3. GC-MS chromatogram of CIR1..……..…….52
Figure 4. Mass spectrum of Hentriacontane……..……..53
Figure 5. ^{1}H NMR (400 MHz, $CDCl_3$) spectra of solid 2 (CIR2)…….……..…53
Figure 6. ^{13}C NMR (100 MHz, $CDCl_3$) spectra of CIR2…….....54
Figure 7. GC-MS chromatogram of CIR2..……..….55
Figure 8. Mass spectrum of squalene……..……..…...55
Figure 9. ^{1}H NMR (400 MHz, $CDCl_3$) spectra of solid 3 (CIR3)…….……..…56
Figure 10. ^{13}C NMR (100 MHz, $CDCl_3$) spectra of CIR3…..……...57
Figure 11. GC-MS chromatogram of CIR3……..……..57
Figure 12. Mass spectrum of 1,30 triacontanediol……..….58
Figure 13. ^{1}H NMR (400 MHz, $CDCl_3$) spectra of solid 4 (CIR4)……..……..…..…..…..….59
Figure 14 .^{13}C NMR (100 MHz, $CDCl_3$) spectra of CIR4……..……..……..…….....60
Figure 15. GC-MS chromatogram of CIR4……..……..……60
Figure 16. Mass spectra of β-Sitosterol……....61
Figure 17. ^{1}H NMR (400MHz, $CDCl_3$) spectra of solid 5 (CIR5)…….……...……..…...….62
Figure 18.^{13}C NMR (100MHz, $CDCl_3$) spectra of CIR5…..……..…..…63
Figure 19. GC-MS chromatogram of CIR5…..……..…...63
Figure 20. Mass spectra of 1-triacontanol……...……..……64
Figure 21. GC-MS chromatogram of hexane stem extract of *C. trifoliata*……....66
Figure 22. UPLC-QTOF-MS chromatogram of the $CHCl_3$ extract of *C. trifoliata*……..…..69
Figure 23. UPLC-QTOF-MS chromatogram of the aqueous extract of *C. trifoliata*…..……...71
Figure 24. PCA of the extracts from the stems of *C. trifoliata* ……..…....73
Figure 25. Pathway analysis of the constituents from the stems of *C. trifoliata*…….……74
Figure 26. UPLC-QTOF-MS chromatogram of F1……..……83
Figure 27. UPLC-QTOF-MS chromatogram of F2……..……84
Figure 28. Extract-ion chromatogram of stilbene derivatives in fraction F1…….……....88
Figure 29. Results of the Z- score of microarrays……..……..…90

LIST OF ABBREVIATIONS

A431	Human epidermoid carcinoma in cell line
A549	Human alveolar lung cancer cell line
ABC	ATP-binding cassette
ABCC1	Multidrug resistant protein 1
AcOEt	Ethyl acetate
ACOT11	acyl-coenzyme A thioesterase 11
AIFM1	Apoptosis-inducing factor 1
Akt1	RAC-alpha serine threonine-protein kinases 1
ALK	Anaplastic lymphoma kinase
ANOVA-LSD	Analysis of Variance Least Significant Difference
ANOVA	Analysis of Variance
AP-1	Activator protein-1
AR	Androgen receptor
ATCC	American Type Culture Collection
Bcl-2	B-cell lymphoma 2 protein
BclxL	B-cell lymphoma extra-large protein
BCRP	Breast cancer resistance protein
BLEE	Extended spectrum beta-lactamase
BMPR2	Bone morphogenetic protein receptor type-2
BuOH	Buthanol
C.	Cissus
C_6H_{14}	Hexane
CaCo-2	Human colon caucasian colon adenocarcinoma
CDC	Centers for Disease Control and Prevention
$CDCl_3$	Deuterated chloroform
cDNA	Complementary DNA
CDKs	Cyclin-dependent kinases
CFU	Colony forming units
CITED4	Cbp/p300-interacting trans activator 4
$CHCl_3$	Chloroform
CKM	creatine kinase M-type
c-Myc	c-MYC oncogene
CO_2	Carbon dioxide
COX-2	Cyclooxygenase-2
CREBBP	CREB binding protein
CYB561D2	Cytochrome 561D2
Cyclins	Protein family involved in cell cycle regulation
DAG	1,2-diacylglycerol
DAVID	Database for Annotation, Visualization and Integrated Discovery
DMSO	Dimethylsulfoxide
DNA	Desoxyribunocleic acid
EBC-1	Non-small cell lung cancer cells
Ecadherin	Cell-cell adhesion molecule in epithelial tissues
ED50	Effective dose 50
EGFR	Epidermal growth factor receptor
EI	Electron ionization
eIF4H	Eukaryotic Translation Initiation Factor 4H
EMT	Epithelial-mesenchymal transition
ER	Estrogen receptor
ERCC1	Excision repair cross complementing 1 proteins

ESBLs	Extended spectrum beta-lactamases
ESI	Electrospray ionization
EtOH	Ethanol
FAAH2	Fatty-acid amide hydrolase
FCQ	Faculty of Chemical Sciences
FCGR1A	High affinity immunoglobulin gamma Fc receptor I
FDR	False Discovery Rate
FIDs	Free induction decays
Fig	Figure
FLIP	Caspase inhibitors
FT-ICR-MS	Fourier-transform ion cyclotron resonance mass spectrometers
G6PD	Glucose 6 phosphate dehydrogenase
GC	Gas Chromatography
GJA1	Gap junction alpha-1 protein
GLP1R	Glucagon-like peptide 1 receptor
GLUT1	Glucose transporter
GR	Glucocorticoid receptor
h	hour
H_2O	Water
HCA	Hierarchical cluster analysis
HDAC3	Histone deacetylase 3
HeLa	Human cervix adenocarcinoma cell line
Hep3B	Human Hepatocellular Carcinoma cell line
HepG2	Human Hepatocellular Carcinoma cell line
Hex	Hexane
HGT	Horizontal gene transfer
HIF1A	Hypoxia-Inducible Factor 1
HK2	Hexokinase 2
HMX2	H6 family homeobox 2
Hox-A3	Homeobox A3
Hox D12	Homeobox D12
HMDB	The Human Metabolome Database
HPLC	High performance liquid chromatography
HRMS	High-resolution mass spectrometry
HSD	Honestly significant difference
IAPs	Inhibitor of apoptosis proteins
IC_{25}	Inhibitory concentration 25
IC_{50}	Half maximal inhibitory concentration
IGFBP6	Insulin-like growth factor-binding protein 6
IGF-II	Insulin growth factor II
IGF1-R	Insulin-like growth factor 1
IKZF1	Ikaros family zinc finger 1
IL-1β	Interleukin 1 beta
iNOS	Inducible nitric oxide
IP3	Inositol 1,4,5-trisphosphate
JAK2	Janus kinase 2
JMJD2B	Jumonji domain containing 2B
JUND	Transcription factor JunD
KB-V1	Multidrug-resistant human cervical carcinoma
KLF14	Krüppel-like factor 14,
KW	Kruskal Wallis
LC	Liquid chromatography
LHX8	LIM homeobox 8
LMSD	LIPID MAPS Structure Database
LNCaP	Human prostate cancer cell line
MCF7	Human breast carcinoma cell line

MDA-MB-453	Cell line of breast carcinoma
MDM2	Murine doble minute 2
MDM4	p53-binding protein Mdm4
MDR	Multidrug resistant
MeOH	Methanol
MIC	Minimum Inhibitory Concentration
MLL3	Methyltransferase mixed-lineage leukemia protein 3
MP	Melting point
MRP1	Multi-drug resistance protein 1
MRSA	Methicillin-resistant S. aureus
MS	Mass spectrometry
MS^2	Sequential stages of mass spectrometric analysis
MSI	Metabolomics Standards Initiative
MT-CO1	C oxidase subunit 1
MTS	[3-(4,5-dimethylthiazol-2-yl)-5-(3-carboxymethoxyphenyl)-2-(4-sulfophenyl)-2H-tetrazolium
MSX-2	Msh Homeobox 2
MYO7B	Unconventional myosin-VIIb
NANOG	Homeobox protein NANOG
NCI	National Cancer Institute
NDN	Necdin
NDM-1	New Delhi metallo-beta-lactamase
NDST2	Bifunctional heparan sulfate N-deacetylase/N-sulfotransferase 2.
NF-κB	Nuclear factor-κB
NIST	National Institute Standard and Technology
NNT	NAD(P) transhydrogenase
NMR	Nuclear Magnetic Resonance
NO	Nitric oxide
NorA	Protein associated with quinolone resistance in *S. aureus*
NP115991	Gap junction alpha-10 protein
NSCLC	Non-small cell lung carcinoma
ODS	Octadecylsilane
oTOF	Orthogonal time-of-flight
Oxa-48	Carbapenemase-producing *Klebsiella pneumoniae* strains
p21	Cyclin-dependent kinase inhibitor
p27kip1	Cyclin-dependent kinase inhibitor 1B
PA26	p53-induced protein sestrin
PARD6G	Partitioning defective 6 homolog gamma
PBPs	Penicillin-binding proteins
PBS	Phosphate buffered saline
PC3	Human prostate cancer cell line.
PCA	Principal Component Analysis
PCAF	P300/CBP-associated factor
PDCD4	Programmed Cell Death 4
PFK1	Phosphofructokinase
PGAM	Phosphoglycerate mutase
PGE2	Prostaglandin E2
PI3K	Phosphoinositide 3-kinase
PIK3R2	Phosphatidylinositol 3-kinase regulatory subunit beta
PKNOX1	PBX/knotted homeobox 1
PLA2	Phospholipase A2
PLCG1	Phospholipase C gamma
PLS-DA	Partial Least Squares Discriminant Analysis
POR	NADPH P450 reductase
POU4F2	POU class 4 homeobox 2
PTPLA	Very-long-chain 3-hydroxyacyl-CoA dehydratase
Q	Quadrupole

QIT-MS	Quadrupole ion traps
Qnr proteins	Quinolone resistance proteins
QqQ	Triple quadrupoles
QR-2	Quinone reductase-2
QTOF	Quadrupole time of flight
RAW 264.7	Murine macrophage cells
RBL-2H3	Rat basophilic leukemia cells
RBPSUH	Recombining binding protein suppressor of hairless
ReSpect	Spectral database for phytochemicals
RNAi	RNA interference
RP	Reversed-phase
SARDH	Sarcosine mitochondrial dehydrogenase
SD	Standard Deviation
SDC2	Syndecan-2
SETD1B	Histone-lysine N-methyltransferase
SETD3	SET domain containing 3
SFB	Serum Fetal Bovine
SIRT5	NAD-dependent protein deacylase sirtuin-5, mitochondrial.
SK-OV3	Ovary cancer cells
SLC25A1	Tricarboxylate mitochondrial transport protein
SLC27A1	Long-chain fatty acid transport protein 1 ligase
Smad7	Mothers against decapentaplegic homolog 7
Spp	Subspecies
STAT3	Signal transducer and activator of transcription 3
STK17A	serine/threonine kinase 17a
TBX1	T-box 1 protein
TGF-α	Transforming growth factor alpha
THRAP3	Thyroid hormone receptor associated protein 3
TJP2	Tight junction protein ZO-2
TKT	Transketolase
TLC	Thin layer chromatography
TMS	Tetramethylsilane
TNF-α	Tumor necrosis factor alpha
Tp53	Tumor protein p53
TSG101	Tumor susceptibility gene 101
UANL	Universidad Autonoma de Nuevo Leon
UHPLC	Ultra High performance liquid chromatography
UPLC	Ultra High Performance Liquid Chromatography system
VEGF	Vascular endothelial growth factor
Vero	Kidney epithelial cells from green monkey
WST-1	1-methoxy-5-methyl-phenazinium methyl sulfate
ZDHHC20	Palmitoyltransferase
ZDHHC9	Palmitoyltransferase specific for HRAS

CHAPTER I

1. INTRODUCTION

1.1. Cancer

Cancer is the second leading cause of morbidity and mortality worldwide, with approximately 14 million newly diagnosed cases per year. Almost 9 million people die from cancer every year, representing one of every six deaths and one trillion dollars just in the United States. Furthermore, the number of diagnosed cases is expected to rise 70% over the next two decades because of the increasing longevity and sedentary lifestyle of population [1]. In Mexico, cancer is the third leading cause of death in adults. The most common tissues affected with cancer in males are originated in the digestive (24%) or genitourinary (12%) tract whereas in females neoplasia begins in the breast (30%), genitourinary (17%) or digestive (14%) tissue [2]. Cancer is traditionally defined as the uncontrolled growth of abnormal cells that impairs the normal biological process of healthy cells. As the tumor progress, the malignant cells spread by the invasion of nearby tissues or metastasize distant organs compromising its functions and ultimately might result in death. The altered process in cancer cells includes the constant activation of proliferation, the evasion of growth suppressors, increased resistance to cell death, the acquisition of replicative immortality, genome instability, metabolic changes, invasion, and metastasis. Additionally, tumors may induce angiogenesis, inflammation, and immune system evasion in the affected tissues fostering cancer progression [3].

Cancer treatment includes surgery, radiation and systemic treatment with conventional cytotoxic therapy, endocrine treatment (in case of hormone-dependent tumors), or targeted agents. The selective therapies were developed to target biomarkers of certain

tumors, such as oncogenes or tumor suppressors. This therapy includes drugs based on RNA interference, kinase inhibitors or monoclonal antibodies with fewer side effects [4]. On the other hand, cytotoxic therapy lacks selectivity and generates deoxyribonucleic acid (DNA) damage or the inhibition of essential enzymes, microtubules, and topoisomerases, which ultimately leads to cell death. Therefore, patients may suffer severe side effects such as vomits, alopecia, diarrhea, constipation, myelosuppression, infection, cystitis, ulcers, lung fibrosis, cardiotoxicity, hepatotoxicity, mucositis and nephrotoxicity [4]. Despite the adverse side effects, some protocols of cytotoxic therapy remain as the gold standard regardless of the little impact offered in overall survival. For example, in ovarian cancer, the combination of cyclophosphamide, adriamycin, vincristine, prednisolone, and platinum, has been used for twenty years despite the lack of effectiveness. Likewise, in lung cancer, survival has increased only two months in the same period, and less than 5% of patients benefit from the treatment. Similar results in the treatment of breast, colon, and head and neck cancers are observed [5]. Additionally, radiotherapy and chemotherapy regiments might spur the development of secondary tumors. The most common type of secondary cancer is leukemia one year after the treatment [6]. Moreover, cancer drugs are expensive and offer limited results because of the development of tumor resistance [7].

1.1.1. Cancer Drug Resistance

Major challenges in treating cancer include delayed diagnosis, metastasis and the emergence of drug resistance. Over 50% of patients are diagnosed in advanced stages or with metastasis in which therapies are almost ineffective. Moreover, on average within six months tumors become refractory to therapy as a result of the emergence of drug-

resistance [8]. Modifications to overcome drugs include genetic changes that modify the DNA sequence (mutations) or its conformation (epigenetics). Among the molecular mechanisms regularly identified as culprits for tumor resistance are gene amplification, mutations, silencing, overexpression, downregulation or reactivation [3]. The overexpression of the ATP-binding cassette (ABC) transporter family of transmembrane proteins has been studied extensively for multidrug resistance (MDR). These proteins regulate the efflux across the plasma membrane of multiple structurally and mechanistically unrelated chemotherapeutic drugs and confer MDR. The family is composed of 49 members, but the most studied proteins are the multi-drug resistance protein 1 (MRP1); the MDR-associated protein 1 (MRP1); and the breast cancer resistance protein (BCRP). They promote the elimination of hydrophobic compounds, such as the topoisomerase inhibitors and the antimetabolites [9]. Another mechanism relevant to drug resistance is the enzymatic inactivation or the lack of drug activation. For example, platinum drugs can be inactivated by the enzyme glutathione [10], and downregulation of enzymatic activities confers lack of activation of the antimetabolites 5-fluorouracil and methotrexate [11]. Drug response and resistance are affected by alterations of the drug target by mutations or increased concentration. Examples include the mutation or amplification of the androgen receptor (AR) in prostate cancers that develop resistance to therapy of androgen deprivation using leuprolide and AR antagonists such as bicalutamide [12]. Cancers often develop mutations in the protein kinases targeted by drugs. For example, mutations in anaplastic lymphoma kinase (ALK) have been identified in neuroblastoma and non-small cell lung carcinoma (NSCLC). For example, the initial tumor responses of 60% to the tyrosine kinase, ALK inhibitor crizotinib, disappear in less than one year due to mutations in the tyrosine kinase domain and patients relapse [13]. In the

case of drugs that induce DNA damage, cancer cells increase the production of enzymes involved in repair and confer resistance to platinum compounds or topoisomerase inhibitors. For example, the mutations in the tumor protein p53 (p53) disrupt the cell cycle arrest induced by DNA damage [14] and overexpression of the protein excision repair 1, endonuclease non-catalytic subunit (ERCC1) has been linked with poor responses. The ERCC1 overexpression allows the efficient nucleotide excision repair mechanisms required for the survival of cells exposed to DNA damage [15]. Cancer cells often overexpress anti-apoptotic proteins such as the members of the B-cell lymphoma 2 (Bcl-2) family, the inhibitor of apoptosis proteins (IAPs) and the FADD-like IL-1β-converting enzyme inhibitory protein the caspase inhibitors (FLIP). Several mechanisms of deregulation in these proteins have been associated with various malignancies and drives resistance to apoptosis [16]. The overexpression of the transcription factors such as, the nuclear factor-κappa B (NF-κB) and signal transducer and activator of transcription 3 (STAT3) is activated by oncogenic mutations in kinases and regulate upstream the anti-apoptotic pathways that increase survival of cancer cells [17]. It has been estimated that 90% of failures in cancer therapy are related to tumor resistance. Additionally, toxicity produced in normal tissues limits the amount of drug that can be administrated and pharmacokinetic effects (absorption, distribution, metabolism, and elimination) limit the amount of drug that effectively reach the tumor. Furthermore, several mechanisms operate at the same time, and tumor resistance can be intrinsic or acquired throughout the treatment. Moreover, tumors are heterogeneous; and resistance can arise by a positive selection of tumor cell subpopulations. Thus, tumor resistance and toxicity remain the biggest limitations for the survival of cancer patients [18].

1.2. Bacterial infections.

Infectious diseases remain the second leading cause of death worldwide. It has been estimated that 15 million deaths each year are directly caused by infectious diseases [19]. The main causes of death are respiratory infections (3.2 million), diarrhea (1.4 million), tuberculosis (1.4 million) and the human immunodeficiency virus infection and the acquired immune deficiency syndrome (HIV/AIDS) (1.1 million). Bacterial diseases are responsible for more than half of those deaths [20]. Bacterial diseases are re-emerging due to resistance to antibiotics that is responsible for an increased rate in the costs, morbidity, and mortality. The group of bacteria that frequently originates life-threatening nosocomial infections is called “ESKAPE”. That name is an acronym for Gram-positive and Gram-negative bacteria, conformed by *Enterococcus faecium*, *Staphylococcus aureus*, *Klebsiella pneumoniae*, *Acinetobacter baumannii*, *Pseudomonas aeruginosa*, and *Enterobacte*r species, all of them are characterized by mechanisms of drug-resistance [21].

The most common pathogens causing nosocomial infections in Mexico are *Escherichia coli* (20%), *S. aureus* (14%) and *P. aeruginosa* (17%). The rest of the infections are produced by *A. baunanni, K. pneumoniae, Providencia rettgeri, Stenotrophomonas maltophilia, S. epidermidis, S. haemolyticus and E. faecium* [22]. In Mexico a study showed that nearly 70% of *E. coli* from clinical isolates was resistant to levofloxacin, 28% to amoxicillin-clavulanic acid and 40% produced the extended-spectrum beta lactamases (ESBLs). In the case of *K. pneumoniae* from clinical isolates, 32% were resistant to levofloxacin and 28% produced ESBLs. In the same study, half clinical isolates of *S. aureus* were resistant to oxacillin (MRSA), and to levofloxacin. In the case of *P. aeruginosa* 40% were resistant to ceftazidime, imipenem, levofloxacin, and 20% to

amikacin. Isolates from *E. faecium* were resistant to vancomycin (33%) and *A. baumannii* presented resistance to amikacin (40%), ceftazidime (70%), levofloxacin (50%), and piperacillin-tazobactam (50%) [23]. Additionally, authors report that nearly 70% of *Streptococcus pneumoniae* samples were resistant to penicillin, cotrimoxazole, and clindamycin and 30% of *H. influenzae* clinical isolates were resistant to cotrimoxazole, ampicillin and clarithromycin [24].

It is considered that Mexico possesses conditions that foster antibiotic resistance, such as abuse of antibiotics in animal production, self-prescription and the use of low-quality drugs. Additionally, in the clinical setting, the overcrowded facilities, poorly trained staff, and low equipped hospitals allow the rapid spread and slow detection of MDR infections. Moreover, patients are often in malnourished conditions with scarce access to medical services and drugs, thus MDR infections frequently become fatal [23].

1.2.1. Mechanisms of Antibiotic Resistance

Resistance to antibiotics is the expected result of the interaction of many organisms with their environment during evolution. Most antibiotics are naturally metabolic products derived from fungi and bacteria. Thus, microorganisms are intrinsically endowed with a mechanism to evade them and survive. However, in the clinical setting the main concern is the acquired antibiotic resistance of bacteria that was originally susceptible [25]. The mechanism by which bacteria become antibiotic-resistant is generally through mutations in the genes that codify for the targets of the antibiotics or by the acquisition of foreign DNA that codify for proteins of resistance through horizontal gene transfer (HGT) [25].

Mutations that result in antimicrobial resistance can origin from the modification of the target. Thus, variations decrease drug affinity or decrease drug uptake. Additionally, the activation of drug pumps allows the clearance of antibiotics by expelling antibiotics outside the cells. The acquisition of foreign DNA through HGT is one of the most important factors driving MDR. Bacteria can acquire external genetic material through transformation (incorporation of DNA), transduction (phage mediated) and bacterial conjugation [26].

Antibiotic resistance can be triggered by different mechanisms and at the same time in bacteria. For example, fluoroquinolone resistance can be induced by mutations in the genes of DNA gyrase that modifies the target site, and by the expression of Qnr proteins (quinolone resistance proteins), that protects the target site, while over-expression of efflux pumps can pull-out fluoroquinolone from the cells [27]. In other cases, bacteria seem to prefer some mechanisms of resistance over others. For example, the predominant mechanism of resistance to β-lactams in gram-negative bacteria is the production of β-lactamases, whereas gram-positive organisms prefer the production of the penicillin-binding proteins (PBPs) [28].

1.3. Antibiotic resistance in cancer patients.

Cancer patients are at risk of bacterial infections in the bloodstream due to chemotherapy-induced neutropenia, especially hematological patients undergoing hematopoietic stem cell transplantation [29]. Immunosuppressed patients with cancer suffer from that complication and increase the morbidity, mortality and economic costs. According to the US Centers for Disease Control and Prevention (CDC), every year, about 650 000 patients

with cancer receive chemotherapy and 10% will acquire an infection that requires hospitalization [30]. Chemotherapy produces oral mucositis and the use of central venous catheters, plus the antimicrobial prophylaxis against enteric gram-negative bacilli leads to infections with gram-positive cocci, especially the viridans group, streptococci, and coagulase-negative staphylococci. Despite that antibiotic therapy is used in neutropenic febrile cancer patients, half of the patients become infected with antibiotic-resistant bacteria that increase eleven times their mortality rate from infection [30].

1.4. Plants as a potential source of new drugs

Plants have evolved for over 350 million years mechanisms that allow them to survive a wide range of stressors. They are continuously exposed to environmental stresses that include abiotic factors (a nutrient deficiency, hypoxia/anoxia, drought, salinity, lack of oxygen, temperature fluctuations and light intensity) and biotic factors (bacteria, fungi, viruses, nematodes, insects and herbivore pests). Plants can trigger immune responses and reinforce their cell walls, biosynthesize lytic enzymes, and produce secondary metabolites as a response of stressors [31]. Secondary metabolites refer to a broad array of chemical defenses, produced constitutive or inducible in response to pathogens or stressors. Phytoanticipins (include saponins, cyanogenic glycosides, and glucosinolates) are present in the plant before microorganism attack or produced after infection from pre-existing precursors. They are usually found at the plant surface while others are present in vacuoles or organelles and are released through a hydrolyzing enzyme after pathogen challenge. On the other hand, phytoalexins (including terpenoids, glycosteroids, flavonoids, and polyphenols) are small molecules (molecular weight < 500) which are both

synthesized and accumulated in the plant after induction. Phytoalexins showed several medicinal properties against cancer, diabetes, inflammation, malaria, bacteria, nematodes, insecticide and nematodes [32]. Thus, plants are excellent candidates for drug discovery. Medicinal plants are typically collected and identified by a trained botanist. In other cases, the plant is generally used in traditional medicine but often the chemical content is unknown. A plant can also be selected based on the genetic relationship (chemotaxonomy) with a recognized medicinal plant. Once plants are collected the phytochemist is the professional that performs the extraction process and the fractionation to isolate and characterization the active compounds through chromatographic and spectroscopic techniques. The molecular biologist also plays a major role in drug discovery, they select the pharmacologically relevant assays, to find the compounds that possess the biological activity. Furthermore, pure compounds can be tested to find the relevant molecular target or to explore the mechanism of action that underlies the therapeutic effects [33].

Pharmacognosy is the science that studies the physical, chemical, biochemical and biological properties of drugs, drug substances, or potential drugs of natural origin as well as the search for new drugs from natural sources. Despite the recent interest in molecular modeling, combinatorial chemistry, and other synthetic chemistry techniques, natural products derived from plants remain as one of the most important sources of new drugs, new drug leads, and new chemical entities [34].

1.4.1. Drugs derived from plants to treat cancer and bacterial infections

Drug discovery from medicinal plants has played an important role in cancer therapy. Sixty percent of clinically approved anticancer drugs were isolated from medicinal plants. Most of them belong to four classes of phycompounds: the vinca alkaloids, epipodophyllotoxins, taxanes, and camptothecins. Vinblastine and vincristine were isolated from *Catharanthus roseus* and have been used clinically for over 50 years. Podophyllotoxin was isolated from the resin of *Podophyllum peltatum* (*Berberidaceae*) and the first derivative approved for clinical use was the etoposide. Paclitaxel was originally isolated from *Taxus brevifolia* (*Taxaceae*) and camptothecin was isolated from *Camptotheca acuminate,* both were clinically introduced in the mid-1990s. Currently, derivatives of all four compound classes remain in clinical use [35]. The initial screenings of plants for anticancer drug discovery include the use of established cancer cell lines, in which the cytotoxic effects of plant extracts or the isolated compounds are measured. According to the National Cancer Institute (NCI), plant extracts and pure compounds are considered cytotoxic active if their half-maximal inhibitory concentration (IC_{50}) is ≤30 μg/ml or ≤4 μg/ml, respectively [36]. In the case of antibacterial drugs approved by the FDA, only 3% are derived from plants. The 97% were isolated or derived from microbes (51% from bacteria and 46% from fungi). In 1968 the aminosalicylate became the first antibacterial FDA approved derived from plants (*Salix alba*) and the azelaic acid, isolated from cereals like rye and barley was last marketed in 1995 [37]. The evaluation of the antibacterial activity *in vitro* of plant extracts or isolated compounds relies in the methods of disk-diffusion and broth or agar dilution. Dilution methods are the most appropriate for the determination of the minimum inhibitory concentration (MIC) value, which is the lowest concentration of the assayed antimicrobial agent that inhibits the visible growth and it is usually expressed in μg/ml or mg/l. The

concentration of the extracts evaluated should not exceed the range of 1 mg/ml for extracts and 0.1 mg/ml for isolated compounds [38]. An extract is considered active if the MIC is ≤ 30 µg /ml, and isolated compounds when the MIC is ≤ 8 µg/ml [39, 40].

1.4.2. Targeting drug-resistance with phytochemicals.

The toxic effects derived from cancer chemotherapy and the emergence of drug resistance limits cancer survival. Regarding bacterial infections, the spread of multidrug-resistant strains of bacteria represents a big threat to their successful treatment. Medicinal plants potentially contain new compounds with diverse chemical structures and mechanisms of action. Some of them might be more effective, selective or can inhibit the resistance mechanisms. Compounds that showed inhibition of the resistance mechanisms, and restore the sensitivity to drugs are called chemo-sensibilizators in cancer [41], and resistance modulators in bacteria [42]. The use of a compound that inhibits bacteria resistance was marketed by the name of Augmentin. The drug is a combination of amoxicillin (a beta-lactam antibiotic) and clavulanic acid, a microbially derived inhibitor of beta lactamases. Resistance modulators may also inhibit multidrug resistance (MDR) in bacteria, a process that generates intracellular ineffective concentration of drugs. Epicatechin gallate is a weak antibacterial (MIC = 280 µg/ml), but reverse the methicillin-resistance by inhibiting the synthesis of PBPs in methicillin-resistant *S. aureus* (MRSA) [43]. The diterpenes totarol showed strong antibacterial activity (MIC = 2 µg/ml) against *S. aureus* but also potentiate methicillin activity against MRSA via interference of PBPs. When incorporated into the medium at 1 µg/ml, it caused an eight-fold increase in methicillin activity against MRSA [44]. The 5´-methoxyhydnocarpin and berberine can inhibit

the NorA (protein associated with hydrophilic quinolone resistance in *S. aureus*), which is a drug efflux pump in *S. aureus* [45]. Kaempferol did not display relevant antibacterial activity against MRSA (MIC = 256 µg/ml), however, also inhibits the expression of NorA. In combination with antibiotics a reduction in the MIC was observed for norfloxacin (16-fold), ciprofloxacin (16-fold), lomefloxacin (four-fold) and ofloxacin (two-fold) [46]. On the other hand, phytochemicals can sensitize tumor cells to chemotherapeutic agents by inhibiting pathways that lead to resistance. Additionally, those compounds protect from therapy-associated toxicity [42]. For example, treatment with genistein before docetaxel or cisplatin administration enhanced tumor cell death in pancreatic cancer cell lines compared with the treatment with drugs alone. This effect may have been mediated by the inhibition of NF-κB, causing increased apoptosis. In liver and colon cancer cell lines, genistein plus dexamethasone resulted in enhanced expression of the CDK-interacting protein 1 (p21CIP1), halting cell cycle progression [47]. Resveratrol administered before (10 µM for 3 days) paclitaxel increased p21CIP1 expression approximately four-fold, lowering the threshold of cell death by paclitaxel in non-small cell lung cancer cells (EBC-1). Additionally, the combination increase the expression of the cyclin-dependent kinase inhibitor 1B (p27kip1), and the cell-cell adhesion molecule of epithelial tissues the E-cadherin, the epidermal growth factor receptor (EGFR), and Bcl-2 [48]. Curcumin potentiated the cytotoxic effects of doxorubicin, fluorouracil, and paclitaxel in prostate cancer cells, and suppressed activation of NF-κB. Curcumin has also been shown to modulate the activity of the MDR genes, suppressing MDR1 protein leading to chemosensitization [49]. Another two examples of inhibition of MDRs are the effects of flavopiridol in enhancing the cytotoxic effects of paclitaxel, cytarabine, topotecan, doxorubicin, and etoposide in non-small cell lung cancer cells [50], and the flavonols

quercetin and kaempferol markedly increasing the sensitivity of the multidrug-resistant human cervical carcinoma KB-V1 cells to vinblastine and paclitaxel in a dose-dependent fashion [51].

1.4.3. Cell differentiation by phytochemicals for cancer treatment.

The strategies that relay in the suppression of the hallmarks of cancer (proliferation, de-differentiation, immune avoidance, inflammation, angiogenesis, etc,) instead of inducing the cell death of tumor cells remain as a relatively new field. The description of the mechanism behind the effects of the phytochemicals on those processes will provide insights into their potential therapeutic value as drugs or chemopreventive agents. One of the most promising and powerful approaches in cancer treatment is the therapy called cytoeducation, which is the induction of differentiation of cancer cells. In general, differentiation means structural and functional changes that lead to the maturation of cells throughout development pathways into lineages or to a cell phenotype [52]. Cancer cells are unable, to varying degrees, to achieve maturation, and thus malignant neoplastic cells show a lack of, or only partial evidence of differentiation, known as anaplasia. Since the basic underlying cause for the failure to differentiate can be attributed to structural changes in the cell's DNA, i.e. mutations, which are essentially irreversible, it is remarkable that some compounds can induce several types of malignant cells to undergo differentiation toward more mature phenotypes [53].

Examples of differentiation therapy in cancer include the treatment of acute promyelocytic leukemia (APL) and other leukemias with all-trans retinoic acid (ATRA), a vitamin A derivative [54, 55] and the induction of differentiation of myeloid leukemia cells to monocytes

with 1α,25-dihydroxyvitamin D3, which also can induce differentiation of prostate and breast cancer cells lines [53]. Phytochemicals with empirical evidence of induction of differentiation in cancer cells belong to the class of coumarins and flavonoids. The coumarin daphnetin (7,8-dihydroxycoumarin), showed potent anti-proliferative effects in the A-498 (human renal carcinoma) cell line at 50 μM, by inhibition of the constitutively active ERK1/ERK2 kinases and induce differentiation (increased expression of cytoskeletal proteins such as the cytokeratins, an epithelial marker) plus concomitant S phase accumulation by inhibition of the cell cycle in the G1-S phase transition (the stage in the cell cycle in which the cell grows) [56]. Other coumarins, the 5-methoxy-6,7-methylenedioxycoumarin, and 5-(3-methyl-2-butenyloxy)-6,7-methylenedioxycoumarin, induce the differentiation human leukemia U-937 to monocytes at doses of 42.75 μM , and 22.16 μM, respectively [57]. Procyanidin (oligomers of flavan-3-ols, such as catechin and epicatechin) also causes irreversible growth-inhibitory in the MDA-MB468 breast carcinoma cell line by induction of accumulation in G1 phase of the cell cycle in a dose-dependent manner and showed an increased expression of cytokeratin 8 (a marker of differentiation). These effects were accompanied by inhibition of the mitogen-activated protein kinase (MAPK)/extracellular signal-regulated protein kinase1/2 (ERK1/ERK2) in a dose-dependent manner after 72 h of treatment at doses of 75-μg/ml [58]. Other flavonoids such as wogonin and, apigetrin showed induction of differentiation on various leukemia cells. Moreover, a newly semisynthetic flavonoid, designated III-10, induced differentiation of human U937 leukemia cells via PKCδ (Protein kinase C delta) activation. It was designed to improve the oral bioavailability and block the metabolism of flavonoids at its hydroxyl groups via introducing the hydrophilic pyrrolidinyl group and the benzyl group to the hydroxyl position. Results showed that exerts growth inhibition on the cell lines U937,

NB4 (acute promyelocytic leukemia cells), HL-60 (acute myeloid leukemia cells) and K-562 (erythroleukemia cells). And the flow cytometry showed that III-10 could induce U937 cells to differentiate into monocyte-like cells at a concentration of 2μM [59]. The mechanisms underlying the effect of phytochemicals on cell proliferation and differentiation will allow the identification of key molecular targets for this group of compounds to facilitate the development of new pharmacological tools with potential therapeutic value for the management of cancer with minor side effects.

1.5. Plant metabolomics

The metabolome is defined as the total quantitative collection of compounds with small molecular weight present in a cell, tissue or organism. The use of high-throughput analytical strategies for the large-scale identification and quantification of metabolites is termed metabolomics. Metabolomics evolves from the pioneering work of metabolite profiling by GC-MS in the early seventies. Metabolic profiling is used when the aim of the study is the identification and quantification of the metabolites present in an organism. On the other hand, metabolomics refers to the identification and quantification of the metabolites in a biological system in a certain physiological state. Other approaches in metabolomics include the targeted analysis, that studies the changes in certain groups of metabolites by optimizing their separation and detection. This method is only possible for a limited number of compounds and relies on the discriminate analysis or on molecular relationships based upon molecular pathways/networks [60]. The use of metabolomics in the study of plants differs from the classical or traditional targeted phytochemical analysis in various aspects, such as being a data-driven approach that aims to assess all

measurable metabolites without any pre-conception or pre-selection. The advance in analytical tools with a higher degree of sensitivity, selectivity, and reproducibility allowed the emergence of plant metabolomics as a type of large-scale phytochemistry [61]. Phytochemistry in natural product discovery focuses on identifying individual, bioactive metabolites, while plant metabolomics seeks to extract meaning from complex data sets. Those fields evolve independently however, both use the same equipment for metabolite analysis and evaluation of the qualities of medicinal plants [62].

1.5.1. Mass spectrometry-based plant metabolomics platforms

Mass spectrometry approaches allow the comprehensive profiling of the metabolome of medicinal plants. The quantitative and qualitative measurements of large numbers of cellular metabolites provide a broad view of the biochemical status of a plant. It is considered that metabolomic approaches provide the most functional information from all the omics technologies. Estimations indicate that number of plant metabolites oscillates between 100,000 and 200,000 ranging from relatively simple primary compounds to highly complex and chemically diverse secondary products. To obtain the most comprehensive visualization of the metabolome of a medicinal plant the use of multiple combinations of solvents, extractions, chromatographic, and spectrometric techniques is necessary [62]. A typical metabolomic analysis comprises three main experimental stages; the preparation of the sample, the acquisition of the data using analytical methods and data mining using chemometric methods followed by compound identification. Plant metabolites are structurally diverse, forming a highly complex spectrum of compounds of different size, solubility, volatility, polarity, quantity and stability. Any extraction method would certainly

produce an inherently multidimensional sample arising from the chemical and physical differences of the constituents. Several methods may be employed to extract metabolites. The choice of method depends on a variety of factors, such as the physicochemical properties of the target metabolites, the biochemical composition of the system under investigation and the properties of the solvent used [63]. Chromatography-mass spectrometry is the most applied analytical techniques in metabolomics. GC-EI-MS is a good approach for targeted analysis of known primary metabolites, whereas LC-ESI-MS is applied for the untargeted analysis of secondary metabolites [64]. To date, gas chromatography coupled to mass spectrometry (GC-MS) is the most widely accepted analytical technique used in studies of plant metabolomics. GC-MS is used for the analysis of very complex matrices such as those of plant extracts. GC-MC provides efficient metabolite separations, resolution, detection, and quantification of metabolites even at low concentrations. The high reproducibility achieved with GC-MS analyses is the result of the electron ionization (EI) method generally employed in GC-MS. In EI, molecules interact with kinetically activated electrons with an accepted average standard energy of 70 eV. Therefore, reproducible mass spectra allowed the building of mass spectral libraries for comparison and identification. Quadrupole (Q) and orthogonal time-of-flight (oTOF) are the most used mass analyzers for GC-MS. TOF-MS analyzers provide higher mass accuracy, higher duty cycles, and faster acquisition times than quadrupole mass analyzers. Those parameters are deconvoluted if necessary in overlapping GC peaks in complex plant extracts. GC-MS technology is used for the analysis of volatile and thermally stable metabolites or metabolites that can be chemically modified to produce volatile derivatives [65].

The most-important complementary technology to GC-MS is the liquid chromatography coupled to mass spectrometry (LC-MS). This technique is used to analyze thermolabile, polar metabolites, and high-molecular weight compounds. Most LC-MS applications use reversed-phase (RP) stationary phases of silica particles functionalized with hydrophobic alkyl chains; such octadecylsilane (ODS). In RP separations the most used mobile phases are mixtures of organic solvents and water. Thus, less polar compounds interact more with the stationary phase and are more retained than polar molecules. Ultra-high performance liquid chromatography (UHPLC) is a related HPLC technique that uses sub-2 mm particles, smaller diameter columns (1-2.1 mm), and higher pressures around 16,000 psi (compared to ca. 6,000 psi for traditional HPLC systems) [66]. Thus, UHPLC provides better resolution and faster analysis. Applications of LC-MS use ESI to allow the analysis of biomolecules directly from the liquid phase and is suitable for LC coupling. ESI is a soft-ionization technique, which introduces little internal energy. Thus, few fragments are generated and provide few structural information of compounds. To obtain detailed structural information from intact ionized species, fragmentation can be achieved by the collision of the analyte ions with inert gas molecules (e.g., He, Ar, or N2). This process is carried out on a tandem MS instrument that allows two or more sequential stages of mass spectrometric analysis [67]. The most common tandem in time instruments is the ion trapping mass spectrometers such as quadrupole ion traps (QIT-MS), the Orbitrap, and the Fourier-transform ion cyclotron resonance mass spectrometers (FT-ICR-MS). Ion trap instruments are particularly useful for unknown plant metabolites because of the multiple MS stages and the provided information for structural elucidation. Tandem-in-space instruments have two mass analyzers separated by a collision cell and allow two sequential stages of mass spectrometric analysis (MS^2). MS^2 is achieved through the

spatial separation of the precursor and fragment ions. Examples of these instruments include triple quadrupoles (QqQ) and quadrupole time-of-flight instruments (qTOF). The study of plant metabolomics by LC-ESI-MS methods present co-eluting interfering compounds due to the complexity of the plant extracts. The presence of multiple metabolites influence the ionization and the transfer of analytes from liquid to the gas phase and potentially compromise the accurate quantification of metabolites. Consequently, the optimization of chromatography is essential to reduce the impact of matrix-induced effects in the mass spectrometer. One major limitation of the target metabolite analysis with LC-MC is the requirement of reference compounds for the identification and quantification of the measured metabolites. Thus, the analysis is limited to compounds commercially available [68].

1.5.2. Data analysis and compound identification

The mass spectral data provides a pattern that is characteristic of specific compounds. Additionally, the identification of analytes uses the accuracy of the mass in the elucidation of metabolites. The procedure for metabolite assignments from MS data consists of the acquisition of accurate mass measurement and the fragmentation patterns, calculation of the elemental composition formula and the spectral comparison in a database for comparison of the fragmentation pattern or with authentic pure standards (when commercially available) [69]. According to recommendations of the Metabolomics Standards Initiative (MSI), the identification of a compound at the highest level of confidence (MSI level 1) requires the comparison of orthogonal parameters of the unknown to an authentic standard measured in the same laboratory and under the same

conditions. The MSI level 2 (“putatively annotated compound”) is for identification by comparison with parameters available in databases. The MSI level 3 (“putatively characterized compound classes”) is for comparison with chemical literature and spectral databases [70].

Various databases have been developed to assist in the assignment of the spectral peaks observed in metabolomics experiments [71]. METLIN is a database that contains about 62,000 MS^2 spectra for more than 12,000 metabolites. All spectra were acquired under standardized conditions (electrospray ionization, positive and negative polarity, high mass accuracy, four different collision energies) on a quadrupole time of flight (QTOF) mass spectrometer [72]. ReSpect is an MS^2 database specific for plant metabolites. Spectral records are annotated with taxonomic information about the species from which the metabolite has been extracted and the chemical class of the metabolite. Flavonoids are the best-represented class (1,360), followed by terpenoids (519), phenylpropanoids (341), alkaloids (256), amino acid derivatives (236), and glucosinolates (93) [73]. The Human Metabolome Database (HMDB) identifies mainly human metabolites. It is used for metabolomics, clinical chemistry and biomarker discovery. It contains information of 2280 drugs, 3670 toxins and 28,000 food components [74]. PhytoHub is a database that contains detailed information about dietary phytochemicals and their metabolites. Around 1,200 polyphenols, terpenoids, alkaloids and other plant secondary metabolites present in foods [75]. The LIPID MAPS Structure Database (LMSD) is a database with structures of and annotations of biologically relevant lipids. The LMSD contains 43307 lipid structures, among them fatty acyls, glycerolipids, glycerophospholipids, sphingolipids, sterol, lipids, saccharolipids, and polyketides [76].

1.5.3. Data mining and data processing

A single GC-MS analysis can identify 500 molecules and provide abundant information that requires simplification and interpretation. Specialized software provides the tools for the statistical analysis to identify differences or similarities in samples, reduction in the dimensionality of data and their visualization. The most popular approaches include unsupervised methods such as principal component analysis (PCA), hierarchical clustering (HCA) and K-means clustering [77]. The PCA is the most used multivariate technique and describe the variance in a set of multivariate data in terms of a set of underlying orthogonal variables (principal components). The original variables can be expressed as a linear combination of the principal components. PCA is a linear additive model, in the sense that each principal component (PC) accounts for a portion of the total variance of the data set. Often, a small set of principal components (2 or 3) account for over 90% of the total variance, and in such circumstances, one can resynthesize the data from those few PCs and thus reduce the dimension of the data set. Then, data is plotting in the space defined by the two or three largest PC and provides an easy method for visualizing the similarities in the data sets [77]. Hierarchical cluster analysis (HCA) is a method for grouping samples in a data set by their similarity. HCA involves a progressive pair-wise grouping of samples by distance. Several distance measures can be used in HCA, such as Euclidean distance, Manhattan distance, or correlation. The result of hierarchical clustering is visualized as a dendrogram. Branch lengths can be made proportional to the distances between groups. This can provide a visualization of the similarities of samples within data sets. Clustering is most useful to classify samples in groups. It is often applied to the data after transformation with PCA, in which case it becomes a means of identifying groups in the reduced dimension data space [77]. These

types of methods are unsupervised because they require no other information than the original data set. A different set of methods called supervised, create a calibration using a training data set, i.e. a set of observations that have been classified by independent means. An example of a supervised method is the use of standards to calibrate a protein concentration assay. Supervised methods can thus only be carried out if one is able to provide known examples [77].

The tools of visualization allow the identification of the properties of the data sets. Metabolites can be related by their molecular structure, the polarity of the solvent employed in the extraction, or the plant from which they were extracted, etc. Diagrams representing the networks or metabolic pathways of the biosynthesis of metabolites have been used as a powerful tool for visualizing relationships between metabolites. Such metabolic network diagrams are also useful to visualize metabolomic data and can be combined with data from genomics or proteomics. Metabolic networks can identify the chain of causality that led to the observed metabolic profile [77].

MetaboAnalyst is a web-based system that supports comprehensive metabolomic data analysis, visualization and interpretation. This platform identifies peaks from raw data, align the peaks among different samples and replicates, and identify and quantify each metabolite. The statistical analysis can be carried with the same software and provides graphical results. In MetaboAnalyst data sets from metabolic studies are processed to obtain the PCA, HCA, K-means clustering, metabolite set enrichment analysis, metabolic pathway analysis, and spectra analysis tools [78].

Currently is technologically impossible to extract and analyze all the metabolite content in a plant. Most metabolomic studies characterized a very small fraction of the whole

metabolome of a certain plant. Moreover, the lack of universal metabolite-specific libraries or known reference compounds represents a major limitation to the definitive identification of metabolites. Another major technological challenge encountered in metabolomics is the dynamic range, which is the presence of some excessive metabolites that cause significant chemical interferences that limit the range in which other metabolites may be successfully profiled. Finally, plants present many biological variations that represent another problem for reproducibility in the results. The goal of a comprehensive quantitative and qualitative analysis of all the metabolites present in a medicinal plant remains an ambitious goal far from reality, but substantial analytical progress was made in the last decade [79].

1.6. Bioassay-guided study of medicinal plants

The ethnobotanical knowledge often leads to the targeted evaluation of the plant extracts or bioassay-guided studies to characterize or isolate the active compounds. Then, using complementary techniques the mechanism of action can be elucidated increasing the understanding of the biological effects of the medicinal plants. Together, those techniques help in the validation of the ethnomedical use of the plant and provide useful lead compounds for further drug development. The characterization of the metabolomic profile of a medicinal plant by chromatography-mass spectrometry techniques allows the fast identification of biologically active constituents [80], however, for the isolation of the biologically active molecules, a bioassay-guided fractionation of the plant extracts linked to column chromatography should be carried out. The bioassay-guided study refers to the isolation of the pure chemical agent from the complete plant extract by the fractionation

of the sample. The separation of the extracted components is based on differences in their physicochemical properties, and the results in biological activity. After several rounds of separation and biological tests, the therapeutically active phytocompounds can be isolated. The field of natural products has provided many effective drugs based on this rationale [81]. However, a common problem with this approach is the loss of activity during the fractionation. The reason obeys to several factors that include but are not limited to next possibilities: an extract may contain a large amount of only moderately active compounds and be very active, may contain small amounts of highly active compounds, and synergistic interactions may be responsible for the bioactivity [80]. Traditionally methods for drug discovery from medicinal plants have additional drawbacks, such as their complexity and the long timescales, and the use of a big amount of solvents need it before an active compound from the complete extracts will finally emerge, and that most compounds obtained by this method are already characterized [82].

The use of the metabolomic profile in combination with a bioassay-guided study provides an overview of the chemical complexity of the active fractions without the need for the time-consuming isolation procedures [60]. This approach enables the profiling of the entire metabolome of the extracts or specific fractions before testing for biological activity. Additionally, allow the rapid analysis of the active fractions and the assessment of the characterization and quantification of the chemical constituents. Recent algorithms can also infer the bioactivity of a medicinal plant based on its metabolic profile [83]. This method is currently employed in drug discovery research due to its effectiveness to directly link the metabolomic profile with bioactivity results and the advantages that represent in cost-effectiveness [81, 84].

CHAPTER II

2. BACKGROUND

2.1. *Cissus trifoliata*

Plants of the genus *Cissus* belong to the *Vitaceae* family that includes the common fruit grapes (*Vitis vinifers*). The tribe *Cisseae* is monogeneric, with about 300 species widely distributed in the tropical and subtropical regions in Asia (85 spp.), the Americas (70 spp.), Africa (135 spp.), and Australia (12 spp.) [85]. These plants are lianas, sometimes succulent, with climbing tendrils, hermaphrodite or polygamomonoecious. Branches contain adherent bark; tendrils unbranched or 2-branched or occasionally 3-6 branched, without adhesive discs. The leaves are simple or ternate, usually succulent with flowers mostly perfect, 4-parted, cymose or corymbose. The ovary is two-celled and fruits with one to four seeds. In the case of *C. trifoliata,* plants are glabrous or sparsely pubescent; leaves mostly trifoliolate, the leaflets of two to nine cm long, usually broadly cuneate, coarsely dentate or lobate; cymes equaling or longer than the leaves; fruit purple or nearly black, with five to eight mm long. Some of the Mexican specimens have been referred to as *C. incisa* (Nutt.) Des MouL, but is doubtfully distinct from *C. trifoliata* [86]. Recent studies confirm no genetic differences between herbariums specimens of *C. incisa* and *C. trifoliata* [87]. Based on phylogenetic relationships, molecular (plastid, nuclear ribosomal sequences) and morphological characters (leaf shape) *C. trifoliata* is closer to *C. descoingsii and C. verticillate,* than *C. quadrangularis, C. repens and C. assamica* which lay in different clusters [85, 88].

The accepted botanical name is *C. trifoliata* (L.); although it is also referred to as *C. acida* (L.), *C. carnifolia*, *C. incisa*, *C. parvifolia*, *Kemoxis acida*, *Sicyos trifoliatus, Vitis acida*, *Vitis incisa, Vitis trifoliata,* possum-grape, and vine-sorrel [86].

C. trifoliata is widely distributed in tropical America and the Mexican territory. It is native of Baja California, Chihuahua, Coahuila, Durango, Nuevo Leon, San Luis Potosi, Sinaloa, Sonora, Tamaulipas, Puebla, Michoacan, Veracruz, Oaxaca, Quintana Roo and Yucatan. Is also present in the United States, Venezuela, Colombia and Ecuador [89] and dispersed in the Caribbean islands such as Bahamas, Cuba, Haiti, Jamaica and Puerto Rico [86].

In Mexico, this plant is also known as "*Hierba del buey*" in Spanish and called *Xbolontibi* in Maya. *C. trifoliata* is an important medicinal plant for the Mayan tribes in Yucatan for the management of gastrointestinal illnesses, sores, cutaneous infections and tumors [90, 91]. The plant is macerated with salt and applied as poultices in the affected site, or prepared as infusion [92]. In Nuevo Leon, at the Northeastern of Mexico, is used for the native population to treat skin infections, inflammation, abscesses and tumors [93]. Ethnobotanical uses documented for *C. trifoliata* in the rest of America include caustic, poison (tubers), burns, sore and tumors [86]. The chemical content of *C. trifoliata* remains unknown; however, in murine models showed anti-inflammatory activities [94].

2.2. Medicinal properties of plants from the genus *Cissus*

Cissus plants are considered medicinal as they have been used in all the continents for the management of several diseases that include arthritis, menopause, obesity, pain, infections, cancer and diabetes [95] (Table 1). Thus, *C. trifoliata* is a potential source of bioactive compounds as suggested by its chemotaxonomic relationship with other medicinal plants, and with its ethnobotanical use in the Mexican traditional medical systems [33].

Table 1. Medicinal properties of *Cissus* plants in different countries

Country	Specie	Traditional use
Australia	*C. hypoglauca*	Sore throats [96].
Brazil	*C. sicyoides* *C. verticillata*	Diabetes [97]. Sore throats [98].
Cameron	*C. aralioides*	Infections [99].
Congo	*C. rubginosa*	Diarrhea [100].
China	*C. assamica* *C. pteroclada* *C. repens*	Diabetes [101]. Pain [102]. Arthritis [103].
India	*C. quadrangularis* *C. ibuensis* *C. hamaderohensis*	Bone healer, menopause, obesity [104]. Infections [105]. Infections [106].
Nigeria	*C. cornifolia* *C. populnea* *C. ibuensis*	Infections [107]. Fertility and malaria [108]. Infections, arthritis [109].
Mexico	*C. trifoliata* *C. verticillata*	Infections [110] Tumors [90].
Tanzania	*C. rotundifolia*	Headaches, infections [111].
Trinidad	*C. verticillata* *C. debilis*	Diabetes, infections[112]. Headaches [113].

Several extracts of *Cissus* species have been tested in relation to the traditional uses. In this regard, hypoglycemic activities have been found for *C. assamica* [114] and *C. sicyoides* [115]. *C. pteroclada* and *C. repens* showed antioxidant, anti-inflammatory and analgesic activities [102] respectively. *C. quadrangularis* demonstrates anti-inflammatory, analgesic, anti-oxidant and hepatoprotective properties [104] and anti-osteoporotic activity [116].

2.2.1. Antibacterial and cytotoxic activity of *Cissus* extracts

Reports in relation to their antibacterial and cytotoxic properties of plants from the genus support the search of bioactive molecules in *C. trifoliata*. The ethyl acetate and petroleum

ether extracts of the stem part of *C. quadrangularis* showed zone of inhibition against *S. aureus, B. cereus, E. coli* and *S. typhi* at a concentration of 1000µg/ml. At a concentration of 250 µg/ml, no significative activity was founded and the ethyl acetate extract was the most active, against *S. aureus* and *S. typhi* [117]. Another study of the antibacterial activity of the extracts from the stems of *C. quadrangularis* by the determination of the MIC with broth microdilution method found the positive activity of the ethyl acetate extract against *B. subtilis* (0.9 mg/ml), *P. aeruginosa* (1.8 mg/ml), *S. typhi* (3.7 mg/ml), *S. aureus* (0.9 mg/ml), and *S. pyogenes* (3.7 mg/ml). For the acetone extract against the estimated MICs were against *P. aeruginosa* (3.1 mg/ml), *S. typhi* (6.2 mg/ml), and *S. aureus* (1.5 mg/ml). The methanolic extract show activity against *B. subtilis* (0.4 mg/ml), *P. aeruginosa* (3.1 mg/ml), *S. typhi* (1.2 mg/ml), *S. aureus* (0.4 mg/ml), and *S. pyogenes* (0.9 mg/ml) [118].

Extracts from the leaf and roots from *C. welwitschii* showed MIC values of 2 mg/ml and 0.5 mg/ml against *B. cereus* and *E. coli* respectively. The range of concentrations used for antibiotics ranged from 1 µg/ml to 4 mg/ml. They include ampicillin, kanamycin, and norfloxacin, showing that strains used were drug-sensitive and that extracts are not as effective as antibiotics. Authors claim that the interactions between compounds may reduce the effectiveness of the plant extracts [119]. The antibacterial activity of extracts from the stems of *C. quadrangularis* was also tested against drug-resistant bacteria from clinical isolates by the method of agar well diffusion. However, the concentrations used for the assay were 1g/ ml and 1.5 g/ml. The hexane, ethyl acetate, and methanol extracts were evaluated against *E. coli* resistant to ciprofloxacin, *K. pneumoniae* resistant to amoxycillin and ciprofloxacin, and *P. aeruginosa* resistant to Amoxycillin, Ciprofloxacin, and Cephaloridine. All of the extracts showed positive inhibition of bacterial growth, and

the zone of inhibition range between 8 and 19 mm, but *Klebsiella* was the most sensitive bacteria [120]. Several extracts from *Cissus* plants have also shown antimicrobial activity *in vitro* against *B. subtilis, K. pneumonia, S. aureus, E. coli,* and *P. aeruginosa*. Those species include *C. pallida* [121], C. *welwitschii* [119], *C. cornifolia* [122], *C. rotundifolia* [106], *C. ibuensis* [123], and *C. rubiginosa* [100].

Regarding the activity of *Cissus* plant extracts against cancer cell lines, cytotoxic activity was found by the MTT technique in extracts from the stems of *C. quadrangularis*. They estimate an IC_{50} of 200 µg/ml for the hexane extract against the skin carcinoma cell line A431 [124], and 48 µg/ml for the acetone extract against the epidermic carcinoma cell line KB [124]. The ethyl acetate extract from the stems of *C. sicyoides* showed an IC_{50} of 43 µg/ml against the liver carcinoma cells HepG2 [125] and the ethanolic extract from their leaves showed activity against lung carcinoma NCI-H292 and mouth KB carcinoma cell lines with an IC_{50} of 50 µg/ml [126]. Finally, the methanolic extract from the stems of *C. debilis* caused proliferative inhibition in the carcinoma cell line from colon CaCo-2 with an estimated IC_{50} of 50 µg/ml [127]. Even though extracts are not as effective as antibiotics or cytotoxic agents is important to mention that side-effects are minimum for human consumption. Studies showed that at doses as high as 5 g/kg for humans [128] and animals [129] there are no signs of any adverse side effects at least for *C. quadrangularis* extracts.

2.2.2. Bioactive compounds isolated from *Cissus* plants

Some of the properties of *Cissus* plants are attributed to bioactive compounds such as flavonoids, triterpenes, sterols, coumarins and stilbenes with anti-inflammatory,

antimicrobial [130] and anticancer activities [131] (Table 2). They exert their action mechanism through the modulation of enzymes as phospholipases, cyclooxygenases, lipoxygenases [132], and steroid and kinase pathways [133]. Some of the isolated and characterized compounds on *Cissus* plants possess both, antibacterial and cytotoxic activities. For example, kaempferol induced the apoptosis via cell cycle arrest in the cell line of breast carcinoma MDA-MB-453 [134] and inhibits the function and expression of the MDR1 in *S. aureus* [46]. Eugenol inhibits MCF7 cell growth, and, in dose and time-dependent manner originates cell shrinkage, membrane changes, and apoptotic body formation. Eugenol downregulates the cyclins D1 and B, the antiapoptotic protein Bcl-2 whereas increases the expression of p21 and p53 [135]. Eugenol has also been shown to be inhibitory for the *E. coli* that produces shigatoxin (O157:H7) through membrane disruption [136]. Ellagic acid induces antiproliferative effects in human prostatic cancer cell lines (PC3) through downregulation of the insulin growth factor II (IGF-II) and the induction of p53/p21 expression [137]. Ellagic acid also shows antibacterial activity against *Aeromonas hydrophila* through unknown mechanisms [138]. Friedelin is another example of a compound with inhibitory activities against *E. faecalis, S. aureus, P. aeruginosa* and Vero cells (kidney epithelial cells extracted from an African green monkey *Chlorocebus*) although the mechanism of action is not well understood [139]. Other compounds isolated in *Cissus* plants with both, *in vitro* activities against cancer and bacterial cells are resveratrol [140], quercetin [141], daucosterol [142], ursolic acid [143], purpurogallin [144], myrecitin [145] and lupeol [146]. Several species of the plants of the genus *Cissus* still lack phytochemical characterization and biological evaluation to support their use as traditional medicine. In Mexico, some communities continue to practice Maya medicine and include the use of *C. verticillata* and *C. trifoliata* for the management of gastrointestinal, skin diseases and tumors [110].

Moreover, according to the chemotaxonomic relationship it is probable that more *Cissus* species from Mexico possess bioactive compounds with anticancer and antibacterial properties [95].

Table 2. Bioactive compounds isolated from the stems of *Cissus* plants

Plant	Solvent	Compounds
C. assamica	BuOH	Ursolic acid, lupeol, isolariciresinol, daucosterine, ellagic acid, β-sitosterol and bergenin [147].
C. pteroclada	EtOH	Stigmasterol, β-sitosterol, daucosterol, taraxerone, eugenol, bergenin, myricetin, gallic acid and oleanolic acid [148].
C. quadrangularis	EtOH MeOH	δ-amyrin, resveratrol, δ-amyrone, piceid, β-sitosterol, kaempferol, quercetin, phytol, lupeol, piceatannol, pallidol, quadrangularin and parthenocissin [116, 120, 133].

2.2.3. Compounds isolated and evaluated from *Cissus* plants

Few reports evaluate the biological activity of compounds isolated in *Cissus* plants. Examples include the isolation of ascorbic acid from the methanolic extract from the stems of *C. quadrangularis.* The administration of the compound produced a significant protection against aspirin-induced gastric toxicity by showing a significant increase in prostaglandin E2 (PGE2), the transforming growth factor alpha (TGF-α), the vascular endothelial growth factor (VEGF), expression accompanied by an inhibition of nitric oxide and regulation of the levels of cytokines in rats. These findings suggest that ascorbic acid from *C. quadrangularis* prevents gastric ulcer formation due to its immunomodulatory effect, antioxidant activity and prostaglandin synthesis modulation [149]. In addition, the new

flavonoid cissusin isolated from the methanolic extracts of *C. sicyoides* stems show inhibitory effects of mast degranulation in the rat basophilic leukemia cells (RBL-2H3) cells [150]. Likewise, the triterpene lupeol isolated from the methanolic extract of *C. quadrangularis* stems showed five times more potent melanin promotion activity when compared with the standard control compound; 3-isobutyl-1-methylxanthine [151]. Moreover, bergenin a phenolic compound isolated from the ethanolic extract of *C. pteroclada* stems exerted *in vitro* anti-inflammatory effects in lipopolysaccharide (LPS) stimulated murine macrophages (RAW 264.7). The molecular effects consist of the inhibition in the production of the pro-inflammatory molecules such as the nitric oxide (NO), PGE2 and the expression of NF-κB, TNF-α, interleukin 1 beta (IL-1β), inducible nitric oxide (iNOS) and cyclooxygenase-2 (COX-2) [102]. Finally, it was recently discovered a new benzolactone from the ethyl acetate extracts of *C. cornifolia* roots. The compound (4,6-dihydroxy-5-methoxy-3-(1,2,3,4,5-pentahydroxypentyl)-2-benzofuran-1(3H)-one) showed antimicrobial activity against six of ten clinical isolates of *S. aureus, S. typhi*, and *C. albicans*. The inhibition zones ranged between 17 and 25 mm [152].

CHAPTER III

3. HYPOTHESIS AND OBJECTIVES

3.1. HYPOTHESIS

The stems of *Cissus trifoliata* possess bioactive compounds with antibacterial or cytotoxic activities with a mechanism of action different from the reported in the literature.

3.2. General Objective

To perform a metabolomic profile and a bioassay-guided phytochemical analysis of *Cissus trifoliata* stems, to evaluate their antibacterial and cytotoxic activities, and to elucidate the mechanism of action of one active compound.

3.2.1. Specific Objectives

- To investigate the ethnomedical uses, chemical composition, and biological evaluation of the plants from the genus *Cissus*.
- To identify the chemical composition of the hexane, $CHCl_3$-MeOH and aqueous extracts from the stems of *C. trifoliata*.
- To study the metabolomic profile of *C. trifoliata* stems.
- To assess the antibacterial and cytotoxic activity of each extract.
- To perform a Bioassay-guided fractionation of the $CHCl_3$-MeOH extract.
- To characterize the metabolomic profile of the active fractions.
- To identify the mechanism of action of one compound present in the most active fraction.

CHAPTER IV

4. MATERIALS AND METHODS

4.1. Phytochemistry

Phytochemistry was carried out in the Pharmaceutical Chemistry Laboratory at the Postgraduate Studies Division of the School of Science in Chemistry, of the UANL.

4.1.1. Plant material

The plant selected for this study was collected in Rayones, Nuevo León and identified by the Biologist Mauricio González Ferrara. A sample of reference was deposited in the Department of Botany, Faculty of Biological Sciences, UANL (voucher 027499).

4.1.2. Fractionation of the extracts and isolation of solids.

Dried and ground stems (756 g) were subjected to exhaustive extractions by maceration with hexane (4 L, 48 h), $CHCl_3$-MeOH (1:1) (9 L, 4 times, 24h each), and distilled water (4 L, 24 h). Solvents used were chloroform ($CHCl_3$) purity 98.8%, methanol (MeOH) purity 99.9%, and hexane purity 98.99% (Baker, USA). The organic extracts were filtered and concentrated using rotavapor (V300, Buchi, Switzerland), at 40 °C and the aqueous extract was lyophilized. The fractionation of the extracts was performed by column chromatography, using silica gel (63-200 μm) (Sigma Aldrich) in a 1:20 relation. Fractionation and purification of compounds were monitored with thin layer chromatography (TLC) of silica gel 60F-254 (Fluka Analytical) using visible and ultraviolet (UV) light at 254 nm and 365 nm (Spectroline, EF160C) and revealed with cerium sulfate. Melting points were calculated using the Fisher-Johns equipment (00590Q).

4.1.2.1. Fractionation of the hexane extract

The hexane extract (3.5 g) was subjected to column chromatography, using silica gel (70 g) as stationary phase and hexane/ethanol in gradient as mobile phase. A total of 224 fractions of 20 ml each were collected. Fractions were pooled in four according to their similarity on TLC (Table 3).

Table 3. Fractionation of the hexane extract

Fractions	Mobile phase	Pooled Fractions	Weight (g)
1-84	Hex 100	I	0.1306
85-98	Hex / EtOH 96:4	II	2.5837
99-144	Hex / EtOH 93:7	III	0.0902
145-224	EtOH 100	IV	0.0941

4.1.2.2. Fractionation of the $CHCl_3$-MeOH extract

The $CHCl_3$-MeOH extract (24 g) was subjected to column chromatography, using silica gel (480 g) as the stationary phase and hexane, ethylacetate and methanol in gradient as mobile phase. A total of 210 fractions of 20 ml each were collected. Fractions were pooled in fourteen according to their similarity on TLC (Table 4).

4.1.3. Isolated solids from the fractionation of hexane extract

4.1.3.1. Solid one (CIR1)

Solid one crystallized out from pooled fraction I, eluted with hexane 100% as a white amorphous solid. The solid was filtrated and washed with cold acetone to remove impurities. The process afforded 50 mg (0.006614%) of a waxy solid. TLC analysis shows that CIR1 was not active under visible or UV light, but stain as a brown spot with cerium sulfate.

Table 4. Fractionation of the $CHCl_3$-MeOH extract

Fractions	Mobile phase	Pooled Fractions	Weight (g)
1-28	Hex 100	A	0.1499
29-36	Hex / AcOEt 85:15	B	1.8797
37-45	Hex / AcOEt 80:20	C	0.9695
46-54	Hex / AcOEt 70:30	D	0.4827
55-72	Hex / AcOEt 60:40	E	2.1402
73-78	Hex / AcOEt 30:70	F	0.4285
79-108	AcOEt 100	G	1.1653
109-117	AcOEt / MeOH 80:20	H	0.4561
118-128	AcOEt / MeOH 80:20	I	0.6795
129-144	AcOEt / MeOH 70:30	J	1.3392
145-168	AcOEt / MeOH 50:50	K	4.1135
169-186	AcOEt / MeOH 30:70	L	3.7527
187-198	AcOEt / MeOH 20:80	M	1.5929
199-210	MeOH 100	N	1.2244

4.1.3.2. Solid two (CIR2)

From pooled fraction II (hexane-ethanol 96:4) precipitated a cream amorphous solid. Its filtration with cold acetone yields 28 mg (0.003703%) of a white solid, soluble in hexane. CIR2 exhibited a single brown spot in TLC stained with cerium sulfate.

4.1.3.3. Solid three (CIR3)

The pooled fraction II (hexane-ethanol 96:4) was re-chromatographed over silica gel (2.35g), eluting with hexane-ethyl acetate (Column II). The subfractions with identical TLC patterns were combined. From subfraction 30-37 (90:10) precipitated a solid, which was washed with methanol yielded 39 mg (0.005158%) of a white solid. CIR3 was soluble in hexane and appear as a brown spot on a TLC stained with cerium sulfate.

4.1.3.4. Solid four (CIR4)

Subfractions 56-63 (hexane-ethyl acetate 85:15) from column II afford a solid that was purified by successive recrystallization with acetone. The process yields 35 mg (0.004629%) of crystals, which were soluble in chloroform and acetone. CIR4 on TLC stains as a single purple spot with cerium sulfate.

4.1.3.5. Solid five (CIR5)

The solid five precipitated in the mother liquor of CIR3. The white solid was filtered by vacuum and washed with hexane. The process recovered 30 mg (0.003968%) of solid soluble in chloroform. The TLC analysis showed a brown spot with the cerium sulfate stain.

4.1.4. Nuclear Magnetic Resonance (NMR) spectroscopy

The chemical structure of the solids was analyzed by ^{1}H and ^{13}C NMR spectroscopy performed in BRUKER NMR 400 MHz equipment using as solvent deuterated chloroform ($CDCl_3$), and tetramethylsilane (TMS) as a reference. The software Mestrenova version 12.0.2 was used for processing the spectral data.

4.1.5. Gas chromatography-mass spectrometry

The GC-MS analysis was performed in a gas chromatograph 6890 equipped with an MSD 5973 mass detector, both from Agilent technologies, using helium as the carrier gas. A volume of 1µl of samples was injected in split mode (1:15), at an injector temperature of

270 ºC. The quadrupole mass spectrometer was operated in EI mode at 70 eV in scan mode (m/z 50 to 600). Data acquisition and processing were performed using Agilent MSD Chemstation software. The solids and the hexane extract were analyzed by GC-MS, the instrumental conditions are described in table 5.

Table 5. Conditions of GC-MS analysis for the solids and the hexane extract

GC-MS engine model	Agilent. GC 6890, MSD 5973N
GC column	HP-5 (30 m *0.25 mm x 0.25 µm)
Injector	Split 1:15
Carrier gas	Helium
Carrier gas flow	1 ml/min
Injector temperature	270 °C
Source temperature	230 °C
Detector temperature	250 °C
Initial temperature	70 °C, 2 min
Temperature program	70 to 200 °C ,10 °C/min, 200 to 310 °C, 10 °C/min.
Final temperature	310 °C, 5 min.

4.1.6. Liquid Chromatography-Mass spectrometry

Samples were diluted in 50% with LC-MS grade MeOH (Fisher Scientific), filtered using the Supelco (54145-U) Iso-disc, N-4-2 nylon, 4 mm x 0.2 µm filters (Sigma-Aldrich), and transferred to high-recovery amber vials (Agilent Technologies, Inc., Santa Clara, CA). Reverse-phase liquid chromatography was performed using an Agilent 1290 Infinity Ultra High-Performance Liquid Chromatography system (UHPLC). The mobile phase was delivered by a binary pump at a flow rate of 0.250 ml/min using two mobile phases: solvent A was composed of LC-MS grade water and 0.1% v/v formic acid (Proteochem Loves Park, IL) and solvent B was of LCMS grade MeOH and 0.1% v/v formic acid (Proteochem). The solvents were dispensed over a gradient: 0-6 min, 100% solvent B; 10 min, 100% B; 11 min, 30% B. The autosampler was set with an injection volume of 5 µl. The flush port was set to clean the injection needle for 30s intervals. The stationary phase was a C18

column (ZORBAX Rapid Resolution High Throughput (RRHT), 2.1 x 50 mm, 1.8 µm, Agilent Technologies, Inc.) was used. The column was maintained at an isothermal temperature of 38 °C (Table 6).

Table 6. UPLC Parameters

Instrument	Agilent 1290 Infinity Binary LC	
Mobile phases	A) 0.1% formic acid in water B) 0.1% formic acid in methanol	
	Initial 100% B	
Gradient	Gradient	
	Time (min) %A 6 min 0% 10 min 0% 11 min 70%	 %B 100% 100% 30%
Flow rate	0.250 ml/min	
Column	A ZORBAX Rapid Resolution High Throughput (RRHT), 2.1 x 50 mm, 1.8 µm C18 column (Agilent Technologies, Inc.) with an Agilent 2.1 mm × 5 mm, guard column (p/n 821725-911)	
Post run time	4 minutes at initial mobile phase	
Temperature	38 °C	
Injection volume	5 µl	

Mass spectrometric analysis was performed by an Agilent 6530 QTOF LC-MS with an ESI source set for detection mass range from mass-to-charge ratio (m/z) 100 to 1000. A dedicated isocratic pump continuously infused a mix of reference standards (Agilent Technologies, Inc.) at a flow rate of 0.5 ml/min to achieve accurate mass correction. The nebulizer pressure was set at 35 psi with a surrounding sheath gas temperature of 350 °C and a gas flow rate of 11 l/min. Drying gas temperature was set at 300 °C with a flow rate of 10 l/min. Default settings were used to set a voltage gradient for nozzle at 1000 V, skimmer at 65 V, capillary (VCap) at 3500 V, and fragmentor at 175 V (Table 7). The active fractions from the $CHCl_3$-MeOH extract were dissolved in a (50:50 v/v) solution of methanol and water at the concentration of 1000 mg/l. Their analyses were carried out by reverse phase HPLC on an Agilent 1200 series system fitted with an Agilent, Zorbax C18 (4.6 × 100 mm, 3 µm).

Table 7. Q-TOF LC/MS Parameters

Instrument	Agilent 6530 Accurate-Mass Q-TOF LC/MS
Ionization mode	Negative electrospray with Agilent Jet Stream technology
Acquisition rate	1.0 spectra/s
Mass range	100-1,000 m/z
Drying gas temperature	225 °C
Drying gas flow rate	10.0 l/min
Sheath gas temperature	350 °C
Sheath gas flow rate	11.0 l/min
Nebulizer gas	35 psi
Skimmer voltage	65 V
Octopole RF	750 V
Fragmentor	175 V
Capillary	2.5 kV (negative mode)

The HPLC conditions were as follows: flow rate, 0.4 ml/min; solvent A, 0.1% formic acid in water; solvent B, methanol; gradient, solvent B 20-100% over 10 min and kept at 100% for 5 min. The extract was injected (4 µL) in the HPLC system and analyzed by ESI-QTOF-MS in the negative mode using an Agilent 6520 time-of-flight mass spectrometer. Mass spectral data were acquired in the range m/z 100-3000, with an acquisition rate of 1.35 spectra/s, averaging 10,000 transients. The source parameters were adjusted as follows: drying gas temperature 250 °C, drying gas flow rate 5 L/min, nebulizer pressure 45 psi, and fragmentor voltage 150 V. Data acquisition and processing were done using Agilent Mass Hunter Workstation Acquisition v. B.02.00 software.

4.1.7. Identification of plant metabolites and data analysis

Record of LC-MS data was achieved using Agilent MassHunter Acquisition SW Version, 6200 series TOF/6500 series Q-TOF B.05.01 (B5125.1). Agilent MassHunter Qualitative Analysis B.06.00 was used to analyze data and to generate the total ion chromatogram (TIC), extracted ion chromatogram (EIC), the extracted compound chromatogram (ECC), and mass spectra. MS acquisition was performed with three replicate injections to allow

column conditioning and examine reproducibility. The putative compound identification was based on the correct elemental composition generated using the accurate m/z and the molecular formula generator tool (Agilent Technologies). Data were queried against the online METLIN, HMDB, LMSD and Phytohub databases.

4.1.8. Antibacterial activity.

4.1.8.1. Bacterial strains.

The tested bacteria include seven bacteria from the ATCC (American Type Culture Collection, Manassas, VA, USA) and nine resistant strains isolated in the University Hospital of the Universidad Autonoma de Nuevo León (Monterrey, Nuevo León, Mexico). The bacteria from the ATCC include 3 three gram-positive bacteria; *Staphylococcus aureus* (ATCC, 29213), *Staphylococcus epidermidis* (ATCC,14990) and *Enterococcus faecium* (ATCC, 2127) and four gram-negative bacteria, *Acinetobacter baumanni* (ATCC, 13883), *Escherichia coli* (ATCC, 25922), *Pseudomonas aeruginosa* (ATCC, 27853), and *Klebsiella pneumoniae* (ATCC, 19606). The drug resistant gram-positive bacteria were methicillin-resistant *S. aureus* (14-2095), linezolid-resistant *S. epidermidis* (14-583), and vancomycin-resistant *E. faecium* (10-984). The drug resistant gram-negative bacteria were, carbapenem-resistant *A. baumannii* (12-666), extended spectrum β-lactamase (ESBL) *E. coli* (14-2081), carbapenem-resistant *P. aeruginosa* (13-1391), oxacillin-resistant (OXA-48) *K. pneumoniae* (17-1692), and New Delhi metallo-β-lactamase 1 (NDM-1+) *K. pneumoniae* (14-3335).

4.1.8.2. Microdilution method.

The MIC of the extracts and the positive control levofloxacin were determined in duplicate by the micro-dilution broth method in 96-well microplates [153]. The aqueous extract was dissolved in distilled water, while organic extracts and levofloxacin were dissolved in dimethyl sulfoxide (DMSO). The solutions were then diluted in Mueller-Hinton broth (Difco, Detroit, MI, USA), in order to achieve concentrations ranging from 500, 250, 125, 62.5, 31.2, 15.6 and 7.8 µg/ml for extracts and 200, 100, 50, 25, 12.5, 6.25 and 3.12 µg/ml for levofloxacin according to literature [154]. The range of concentrations used for DMSO was from 6% to 0.09% (v/v) and this solution was used as a negative control. The strains were inoculated on plates prepared with 5% blood agar and cultured for 24 h at 37 °C. The strains of *P. aeruginosa* and *S. epidermidis* were incubated for 48 h at 37 °C. One to three colonies from the blood agar plate were selected and transferred to a tube containing 5 ml of sterile saline solution. The suspension was adjusted to 0.5 MacFarland standard (1.5×10^8 CFU). Then, 10 µl of this suspension was transferred into 11 ml Mueller Hinton broth to achieve 1.5×10^5 CFU/ml. One hundred microliter of Mueller Hinton broth was added into each well of the 96-well plate. Further, 100 µl of each solution to be tested was added to the wells of line A. Then, a serial dilution (1:2) was carried out through the plate until line G. Then, 100 µl of bacterial suspension (1.5×10^8 CFU) was added to all the wells except line H which was the sterility control. Plates were incubated at 37 °C for 24 or 48 h depending on the bacteria. After the incubation, the turbidity or bottom deposition was visually evaluated to determine the microorganism viability. The MIC values were determined as the lowest concentration which inhibits the microorganism growth. According to the National Committee for Clinical Laboratory Standards extracts with a MIC value ≥30 µg/ml were considered negative for antibacterial activity [154].

4.1.9. Cytotoxic activity

4.1.9.1. Cells and culture of MTS assay

The cytotoxic activity was investigated on the human cancer cell lines PC3 (prostate), Hep3B, and HepG2 (hepatocellular), MCF7 (breast), A549 (lung) and HeLa (cervical) human cancer cell lines, obtained from the ATCC (American Type Culture Collection, Manassas, VA, USA) [155]. PC3 cells were grown in RPMI-1640 medium (Sigma Aldrich, St. Louis, MO, USA), and the rest in DMEM medium (Invitrogen, Thermo Fisher Scientific, Inc., Waltham, MA, USA), supplemented with fetal bovine serum 10% (SFB, Invitrogen) and with 2 mM glutamine. All cultures were incubated at 37 °C in an atmosphere of 5% CO_2. For the evaluation in the MTS assay, 4000 cells per well were cultured in a 96-well plate. The concentrations used for the extract, the pure compounds, and the positive control paclitaxel were 100, 10, 1, 0.1, 0.001 µg/ml for a dose/response curve, and incubated at 37 °C in 5% CO_2 atmosphere for 72 h according to recommendations [36]. The number of viable cells in proliferation was determined by using CellTiter 96 AQueous One Solution Cell Proliferation Assay kit (Promega, Madison, WI, USA), following the manufacturer's instructions. Cell viability was determined by absorbance at 450 nm using an automated ELISA reader. The experiments were conducted by triplicate in three independent experiments. The concentrations assayed allowed the determination of the half-maximal inhibitory concentration (IC_{50}) by regression analysis with the statistical program Prism5. The recommendations of the National Cancer Institute were used as a guideline. Thus, the extracts were considered cytotoxic when the $IC_{50} \leq 30$ µg/ml [36].

4.1.10. Bioassay-guided cytotoxicity of the $CHCl_3$-MeOH extract by WST-1

The hexane extract (3.5g) was completely processed by column chromatography during the purification of the solids. Thus, the bioassay-guided study was done in the $CHCl_3$-MeOH (21g). The assays were performed in MCF7 and PC3 cell lines. When cells reached a confluence of 80%, were washed twice with phosphate-buffered saline (PBS) solution, followed by 500 µl of 0.25% trypsin for each vial with medium, and incubating for 5 min at 37 °C in 5% atmosphere of CO_2 in an incubator (model 3403 Thermo Scientific ®). After incubation, cells were detached and resuspended in 1 ml of EMEM (Eagle modified essential medium) medium supplemented with 10% fetal bovine serum (SFB) and 1% of an antibiotic (10000 units of penicillin/10 mg streptomycin /ml). The cell suspension was centrifuged at 13000 rpm for 10 min in a refrigerated centrifuge (Sorval Thermo Scientific®). The supernatant was removed, and the pellet was resuspended with 5 ml of EMEM medium, 10 µl of the cell suspension was transferred in the Neubauer chamber to perform the cell counting. The cell suspension was adjusted to $5x10^4$ cells/ml. For the assay, approximately $5x10^3$ cells per well were incubated for 24 h. Then, fractions under study and the controls were added to the 96-well plates. The concentrations of the fractions used were 100, 50, and 25µg/ml. The stock solution of each extract was made of 1 mg of extract and 250 µl of DMSO. From the stocks, 20 µl were transferred to an Eppendorf tube, and 480 µl of EMEM medium were added. Then, 100 µl of the solution was taken and placed in the first well of the plate and subsequently carry out a serial dilution. The procedure was carried out for each fraction and controls in triplicate. The plate was incubated for 48 h at 37 °C. At the end of the incubation period, the supernatant of the plate was substituted with 10 µl of WST-1 and 90 µl of EMEM medium and incubated for 2 h. At the end of the incubation period, the optical density was measured at 450 nm

with an ELISA reader (ELX800, Biotek®). The paclitaxel was used as the reference drug at the same concentrations, and as positive control 1% of triton X in PBS. As negative controls, the cells without any treatment, the solvent/medium EMEM at the same concentrations for the dilutions of the fractions, and 95 µl of EMEM medium and 5 µl of WST-1 other as target of the reaction of wells without cells.

4.1.10.1 Determination of the IC_{50} for pure compounds

Phytochemicals identified in the active fractions are widely distributed in the plant kingdom, except for stilbenes with a narrow distribution that includes the Vitaceae. Thus, resveratrol derivatives were chosen for the determination of the cytotoxic activity and the microarray study. The pure compounds purchased in Sigma Aldrich were the resveratrol (R5010) and piceid (R15721). The IC_{50} was calculated against the PC3 and MCF7 cell lines by the WST-1 protocol previously used in the evaluation of the cytotoxic activity of the fractions. Cells were exposed to 6.25, 12.5, 25, 50 and 100 (µg/ml) of resveratrol or piceid for 24 h. Stocks were prepared with DMSO, and assays were carried out in triplicate and repeated 3 times on different days. The IC_{50} was calculated with Quest Graph™ (AAT Bioquest, Inc. USA).

4.1.11. Microarrays

4.1.11.1 RNA isolation

Traditional methodologies to discover anticancer drugs are based on the determination of the cytotoxic effects of a certain molecule over cancer cells *in vitro* exposed to its IC_{50}. However, recent literature has shown that the exposition to IC_{20-30} [156] or lower

concentrations, but longer incubation periods [157] are useful in the determination of novel anticancer mechanisms of well-known phytocompounds. Thus, PC3 cells were exposed to resveratrol at IC_{25} for 24 h to explore antitumor effects non-related with apoptosis. The concentration of resveratrol used for the assays was 27 µg/ml (115 µM). Cells were counted, and 10 µl were added to the Neubauer chamber to reach a cell suspension of $2x10^6$ of cell/ml. In each flask 1 ml of cell suspension was added in 3 ml of EMEM and incubated for 24 h, at 37 °C in an atmosphere of 5% of CO_2. Further, cells were exposed for 24 h with resveratrol. For the RNA isolation, the media was discarded, and cells were washed with PBS, and 1 ml of trypsin was added to each flask and incubated for 3 min. Then 2 ml of EMEM was added in each flask. Cells were transferred to 15 ml Falcon tubes and centrifugated for 10 min at 1300 rpm.

The supernatant was discarded, and 1 ml of PBS was added to the pellet. Centrifugated 8 min at 13300 rpm at 4 °C. The supernatant was discarded and 500 µl of trizol was added and vortexed for 15 s, followed for incubation of 2 min at room temperature. Then, 500 µl of $CHCl_3$ were added, and vortexed for 15 s, and incubated 3 min at room temperature. Another centrifugation step of 8 min at 13300 rpm was carried out. The aqueous phase was recovered by micropipette and included in 500 µl of isopropanol and mixed by immersion. The centrifugation step was repeated in the same conditions, and the supernatant was discarded. The pellet was washed with 500 µl of ethanol 70% and centrifugated in the same conditions for 5 min. The pellet was left to dry for 5 min at room temperature. Then, 50 µl of Mili-Q water was added to dissolve the RNA pellet. Samples were kept at 4 °C. RNA integrity was evaluated in 1% agarose gel in TBE 1X buffer, run at 80 V for 5 minutes, followed by 120 V for 25 min. RNA was quantified by spectrophotometry, adding 2 µl of each sample in nanodrop 2000 (Thermo Scientific,

USA). The optical density relationship 260/280 was assessed to evaluate RNA purity. Finally, the RNA was precipitated and transferred to cryotubes, adding 5 µl of sodium acetate 3M at pH 5.2 and vortexed. Cold ethanol was added (138 µl) in each sample and mixed by immersion. RNA samples were kept in -80 °C.

4.1.11.2 RNA tagging

For RNA tagging, deoxynucleotides of thymine were marked with fluorescence molecules, Alexafluor 555 for the control and Alexafluor 647 (Thermo Fisher Scientific, MA, USA) for the sample. The RNA of the samples was centrifugated at 14000 rpm for 15 min. The supernatant was discarded, and the pellet washed with 500 µl of ethanol 70%, it was centrifugated and allowed to dry 15 min. Then was resuspended in 15 µl of water treated with diethylpyrocarbonate (DEPC). Tagging was performed by retrotranscription employing mixtures. Mixture A contained Oligo dT 1 µl, random primers 1 µl and water treated with DEPC. The final volume of the mixture was 19 µl and was incubated at 70 °C for 10 min and placed on ice for 5 min. Mixture B consisted in reaction buffer 5X RT (8 µl, MgCl 25 mM, 2 µl, aminoalil-DNTP 4 µl, ditiotreitol (DTT) 0.1 M 4 µl, transcriptase reverse superscript II (200U/ µl) 3 µl. Mixture B was mixed with A, and centrifugated e incubated for 10 min at 25 °C, followed by overnight incubation at 42 °C. After retrotranscription, RNA was hydrolyzed with 5 µl of NaOH 1 N and 1 µl of EDTA 0.5 M and incubated 10 min at 65 °C, then 24 µl of (4-(2-hidroxietil)-1-ácido piperazineetanosulfonico) (HEPES) 1 M, pH 7.5 were added. The cDNA purification consisted of the addition of 7 µl of sodium acetate 3 M and 400 µl of union buffer, mixed and was subjected to column Qiagen. It was incubated 5 min, and centrifugated at 1400 rpm one min, it was washed in triplicated with 500 µl of ethanol at 80%, and centrifugated at 14000 rpm. Finally, ethanol was

evaporated. New tubes were used to recover cDNA of the column with 30 µl of H_2O/DEPC. The sample was centrifugated at 9000 rpm for 1 min in a vacuum centrifuge (Integrated Speedvac system model ISS110, Thermo). Samples were resuspended in 4.5 µl sodium bicarbonate 100 mM, 9.0 pH, vortexed and allowed to rest 10 min.

4.1.11.3 Microarray hybridization

Microarrays used was the H35K, which contains the entire human genome sequence as a blueprint (Arrayit, CA, USA). The microarray chip was hydrated in water vapor at 60 °C for 10 s, tree times. Chip was fixed with ultraviolet light for 1 min, 2x, in the Sprectrolinker (XL-1500). To perform hybridization, the complementary DNA (cDNA) was quantified with Nanodrop. Each sample was adjusted and led to dry, to dissolve them in hybridization solution containing 17.5 µl of saline-sodium citrate (SSC) 5X, 7 µl of Sodium dodecyl sulfate (SDS) 0.1%, 45.5 µl and Tris EDTA buffer (TE). Denaturalization was performed at 94 °C for 5 m and 30 s at 65 °C. The mixture was added to the microarray and covered. The incubation was allowed for 18 h in a water bath at 42 °C. Afterward, the microarrays were washed 3 times with the SSC 1X buffer at room temperature. The microarrays were centrifugated (model Allegra 6, Beckman) at 1500 rpm for 2 min. Once dry, microarrays were read it with the scanner GenePix 4100 (Molecular Devices, CA, USA).

4.1.11.4. Bioinformatic analysis of Microarrays

For the bioinformatic analysis, the upregulated and downregulated genes considered were those with a z-score of ± 2 SD. The database employed for the interpretation was DAVID version 4.0 (The database for Annotation, Visualization, and Integrated Discovery) to identify the functional roles of the affected genes.

4.1.12. Statistical analysis

The analysis of the metabolic profile was carried out using MetaboAnalyst version 4. All data were log-transformed and normalized before statistical analysis. Principal Component Analysis (PCA) was used to determine the metabolomic variation in individual extracts and the hierarchal clustering to visualize the relationship among samples (Euclidean distances). The metabolic pathways analysis employed the library of *Arabidopsis thaliana*. The one-way ANOVAs and the post-hoc analysis (Tukey HSD test) were performed to determine significative differences ($p > 0.05$). Data from experiments of cell proliferation were analyzed by ANOVA-LSD test (Fisher's least significant difference) in the IBM SPSS Statistics Version 20.

4.1.13. Waste disposal

Hazardous waste material was properly collected, stored and disposed in line with the recommendations of the department of waste management of the FCQ, UANL. Accordingly, the halogenated solvents and their mixtures were collected in container D, and non-halogenated solvents in collector C. Waste material generated during the assays of microbiology and cell cultures were disposed in a biohazard red bags and autoclave it before discarding in line with the guideline of the microbiology lab of the University Hospital, and INGEN, UANL. Disposal of organic substances produced during the chromatographic analysis was processed according to the instructions of the department of Medical Toxicology of Cagliari University, Italy.

CHAPTER V

5.1. RESULTS AND DISCUSSION

5.1.1. Plant material and extraction

The sequential maceration of the grounded stems (756 g) yields 3.5 g (0.423%), 24 g (3.201%) and 8.24 g (1.084%) of dry extracts of hexane, $CHCl_3$-MeOH (1:1) and aqueous solvents, respectively.

5.1.2. Structural elucidation of solids from the hexane extract

5.1.2.1. Physic and spectral data of solid 1 (CIR1)

White waxy solid, melting point (MP) 60-62 °C. The ^{1}H NMR of CIR1 (Figure 1) shows the presence of a triplet at δ 0.88 (t, J = 6.8 Hz, H1, H31) integrating for six methyl protons and a singlet of methylenes at δ 1.25 (H2 to H30) integrating for 58 protons which suggest a long chain linear alkane. The ^{13}C NMR spectra (Figure 2) shows five-carbon signals at δ 31.95 (C3, C29), 29.72 (C5 to C27), 29.38 (C4, C28), 22.71 (C2, C30), 14.12 (C1, C31), which corresponds to the observed five resonances for a hydrocarbon chain of $(\alpha CH_3)_2(\beta CH_2)_2(\gamma CH_2)_2(\delta CH_2)_2(\varepsilon CH_2)_2$. The terminal αCH_3 groups, and four CH_2 groups (β, γ, δ, and ε), at 14.3 ppm (αCH_3), 23.0 ppm (βCH_2), 32.2 ppm (γCH_2), 29.7 ppm (δCH_2) and 30.0 ppm (εCH_2) [158]. Thus, CIR1 was assigned as hentriacontane $C_{31}H_{64}$, MW = 436.85 g/mol, according to its NMR signals and previous reports [159].

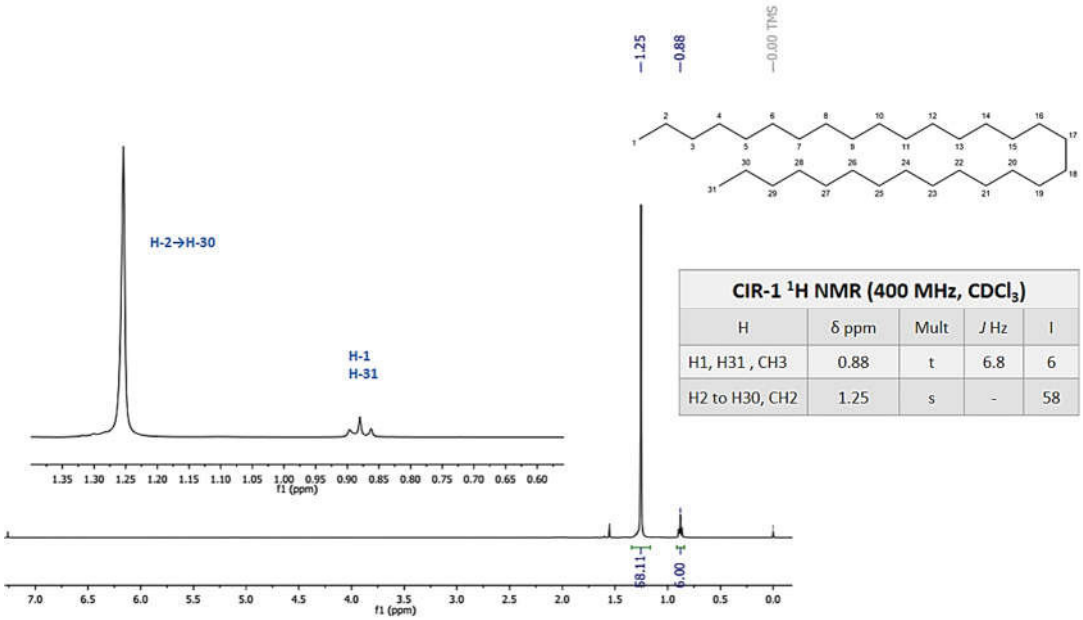

CIR-1 ^{1}H NMR (400 MHz, $CDCl_3$)				
H	δ ppm	Mult	J Hz	I
H1, H31 , CH3	0.88	t	6.8	6
H2 to H30, CH2	1.25	s	-	58

Figure 1. ^{1}H NMR (400 MHz, $CDCl_3$) spectra of CIR1.

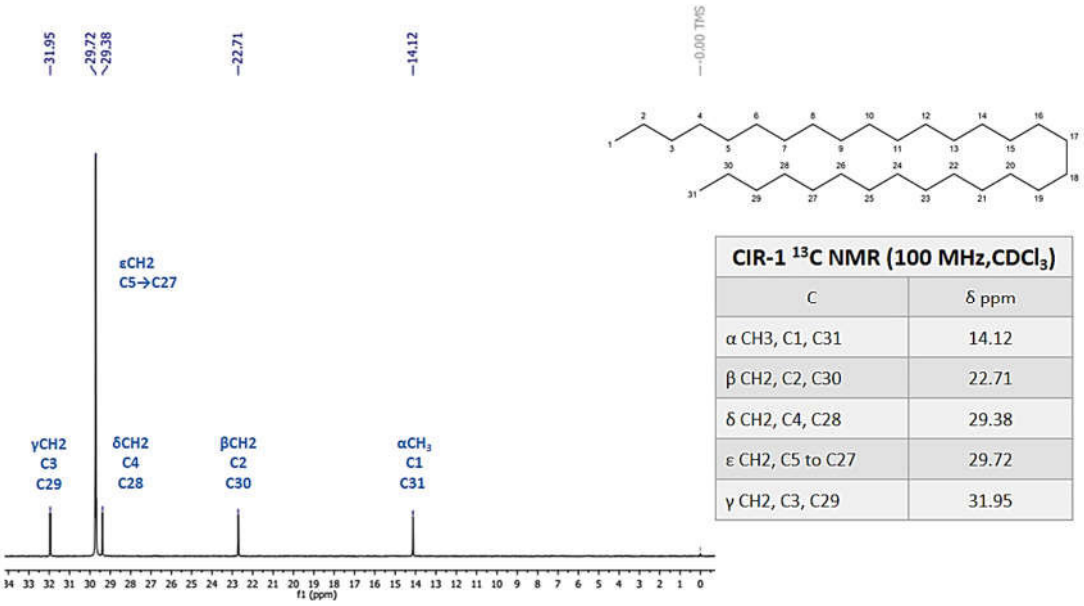

CIR-1 ^{13}C NMR (100 MHz,$CDCl_3$)	
C	δ ppm
α CH3, C1, C31	14.12
β CH2, C2, C30	22.71
δ CH2, C4, C28	29.38
ε CH2, C5 to C27	29.72
γ CH2, C3, C29	31.95

Figure 2. ^{13}C NMR (100 MHz, $CDCl_3$) spectra of CIR1.

The solid 1 was subsequently analyzed by GC-MS and its chromatogram (Figure 3) showed that it was a mixture of long-chain alkanes, and squalene. The retention times, abundance, molecular weight, and molecular formula of the identified compounds are summarized in Table 8.

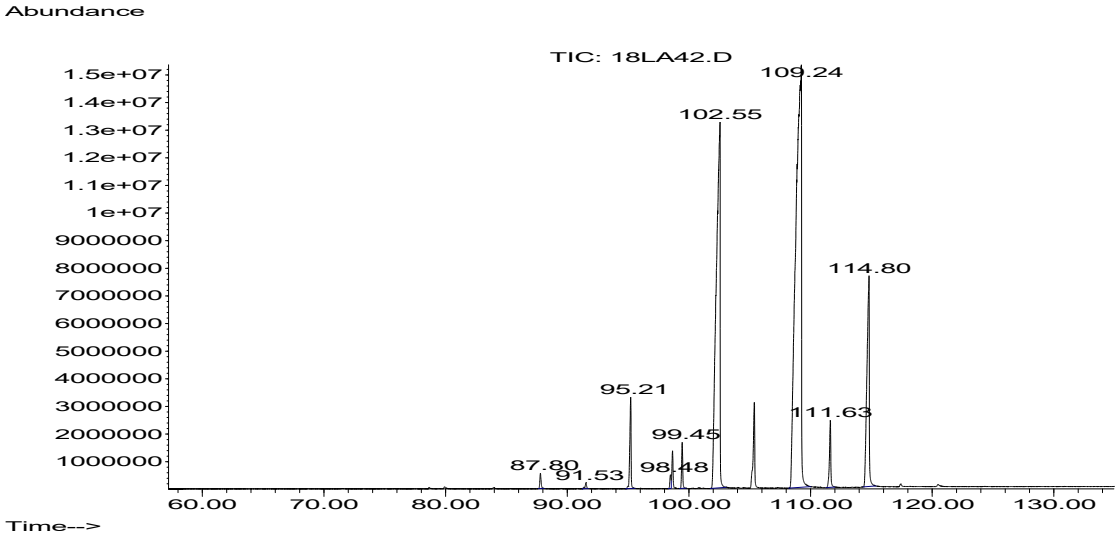

Figure 3. GC-MS chromatogram of CIR1.

90% of the identified compounds corresponds with long-chain alkanes. The GC-MS analysis confirmed the presence of hentriacontane as the most abundant constituent in CIR1. The hentriacontane is a common constituent of plant extracts identified by hyphenated gas chromatography-mass spectrometry [160].

Table 8. GC-MS analysis of CIR1

Peak	RT (min)	Abundance (%)	Compound	Molecular weight	Molecular formula
1	3.289	0.95	Pentacosane	352.6804	$C_{25}H_{52}$
2	87.794	0.41	Pentatriacontane	492.9462	$C_{35}H_{72}$
3	91.532	0.19	Octacosane	394.7601	$C_{28}H_{58}$
4	95.217	2.52	Cyclooctacosane	392.7442	$C_{28}H_{56}$
5	98.481	0.33	Squalene	410.7180	$C_{30}H_{50}$
6	99.454	1.09	Nonacosane	408.7867	$C_{29}H_{60}$
7	102.547	30.26	Dotriacontane	450.8664	$C_{32}H_{66}$
8	109.241	52.35	Hentriacontane	436.8399	$C_{31}H_{64}$
9	114.804	10.75	Triacontane	422.8133	$C_{30}H_{62}$

The EI mass spectrum of hentriacontane is typical for linear saturated hydrocarbons (figure 4). It shows smooth transitions of carbenium ion signal intensities from peak to peak, starting from propyl [$C_3H_7^+$] m/z 43, then intensities rise to butyl [$C_4H_9^+$] m/z 57, then falls notably fall to the molecular ion peak at m/z 436 [$M^{+\cdot}$], in line with the reported

spectrum [159, 161]. GC-EIMS m/z (rel. int.) = 436, $C_{31}H_{64}$, M^+ (15), 99 (27), 97 (35), 85 (50), 71 (65), 57 (100), 43 (70).

Figure 4. Mass spectrum of Hentriacontane

5.1.2.2. Physic and spectral data of solid 2 (CIR2)

White solid of mp 74-75 °C. The ^{1}H NMR of CIR2 exhibited the existence of one triplet at δ 0.88 (t, J = 6.6 Hz, H1, H48) integrating for six methyl protons and a singlet of methylenes at δ 1.25 (H2 to H47) integrating for 92 protons, suggesting the presence of a long-chain linear alkane (Figure 5).

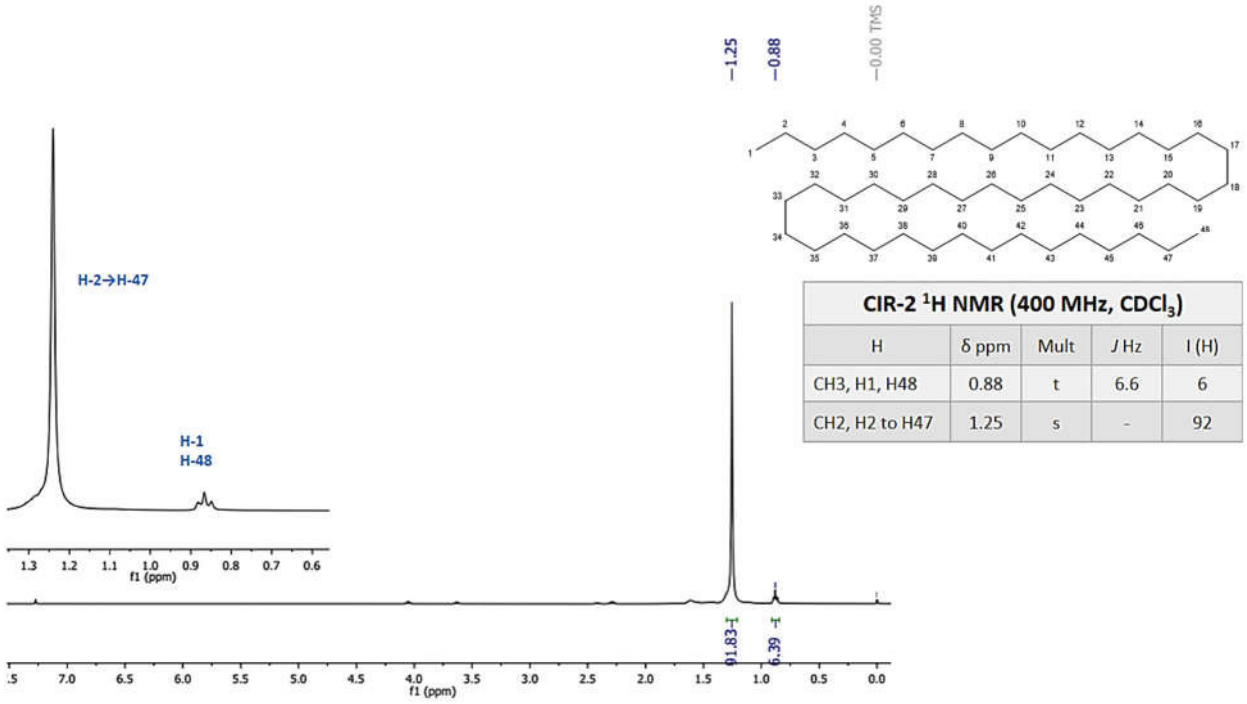

CIR-2 ^{1}H NMR (400 MHz, $CDCl_3$)				
H	δ ppm	Mult	*J* Hz	I (H)
CH3, H1, H48	0.88	t	6.6	6
CH2, H2 to H47	1.25	s	-	92

Figure 5. ^{1}H NMR (400 MHz, $CDCl_3$) spectra of CIR2.

In the ^{13}C NMR spectra are recognized signals of a long hydrocarbon chain, the five-carbon signals at δ 31.95 (C3, C46), 29.72 (C5 to C43), 29.38 (C4, C45), 22.71 (C2, C47), 14.12 (C1, C48) (Figure 6). Based on NMR spectral data the proposed structure for solid 2 has been characterized as octatetracontane, $C_{48}H_{98}$ [162] in mixture with other minority compounds.

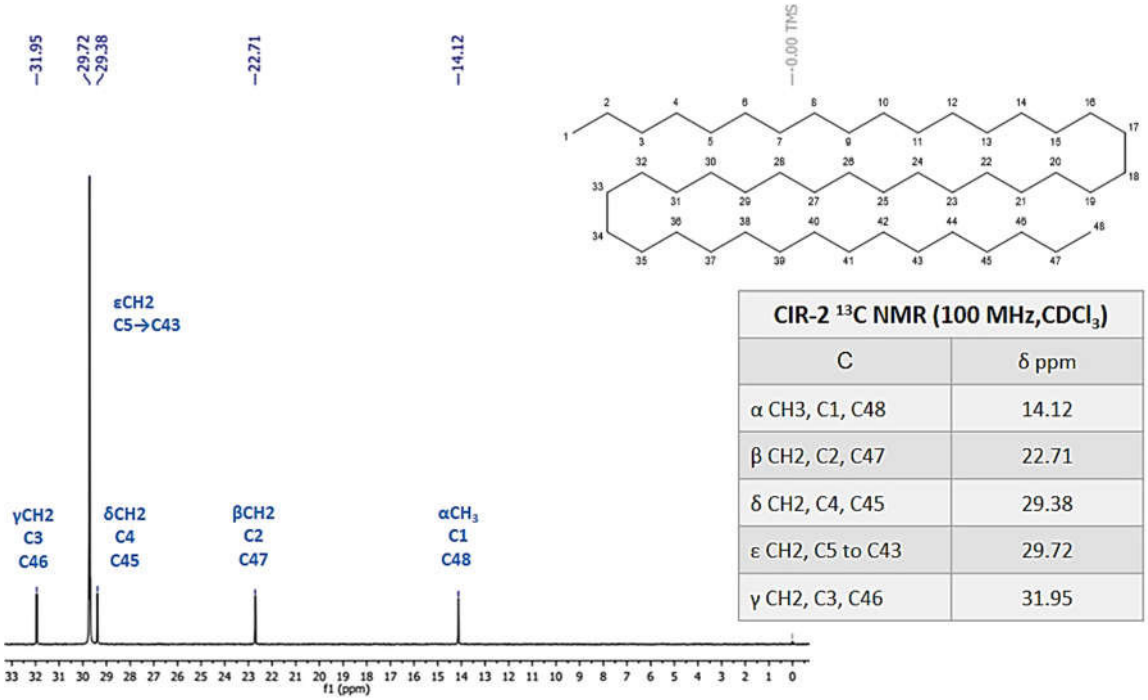

CIR-2 ^{13}C NMR (100 MHz,$CDCl_3$)	
C	δ ppm
α CH3, C1, C48	14.12
β CH2, C2, C47	22.71
δ CH2, C4, C45	29.38
ε CH2, C5 to C43	29.72
γ CH2, C3, C46	31.95

Figure 6. ^{13}C NMR (100 MHz, $CDCl_3$) spectra of CIR2.

The results of the GC-MS analysis support the presence of long-chain aliphatic compounds and allowed the identification of other components in the solid 2. The GC-MS chromatogram is presented in Figure 7, the retention times, abundance, molecular weight, and molecular formula of the ten identified molecules were summarized in Table 9. The solid 2 resulted in a mixture of hentriacontane, octacosane, tricosane, heneicosane, nonacosane, heptacosane, the triterpene squalene, and other unknown compounds.

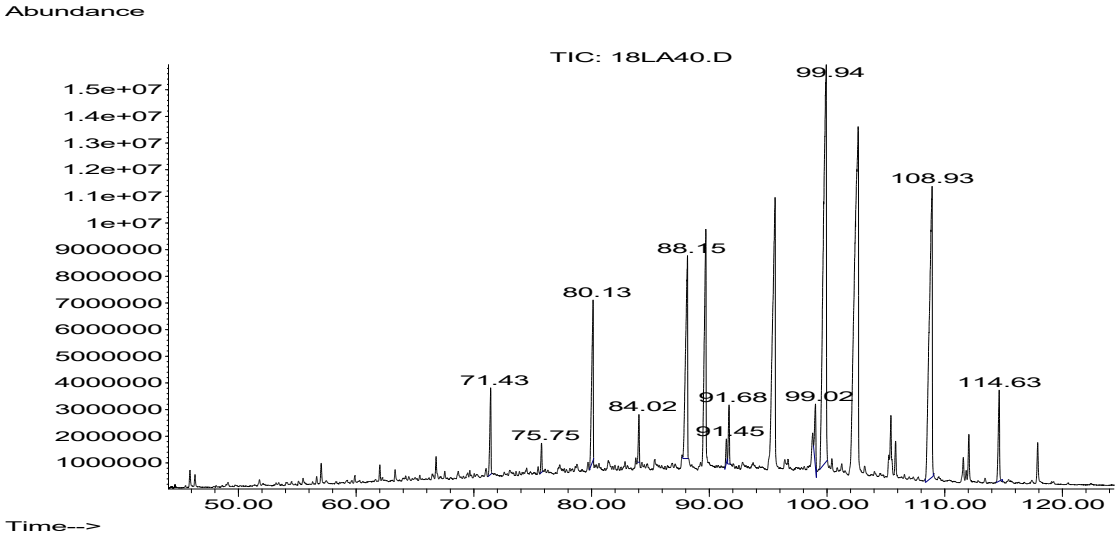

Figure 7. GC-MS chromatogram of CIR2.

Approximately 60% of the identified compounds correspond to alkanes and hentriacontane was the majoritarian long-chain aliphatic compound present in the solid. The mass spectrum of squalene, the next most abundant identified compound in solid 2 is showed in figure 8.

Table 9. GC-MS analysis of CIR2

Peak	RT (min)	Abundance (%)	Compound	Molecular weight	Molecular formula
1	71.425	3.11	Heneicosane	296.5741	$C_{21}H_{44}$
2	75.754	0.87	Docosane	310.6006	$C_{22}H_{46}$
3	80.129	7.92	Tricosane	324.6272	$C_{23}H_{48}$
4	84.017	1.39	Pentatriacontane	492.9462	$C_{35}H_{72}$
5	88.149	12.97	Octacosane	394.7601	$C_{28}H_{58}$
6	91.447	0.78	1-Hexacosene	364.6911	$C_{26}H_{52}$
7	91.677	1.95	Heptacosane	380.7335	$C_{27}H_{56}$
8	99.020	2.41	Nonacosane	408.7867	$C_{29}H_{60}$
9	99.940	37.76	Squalene	410.7180	$C_{30}H_{50}$
10	108.932	27.11	Hentriacontane	436.8399	$C_{31}H_{64}$

The EI-MS spectrum of squalene exhibits a fragmentation pattern typical of cleavage of isoprene units $[C_5H_9]^+$ m/z 69 , in consistency with literature [163]. GC-EIMS: m/z (rel. int.)= 410(3),$C_{30}H_{50}$ $[M^+]$, 137(40), 121(17), 95(17), 81(100), 69(90), 57(19), 55(17) [163].

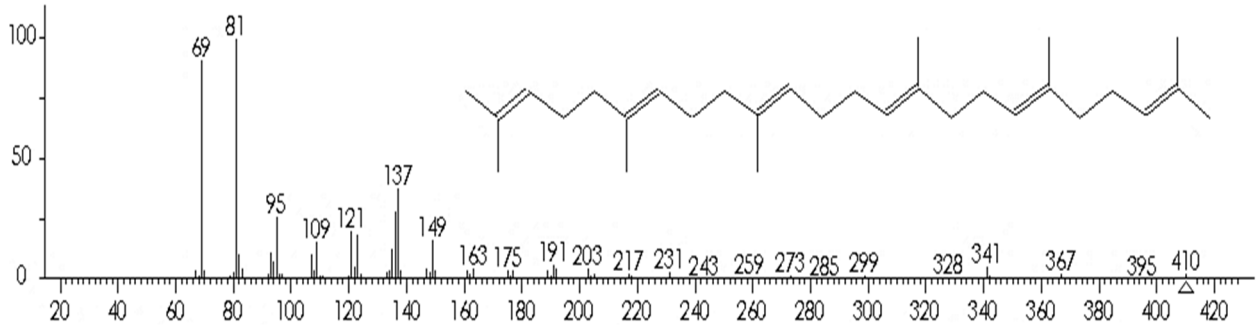

Figure 8. Mass spectrum of squalene.

5.1.2.3. Physic and spectral data of solid 3 (CIR3)

White waxy solid of mp 64-65 °C. The NMR data of CIR3 (Figure 9) shows a triplet at δ 0.88 (t, J = 6.7 H, H28) attributed to three methyl protons, and at 1.25 (H4 to H27) a singlet integrating for 48 protons, which corresponds to 24 units of methylenes, downfield at 1.63 (H3) a multiplet integrating two protons corresponding to a methylene protons beta, in respect to a carbonyl, and at 2.35 (t, J = 7.5 Hz, H2) a triplet integrating for two protons corresponding to an alpha carbonyl methylene protons. The ^{13}C NMR gave signals at δ 178.47 that corresponds to a carboxylic carbon at C1, along with the signals at 33.79 (C2) of the alpha carbonyl methylene, and 31.94 (C26), 29.69 (C4 to C25), 24.72 (C23), 22.70 (C27) and 14.12 (C1). (Figure 10). Overall, the spectral data and the literature comparison suggest the structure of the octacosanoic acid $C_{28}H_{56}O_2$; MW = 424.75 g/mol [164].

The solid 3 was also subjected to GC-MS analysis that revealed four majoritarian compounds from which two were identified. The chromatogram is shown in figure 11 and table 10 summarizes the retention times, abundance, molecular weight, and molecular formula of the identified compounds.

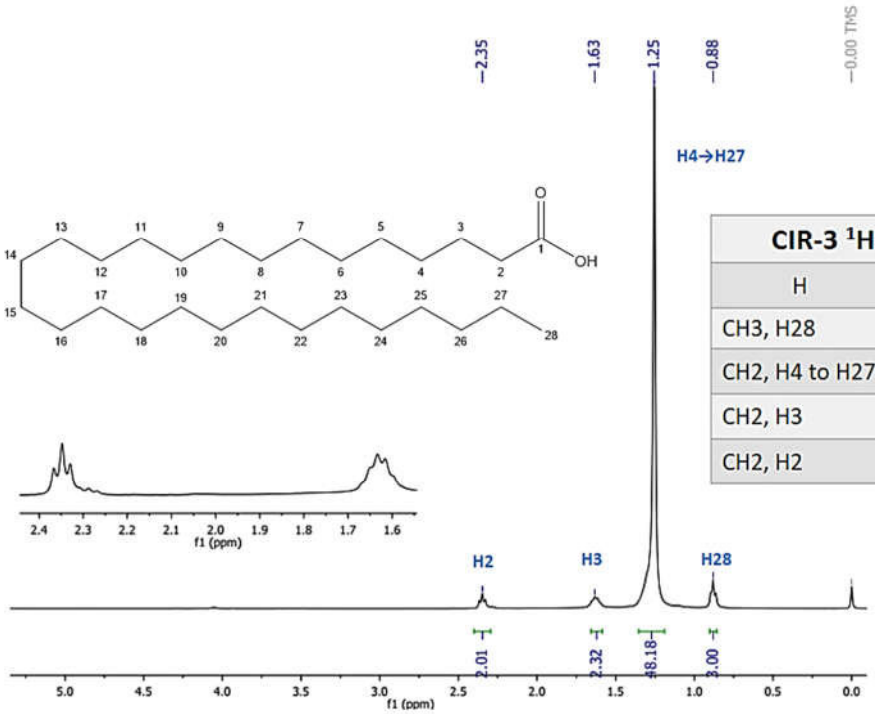

CIR-3 ^{1}H NMR (400 MHz, $CDCl_3$)				
H	δ ppm	Mult	*J* Hz	I (H)
CH3, H28	0.88	t	6.7	3
CH2, H4 to H27	1.25	s	-	48
CH2, H3	1.63	m	-	2
CH2, H2	2.35	t	7.5	2

Figure 9. ^{1}H NMR (400 MHz, $CDCl_3$) spectra of CIR3.

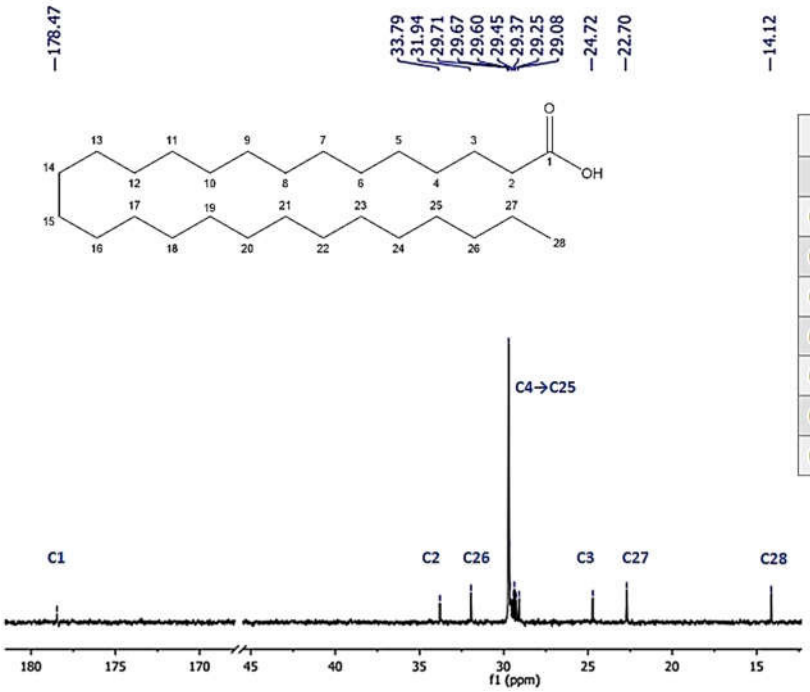

CIR-3 ^{13}C NMR (100 MHz,$CDCl_3$)	
C	δ ppm
CH3, C28	14.12
CH2, C27	22.70
CH2, C3	24.72
CH2, C4 to C26	29.69
CH2, C26	31.94
CH2, C2	33.79
C=O, C1	178.47

Figure 10. ^{13}C NMR (100 MHz, $CDCl_3$) spectra of CIR3.

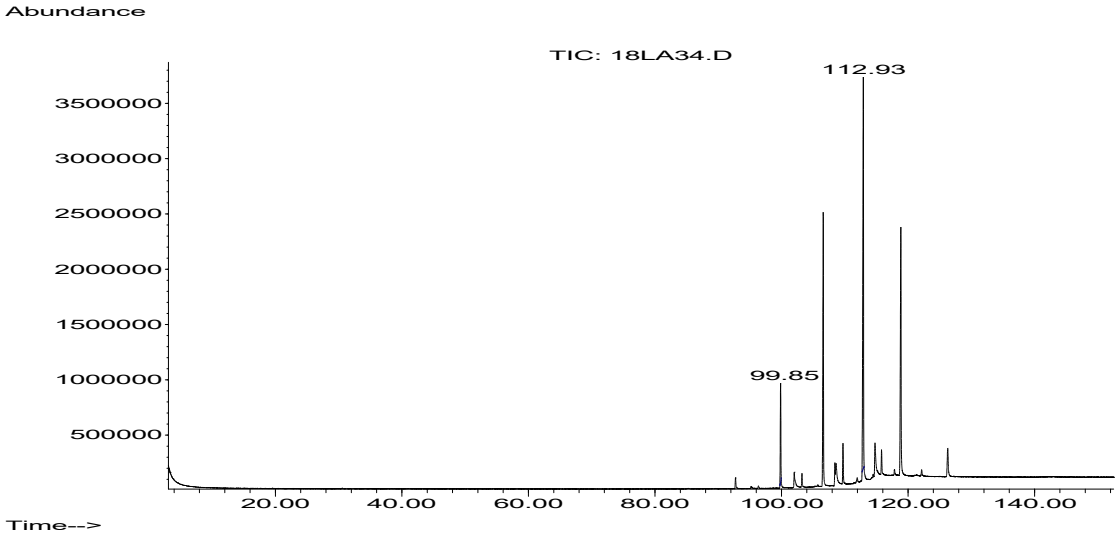

Figure 11. GC-MS chromatogram of CIR3.

The major compound present in solid 3 corresponds to 1,30-triacontanediol, followed by the 2-heptadecyloxirane and other unidentified constituents. Both compounds commonly identified by GCMS analysis of plant extracts [160, 165]. The mass spectrum of 1,30 triacontanediol corresponds with the reported in literature [166] (Figure 12).

Table 10. GC-MS analysis of CIR3

Peak	RT (min)	Abundance (%)	Compound	Molecular weight	Molecular formula
1	99.854	15.32	2-heptadecyloxirane	282.5110	$C_{19}H_{38}O$
2	112.932	84.69	1,30-Triacontanediol	454.8120	$C_{30}H_{62}O_2$

The spectrum lacks the molecular ion peak (typical of aliphatic alcohols). Instead, the [M-36] ion, from the loss of two molecules of water is observed at m/z 418. GC-EIMS: m/z (rel. int.)= 454 (0), $C_{30}H_{62}O_2$ [M^+], 418(15), 96 (68), 82 (90), 69 (74), 55 (100), 43 (70).

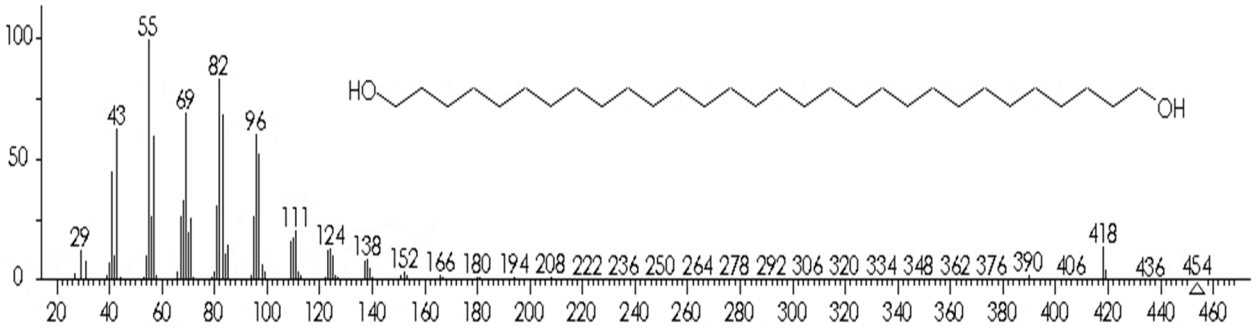

Figure 12. Mass spectrum of 1,30 triacontanediol.

5.1.2.4. Physic and spectral data of solid 4 (CIR4)

Needle shape crystals, mp 135-136 °C. The ^{1}H NMR shows six singlets methyl signals that appeared at δ 1.01 (s, 3H, H19), 0.92 (d, J= 6.5 Hz, 3H, H21), 0.86 (t, J = 7.3 Hz, 3H, H29), 0.84 (d, J = 7.2 Hz, 3H, H26), 0.81 (d, J = 7.2 Hz, 3H, H27), and 0.68 (s, 3H, H18). The spectrum further revealed the presence of a signal at δ 5.53 (psd, J = 4.7Hz, 1H, H6), and δ 3.53 (m, 1H, H3) and less intense signals at δ 5.15 (dd, J = 9, 15 Hz), and 5.01 (dd, J = 9, 15 Hz). Overall, most of the CIR4 ^{1}H NMR spectrum is consistent to the reported literature values for β-sitosterol [167] (Figure 13). The ^{13}C NMR spectra of solid 4 showed twenty-nine carbon signals, including six methyls, two olefinic carbons, and the carbon adjacent to the hydroxyl group. The signals were assigned accordingly to the reported spectra for β-sitosterol [168]; at δ 140.78 (C5), at 121.73 (C6), and 71.83 (C3) for the ring motifs. The methyls were assigned as: at δ 21.10 (C26), 19.83 (C19), 19.41 (C27), 19.05 (C21), 12.00 (C29) and 11.87 (C18) (Figure 14). Thus, based on the spectroscopic data of CIR4 and literature comparison the solid four appears to be composed mainly by β-sitosterol, and the presence of signals at δ 5 in the ^{1}H NMR spectrum indicates a mixture with stigmasterol (the double bond between C22 and C23) [167 169].

Consistent with the spectral data, the GC-MS analysis revealed that solid 4 was a mixture composed mainly of β-sitosterol (73%), stigmasterol (17%) and campesterol (9%). The GC-MS chromatogram of CIR4 is presented in Figure 15. The compound assignment was based on their mass spectra, compared with the NIST database[166]. Table 11 summarizes the retention times, abundance, molecular weight, and molecular formula of the identified compounds.

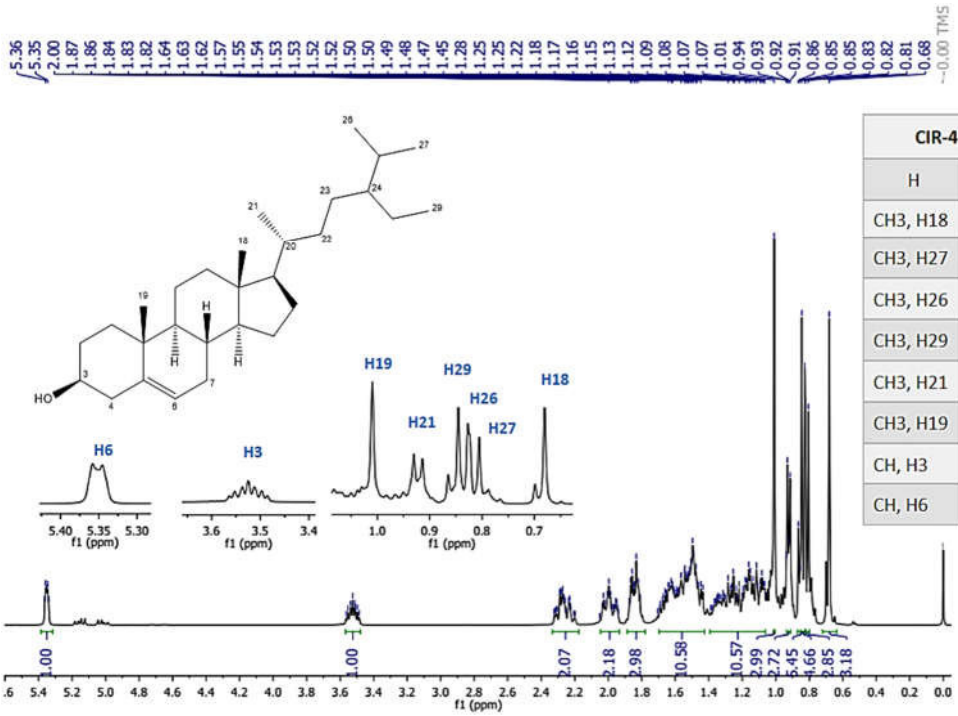

CIR-4 ^{1}H NMR (400 MHz, $CDCl_3$)				
H	δ ppm	Mult	*J* (Hz)	I
CH3, H18	0.68	s	-	3
CH3, H27	0.81	d	7.2	3
CH3, H26	0.84	d	7.2	3
CH3, H29	0.86	t	7.3	3
CH3, H21	0.92	d	6.5	3
CH3, H19	1.01	s	-	3
CH, H3	3.53	m	-	1
CH, H6	5.53	psd	4.7	1

Figure 13. ^{1}H NMR (400 MHz, $CDCl_3$) spectra of CIR4.

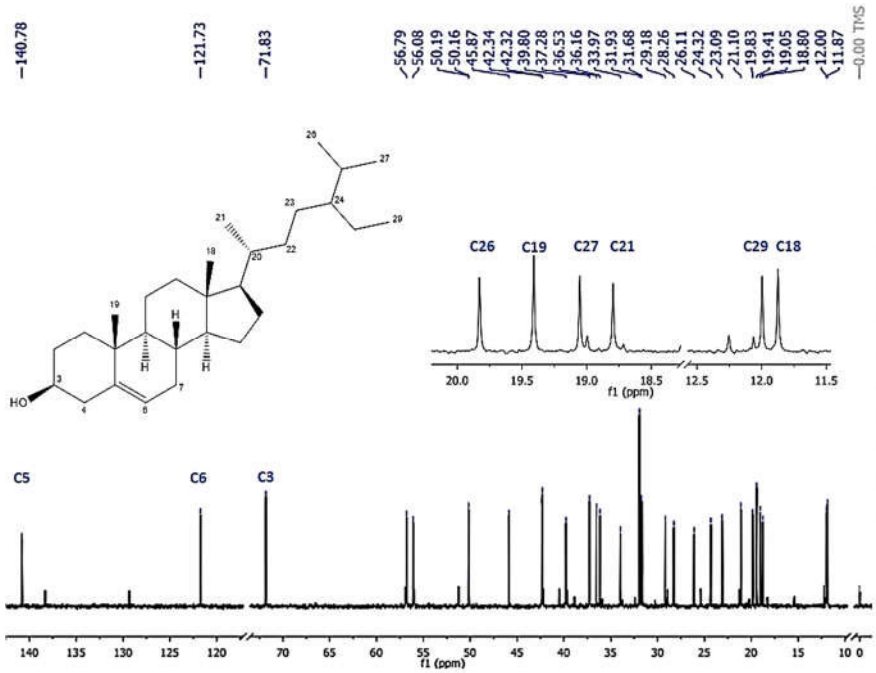

CIR-4 ^{13}C NMR (100 MHz,$CDCl_3$)	
C	δ ppm
CH3, C18	11.87
CH3, C29	12.00
CH3, C21	19.05
CH3, C27	19.41
CH3, C19	19.83
CH3, C26	21.10
CH, C3	71.83
CH, C6	121.73
C, C5	140.78

Figure 14 .^{13}C NMR (100 MHz, $CDCl_3$) spectra of CIR4.

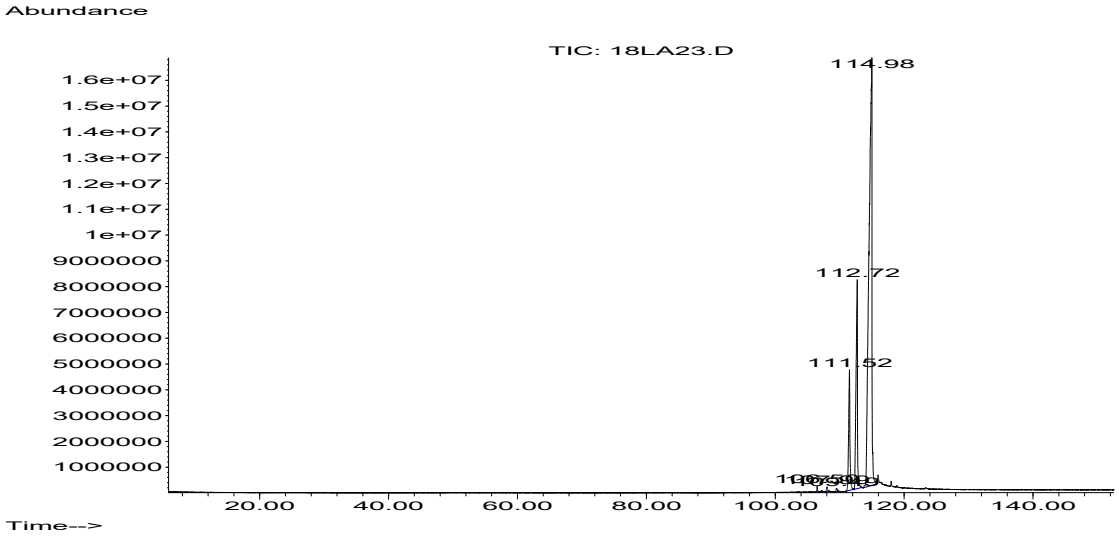

Figure 15. GC-MS chromatogram of CIR4.

The mass spectrum of β-sitosterol is presented in figure 16. The parent molecular ion peak at m/z 414 corresponds with the molecular formula $C_{29}H_{50}O$ [168] and the fragmentation pattern that is characteristic for sitosterols [169].

Table 11. GC-MS analysis of solid 4

Peak	RT (min)	Abundance (%)	Compound	Molecular weight	Molecular formula
1	106.495	0.51	5α-Cholest-5-en-3-β-ol	386.3548	$C_{27}H_{46}O$
2	109.497	0.22	(22E)-Ergosta-5,22-dién-3-ol	398.6642	$C_{28}H_{46}O$
3	111.514	9.17	Campesterol	400.6801	$C_{28}H_{48}O$
4	112.722	17.09	Stigmasta-5,22-dien-3-ol	412.6908	$C_{29}H_{48}O$
5	114.982	73.01	β-Sitosterol	414.7067	$C_{29}H_{50}O$

It shows a peak at m/z 396 resulted from the loss of water molecule from the molecular ion which will further dealkylate to yield peak at m/z 381. Fragments at m/z 273 for fragmentation of C17-C20 cleavage [M-side chain]+, the dehydration of m/z 273 fragment will yield m/z 255 and the peak 231 comes from [273-42 (ring D)]+, 161 [273-70 (ring C)]+, 107 [161-54 (ring B)]+, 92 [107-15 (CH_3)]+ [168].GC-EIMS m/z (rel. int.) = 414, $C_{29}H_{50}O$, M+(40), 396 (20), 381 (14), 329 (18), 303 (25), 255 (18), 213 (23), 145 (30), 107 (47), 95 (48), 81 (50), 43 (100).

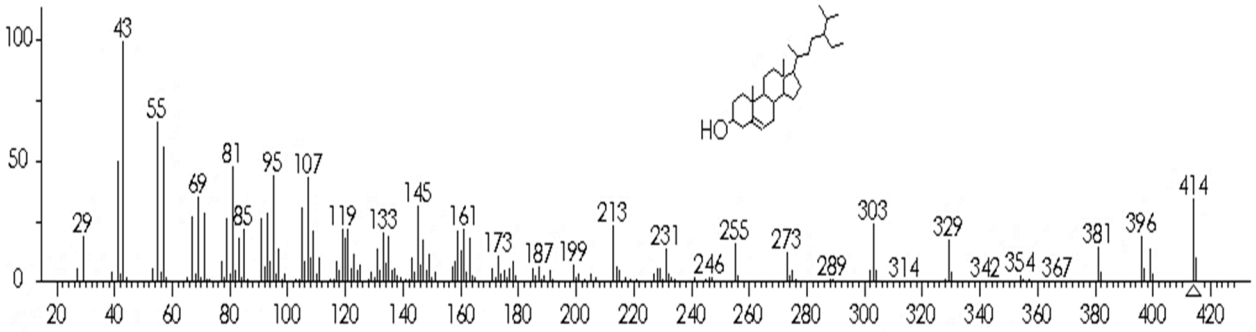

Figure 16. Mass spectra of β-Sitosterol.

5.1.2.5. Physic and spectral data of solid 5 (CIR5)

White solid of mp 62-63 °C. CIR5 ^{1}H NMR had peaks characteristics of aliphatic esters isolated from plant apolar extracts [170]. The spectrum shows the presence of two triplets integrating for two protons each, at δ 4.05 (t, J= 6.7 Hz, H25), and 2.29 (t, J = 7.5 Hz, H2), corresponding with methylene protons adjacent to the carbonyl group of the ester function, and a multiplet at δ 1.60 (H3, H26) integrating for 4 protons corresponding for a couple of methylenes beta position relative to the ester, a singlet at 1.25 (H4 to 23, and H27 to H45) integrating for 80 protons corresponding to a long methylene chain, and a triplet at δ 0.88 (t, J = 6.7 Hz, 6H) for six methyl protons (H24, H47) (Figure 17). The ^{13}C NMR shows the characteristic carbonyl ester at δ 174.04 (C1), and the carbon alpha in respect to the oxygen of the ester at δ 64.41 (C25), subsequently appear a signal of a carbon alpha to the carbonyl at δ 34.44 (C2), and a signal at 31.94 (C22, C45) corresponding to the gamma carbons respect to the terminal methyls, then, appears a signal of a carbon chain at 29.71 (C27 to C44, and C27 to C21. After the methylene chain appears at 25.95 (C26), 25.05 (C3), 22.70 (C46, C23), and at 14.12 (C24, C47) (Figure 18). NMR spectral data suggest the presence of a long chain saturated ester [170], the trycosyl tetracosanoate, with a molecular formula of $C_{47}H_{94}O_2$; MW = 690 g/mol.

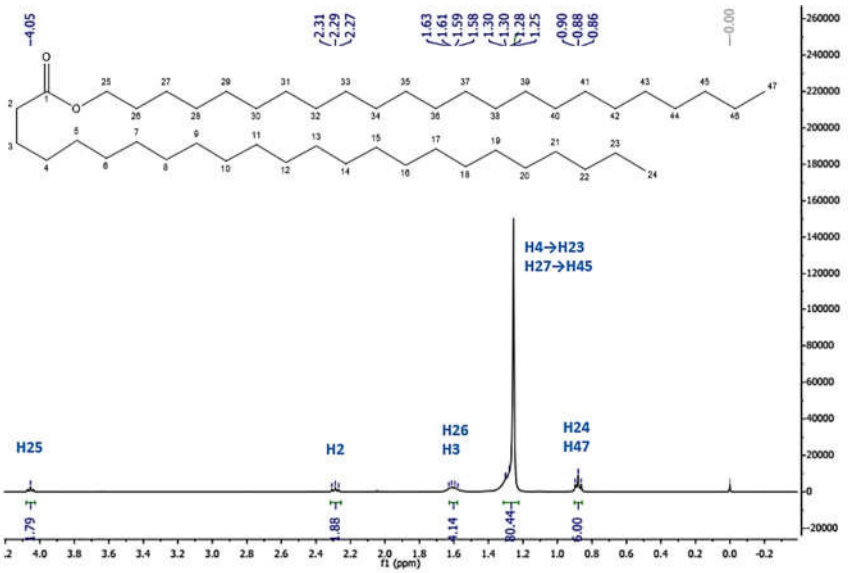

CIR-5 ^{1}H NMR (400 MHz, $CDCl_3$)				
H	δ ppm	Mult	*J* Hz	I
CH3, H24, H47	0.88	t	6.7	6
CH2, H4 to H23 H27 to H45	1.25	s	-	80
CH2, H3, H26	1.60	m	-	4
CH2, H2	2.29	t	7.5	2
CH2, H25	4.05	t	6.7	2

Figure 17. ^{1}H NMR (400MHz, $CDCl_3$) spectra of CIR5.

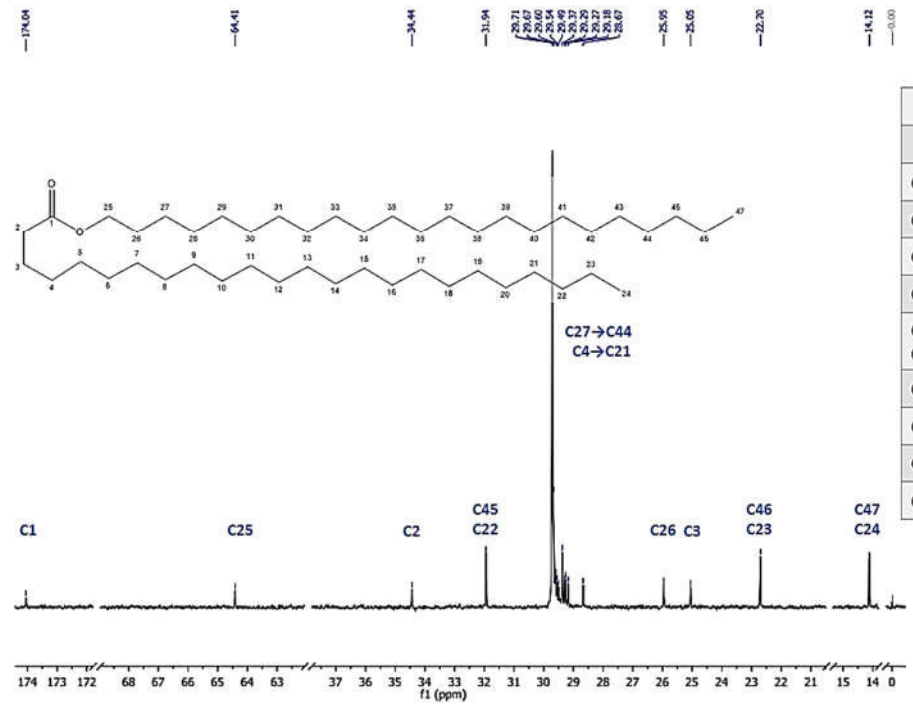

CIR-5 ^{13}C NMR (100 MHz,$CDCl_3$)	
C	δ ppm
CH3, C24, C47	14.12
CH2, C46, C23	22.70
CH2, C3	25.05
CH2, C26	25.95
CH2, C27 to C44 CH2, C4 to C21	29.71
CH2, C22, C45	31.94
CH2, C2	34.44
CH2, C25	64.41
C=O, C1	174.04

Figure 18.^{13}C NMR (100MHz, $CDCl_3$) spectra of CIR5.

The GC-MS analysis of CIR5 revealed a mixture of fatty alcohols, alkanes, and other unidentified compounds. The chromatogram of solid 5 is reported in Figure 19.

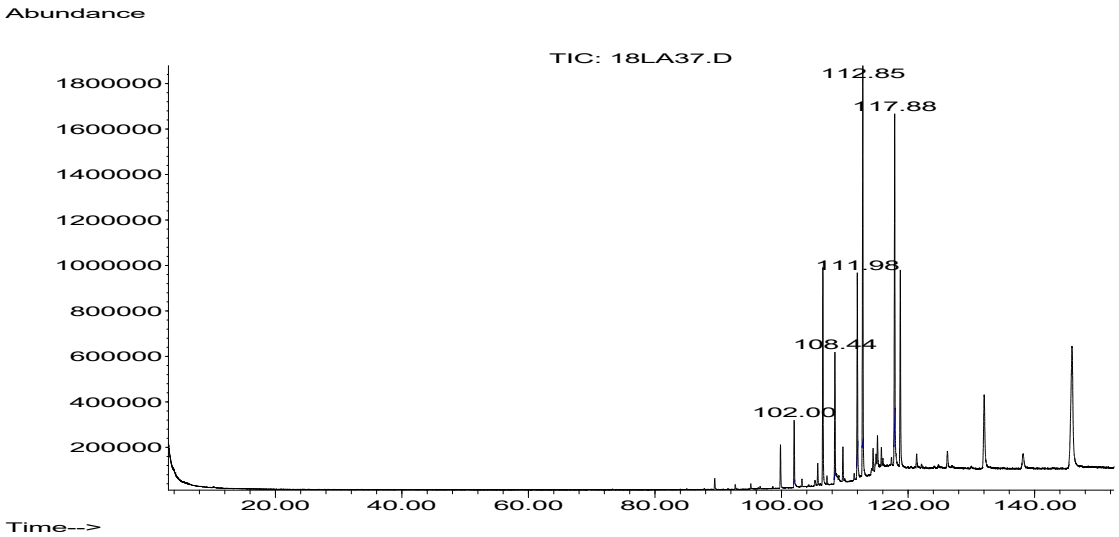

Figure 19. GC-MS chromatogram of CIR5

Based on their mass spectra, and comparison with the NIST database five compounds were identified as major constituents of CIR5, the 1,30-triacontanediol, 1-triacontanol, cyclooctacosane, dotriacontane, and nonacosane. Those constituents are usually identified by GCMS analysis of plant extracts [160] The retention time, abundance, molecular weight molecular formula is presented in Table 12.

Table 12. GC-MS analysis of solid 5

Peak	RT (min)	Abundance (%)	Compound	Molecular weight	Molecular formula
1	101.996	5.78	Nonacosane	408.7867	$C_{29}H_{60}$
2	108.433	11.62	Dotriacontane	450.8664	$C_{32}H_{66}$
3	111.980	16.47	Cyclooctacosane	392.7442	$C_{28}H_{56}$
4	112.847	36.34	1,30-Triacontanediol	454.8120	$C_{30}H_{62}O_2$
5	117.885	29.80	1-Triacontanol	438.8127	$C_{30}H_{62}O$

The mass spectrum of 1-triacontanol is typical of aliphatic alcohols with an absence of molecular ion peak, instead, the [M-18] ion (loss of water) is observed at m/z 392 [166]. GC-EIMS: m/z (rel. int.) = 438(0), $C_{30}H_{62}O$ [M^+], 420(25), 392(3), 125(25), 97(70), 83(70), 57(100). (Figure 20).

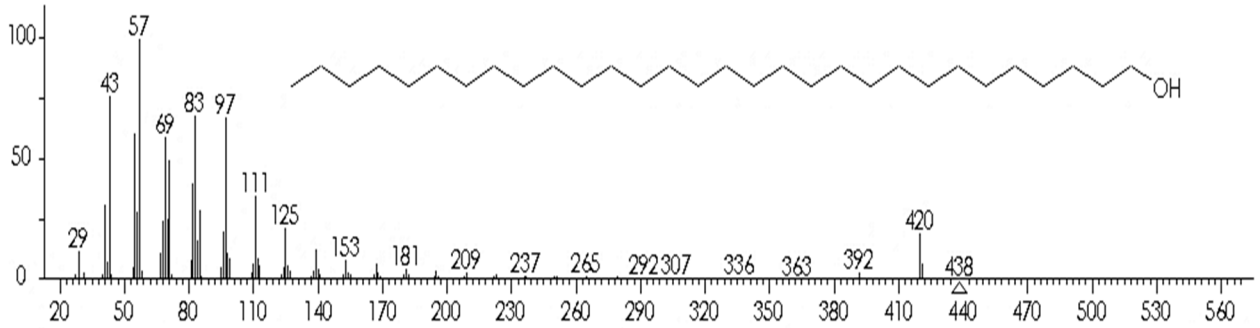

Figure 20. Mass spectra of 1-triacontanol.

5.1.2.6. Isolation of compounds from hexane extract of *Cissus* plants.

The most abundant compounds present in the solids according to NMR signals, correspond with the hentriacontane and octatetracontane, which are unsaturated linear hydrocarbons present in dominant proportions in plant waxes [162, 171]. The octacosanoic acid is a long-chain saturated fatty that is also a common constituent of plant waxes [172]. In the case of the long chain saturated ester suggested for the NMR spectral data as trycosyl tetracosanoate, there are no previous reports, however, similar aliphatic esters have been characterized in the lipid constituents of plants [170]. Moreover, the chain length of wax esters in plants range from C32 to C64, which is also consistent with the chemical composition of plant cuticular waxes [173]. The mixture of sterols such as the present in solid 4 are also constituents in plant cuticular waxes [173]. Furthermore, similar compounds have been isolated from the hexane extract of *C. quadrangularis*. For example, the heptacosane, the pentatriacontane, the isopentacosanoic acid, the β-sitosterol, and the eicosyl eicosanoate [149, 174]. Overall, the GC-MS and NMR spectroscopy of solids from the hexane extract of *C. trifoliata* corresponded with the main constituents of plant cuticular waxes (mixtures of alkanes, alcohols, fatty acids, esters, triterpenes, and sterols) [175]. Accordingly, compounds present in the solids are widely distributed in the plant kingdom [173] and their further purification and biological evaluation were discarded.

5.1.3. GC-MS analysis of hexane extract

The volatile contents of the hexane stem extract of *C. trifoliata* were analyzed by GC-MS. The chromatogram is shown in Figure 21. The name, retention time, abundance, molecular weight, and the molecular formula of the compounds are listed in table 13.

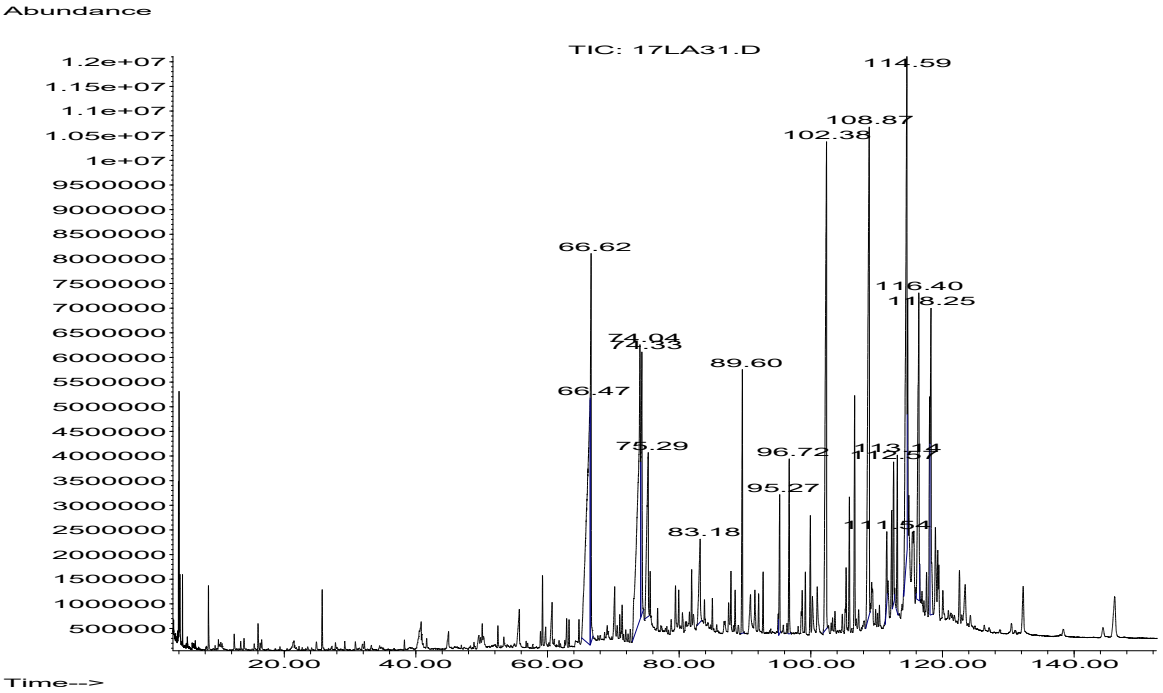

Figure 21. GC-MS chromatogram of hexane stem extract of *C. trifoliata.*

The hexane extract contained sixteen major compounds including alkanes (18.7%), fatty acids (31.3%), terpenes (37.5%), alcohols (6.25%) and esters (6.25%). Overall, the compounds identified in the hexane extract are common constituents of cuticles and membranes in most plants, composed of C16 and C18 esterified fatty acids and waxes (mixtures of homologous series of long-chain aliphatics, such as alkanes, alcohols, aldehydes, fatty acids, and esters, together with variable amounts of triterpenes), glycerolipids, sterols, and sphingolipids [175]. Previous reports of the GC-MS analysis of the hexane extracts of *C. quadrangularis* stems identified as the main components the hexadecanoic acid ethyl ester, the octadecanoic acid ethyl ester and phytol [176]. The alkane

hentriacontane has been previously reported in *C. quadrangularis* stems [177], while the nonacosane in *C. cornifolia* [178]. In agreement, the nonacosane and hentriacontane, are predominant cuticular wax components in plants [179].

Table 13. GC-MS analysis of hexane extract from the stems of *C. trifoliata*

Peak	RT (min)	Abundance (%)	Molecular weight	Molecular formula	Compound
1	66.472	14.39	256.4241	$C_{16}H_{32}O_2$	Hexadecanoic acid
2	66.623	5.35	284.4772	$C_{18}H_{36}O_2$	Hexadecanoic acid ethyl ester
3	74.039	12.60	280.4455	$C_{18}H_{32}O_2$	9Z,12Z-octadecadienoic acid
4	74.328	4.63	282.4614	$C_{18}H_{34}O_2$	9Z-Octadecenoic acid
5	75.294	4.42	284.4772	$C_{18}H_{36}O_2$	Octadecanoic acid
6	83.176	2.01	312.5304	$C_{20}H_{40}O_2$	Eicosanoic acid
7	89.609	1.94	394.7601	$C_{28}H_{58}$	Octacosane
8	95.271	3.15	410.7180	$C_{30}H_{50}$	Squalene
9	102.377	10.45	408.7867	$C_{29}H_{60}$	Nonacosane
10	108.871	12.82	436.8399	$C_{31}H_{64}$	Hentriacontane
11	111.546	1.81	400.6801	$C_{28}H_{48}O$	Campesterol
12	112.571	1.91	412.6908	$C_{29}H_{48}O$	Stigmasterol
13	113.143	1.73	454.4749	$C_{30}H_{62}O_2$	1,30-triacontanediol
14	114.588	11.23	414.7067	$C_{29}H_{50}O$	Beta sitosterol
15	116.401	6.53	426.7174	$C_{30}H_{50}O$	Lupeol
16	118.246	5.03	412.6908	$C_{29}H_{48}O$	Stigmast-4-en-3-one

The hexadecanoic and the octadecanoic acid were also the major fatty acids in the hexane extract from the stems of *C. quadrangularis* [176]. They are structural constituents in the cellular membranes of higher plants [180]. In the case of the n-hexadecanoic acid ethyl ester, it was found as the major constituent of hexane extract from the roots of *C. quadrangularis*

[176]. This is one of the most common esters founded in plant waxes [181]. The eicosanoic acid, is also a major constituent of the hexane extract from the roots in *C. quadrangularis* [176], but in general is a minor constituent of plant cell membranes [181]. The unsaturated fatty acids present in the hexane extract of *C. trifoliata* were the (Z,Z) 9,12-octadiecadienoic acid and the (Z)-9-octadecenoic acid. The former was reported for the first time in the methanolic extract from stems [182] and the other as a major constituent in the hexane extracts from the roots [176] of *C. quadrangularis*. Both fatty acids, the linoleic acid, and the oleic acid play roles in increasing the fluidity of plant membranes [183]. This is the first report of the presence of the alcohol 1,30-triacontanediol in plants from the genus *Cissus*, however, is an alcohol common in the cuticular wax of plants [179] acting as a growth regulator [184]. Among the terpenes identified, the squalene is the simplest and the most abundant in the hexane extract from the stems of *Cissus* plants [116]. Lupeol was the only pentacyclic terpene and was reported as a major constituent in the hexane extract from the stems and roots in *C. quadrangularis* [116, 176]. Its biosynthesis is induced by pathogens and exerts antimicrobial activities [185]. The β-sitosterol, stigmasterol, and campesterol were previously isolated in the hexane extract from the stems of *C. quadrangularis* [116, 176]. In the case of stigmast-4-en-3-one was previously isolated in the ethanolic extract from the stems *C. quadrangularis* [186]. Although all sterols share a structural role in the fluidity of plant membranes [187], changes in plant sterol structure, such as the observed in stigmast-4-en-3-one are associated with infestation with insects, and its biological activity showed to disrupt their metabolism and growth [188].

5.1.4. UPLC-QTOF-MS analysis

5.1.4.1. UPLC-QTOF-MS characterization of the $CHCl_3$-MeOH extract

The total compound chromatogram (TCC) of the $CHCl_3$-MeOH extract of *C. trifoliata* stems is presented in Figure 22. The compounds tentatively identified are summarized in Table 14, with numbers showing the elution order, retention time, the experimental m/z and the molecular formula. All the compounds were characterized based on accurate m/z, the calculation of the molecular formula and data provided by the literature and databases. Eighteen compounds were identified and included simple phenolics (16.6%), fatty acids (22.2%), flavonoids (44.6%), and stilbenes (16.6%).

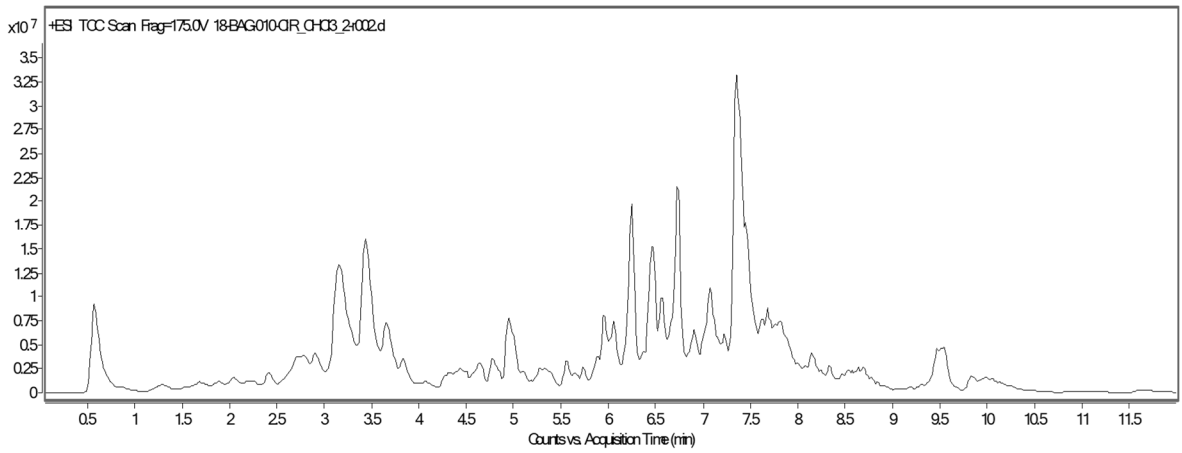

Figure 22. Chromatogram of the UPLC-QTOF-MS analysis of the $CHCl_3$-MeOH stem extract of *C. trifoliata*

Most of the compounds identified by LC-MS were phenolic compounds. The gallic acid derivatives such as the protocatechuic acid, trigallic acid, and methyl digallate are secondary metabolites widely distributed in the plant kingdom. They play a role in the interaction with pathogens [189]. Flavonoids are also widely distributed in plants and were the main chemical class identified. Apigenin, kaempferol and quercetin have been reported on alcoholic extracts from *C. ibuensis* [106], *C. digitate* [190] and *C. quadrangularis* [191].

Table 14. UPLC-QTOF-MS analysis of the $CHCl_3$-MeOH stem extract of *C. trifoliata*

Peak	RT (min)	Experimental m/z $[M-H]^-$	Molecular Formula	Tentatively identified compound
1	0.612	593.1497	$C_{27}H_{30}O_{15}$	Kaempferol-O-α-rhamnosyl-glucopyranoside
2	2.419	625.1436	$C_{27}H_{30}O_{17}$	Myricetin 3-O-rutinoside
3	2.857	507.1147	$C_{23}H_{24}O_{13}$	Syringetin 3-O-galactoside
4	3.226	405.1198	$C_{20}H_{22}O_9$	Piceatannol glucoside
5	3.547	595.1341	$C_{26}H_{28}O_{16}$	Quercetin 3-O-glucosyl-xyloside
6	3.774	310.2052	-	Unknown
7	4.042	315.0717	$C_{13}H_{16}O_9$	Protocatechuic acid hexoside
8	4.807	433.1140	$C_{21}H_{22}O_{10}$	Dihydrokaempferol 3-*O*-rhamnoside
9	5.090	389.1249	$C_{20}H_{22}O_8$	Resveratrol 3-O-glucoside
10	5.813	473.0362	$C_{21}H_{14}O_{13}$	Trigallic acid
11	5.895	431.0939	-	Unknown
12	6.180	335.0403	$C_{15}H_{12}O_9$	Methyl digallate
13	6.423	433.0760	$C_{20}H_{18}O_{11}$	Quercetin arabinoside
14	6.531	336.1840	-	Unknown
15	6.592	615.1869	$C_{34}H_{32}O_{11}$	Pallidol-3-*O*-glucoside
16	6.763	447.0938	$C_{21}H_{20}O_{11}$	Kaempferol 3-O-galactoside
17	7.169	615.0988	$C_{28}H_{24}O_{16}$	Myricitrin O-gallate
18	7.191	297.3810	-	Unknown
19	7.417	253.2161	$C_{16}H_{30}O_2$	Hexadecenoic acid
20	7.534	279.2348	$C_{18}H_{32}O_2$	Octadecadienoic acid
21	7.595	255.2345	$C_{16}H_{32}O_2$	Palmitic acid
22	7.852	283.2649	$C_{18}H_{36}O_2$	Stearic acid
23	8.272	653.2235	-	Unknown
24	9.480	535.1650	-	Unknown

Stilbenes were the second most common class of polyphenolic compounds identified in the stems of *C. trifoliata*. Previously, resveratrol, piceatannol, and pallidol were isolated and characterized in ethanolic extracts from the stems of *C. quadrangularis* [133]. Additionally, stilbene glucosides have been found in *C. repens* [103] and *C. sicyoides* [150].

5.1.4.2. UPLC-QTOF-MS characterization of the aqueous extract

The chromatogram of the aqueous extract of *C. trifoliata* stems is presented in Figure 23. The compounds tentatively identified are summarized in Table 15, showing the elution order, retention time, the experimental m/z and the molecular formula. All the compounds were characterized based on accurate m/z, the calculation of the molecular formula and data provided by the literature and databases, these include flavonoids (83%) and stilbenes (17%).

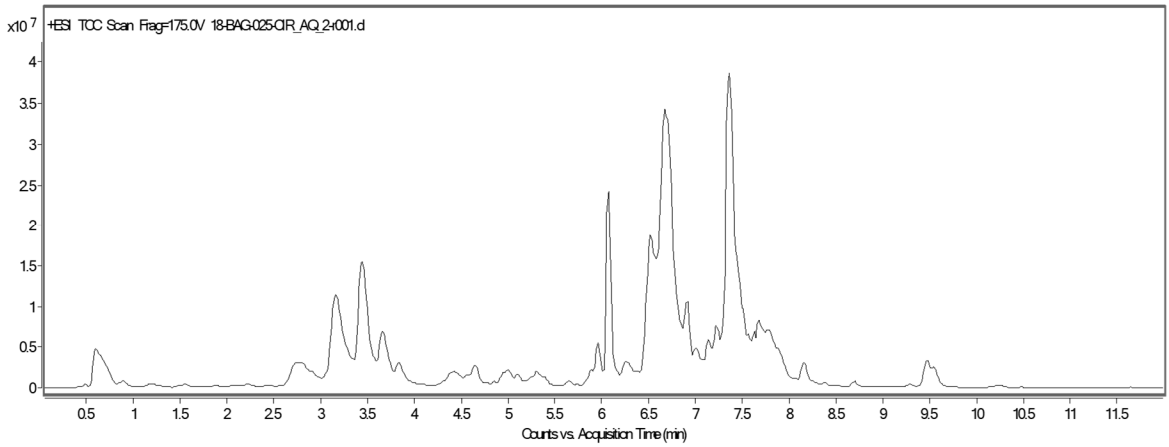

Figure 23. Chromatogram of the UPLC-QTOF-MS analysis of the aqueous stem extract of *C. trifoliata*

The flavonoid glucosides of apigenin, kaempferol, and quercetin were identified in the aqueous extract. Additionally the glucosides of the stilbenes piceatanol and *E*-viniferine were identified. Those resveratrol derivatives were previously reported in *C.*

quadrangularis [133] and *C. repens* [103], whereas the anthocyanidins cyanidin and delphinidin were identified in the methanolic extract of *C. sicyoides* [192].

Table 15. UPLC-QTOF-MS analysis of aqueous stem extract of *C. trifoliata*

Peak	RT (min)	Experimental m/z $[M-H]^-$	Molecular Formula	Tentatively identified compound
1	0.612	592.9786	$C_{27}H_{30}O_{15}$	Apigenin-6,8-di-C- glycoside
2	2.781	563.0218	$C_{26}H_{28}O_{14}$	Kaempferol rhamnosyl xyloside
3	3.180	405.1198	$C_{20}H_{22}O_9$	Piceatannol glucoside
4	3.497	595.1341	$C_{26}H_{28}O_{16}$	Quercetin 3-O-glucosyl-xyloside
5	3.689	609.1451	$C_{27}H_{30}O_{16}$	Kaempferol 3,7-O-diglucoside
6	4.457	374.4914	-	Unknown
7	4.665	593.1497	$C_{27}H_{30}O_{15}$	Kaempferol-O-α-rhamnosyl-glucopyranoside
8	5.078	453.1356	$C_{28}H_{22}O_6$	*E*-viniferin
9	5.395	400.3705	-	Unknown
10	5.973	755.2030	$C_{33}H_{40}O_{20}$	Kaempferol 3-O-glucosyl-rhamnosyl-galactoside
11	6.179	594.1627	-	Unknown
12	6.423	433.0760	$C_{20}H_{18}O_{11}$	Quercetin arabinoside
13	6.779	448.1011	$C_{21}H_{21}O_{11}$	Cyanidin 3-O-galactoside
14	6.954	464.0960	$C_{21}H_{21}O_{12}$	Delphinidin 3-O-glucoside
15	7.384	447.0930	$C_{21}H_{20}O_{11}$	Kaempferol hexoside
16	7.465	576.4380	-	Unknown
17	7.645	302.0060	-	Unknown
18	7.851	426.7290	-	Unknown

Overrall, the phytochemical characterization of the organic and aqueous extracts from the stems of *C. trifoliata* highlighted its taxonomic relationship with Vitaceas. Based on plastid markers *Cissus* plants were founded genetically related to vitis plants [193], additionally, the

metabolomic studies of Vitaceas showed overrepresentation of flavonoid and stilbene metabolites [194]. Moreover, stilbene derivatives accumulate and characterize the lignified stem tissues of Vitaceae [195], which is consistent given the macerated plant material in the present study.

5.1.4.3. Metabolic profile of stems from the medicinal plant *C. trifoliata*

The metabolic profiling of plants refers to the analysis of the plant extracts by hyphenated techniques such as the gas chromatography-mass spectrometry (GC-MS) and liquid chromatography-mass spectrometry (LC-MS) [196]. The plant extracts are very complex matrices and the identification of metabolites requires the use of specific algorithms. Using the accurate mass and the spectral data the molecular formula is recovered. The combined information is then compared with available databases and metabolites are identified [64]. Metabolic profiling has been useful to understand the chemical diversity of a medicinal plant [84, 196]. The information is then used to compare it with taxonomically related studied plants and to infer their bioactivity [82, 83]. Following this approach, forty-six metabolites were identified. The metabolic profile of extracts from the stems of *C. trifoliata* included alcohols, alkanes, esters, fatty acids, terpenes, and phenolic compounds. With the use of MetaboAnalyst tools, the obtained chemical content was processed to perform the PCA, and the metabolic pathway analysis.

5.1.5. Principal Component Analysis

The PCA showed that extracts are three different chemical entities. The polarity of the solvents employed for the extractions may underlie the observed differences [197] (Fig 24).

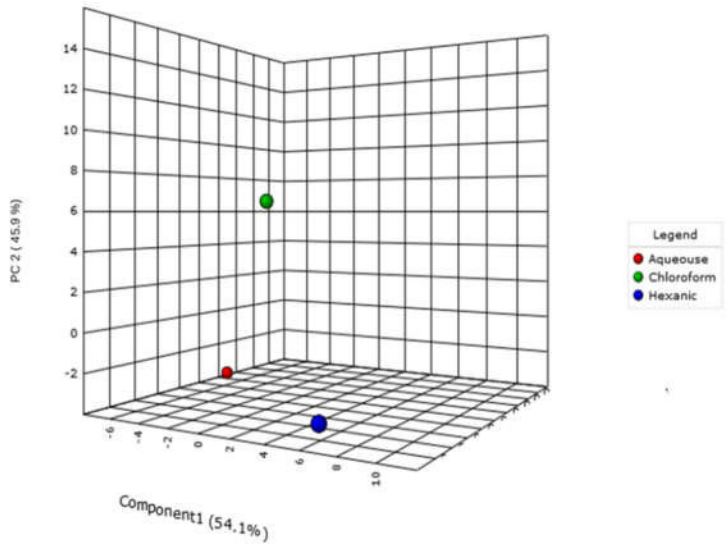

Figure 24. PCA of the metabolomic composition of extracts from the stems of *C. trifoliata*.

5.1.6. Pathway Analysis

The Pathway Analysis module in Metaboanalyst combines results from pathway enrichment analysis with topology analysis to identify the most relevant pathways involved in the production of the metabolites that were identified. Over-representation analysis tests if a group of compounds was present more than expected by chance, and the impact was calculated from pathway topology analysis. The results suggested (figure 25) that extracts from the stems of *C. trifoliata* were overrepresented by the pathways of the biosynthesis of flavone, flavonols (0.8) and stilbene (1.0). Stilbenes occur within a limited distribution in the plant kingdom. Consistent with the results of the pathway analysis, *C. trifoliata* belongs to the Vitaceae family of plants that produce stilbenes in great amounts [198]. *Vitis vinifera* is the most studied Vitaceae, and recent metabolic and molecular studies are consistent with its high production of flavonoid and stilbenes [199]. Stilbene derivatives act as phytoalexins under the elicitation of biotic and/or abiotic agents through the activation of the stilbene synthase gene. The production of stilbenes by *Vitis spp*. as a

response to fungal infection was first reported in 1976. Resveratrol is the most abundant stilbene and accumulates at high levels at the sites of infection [194].

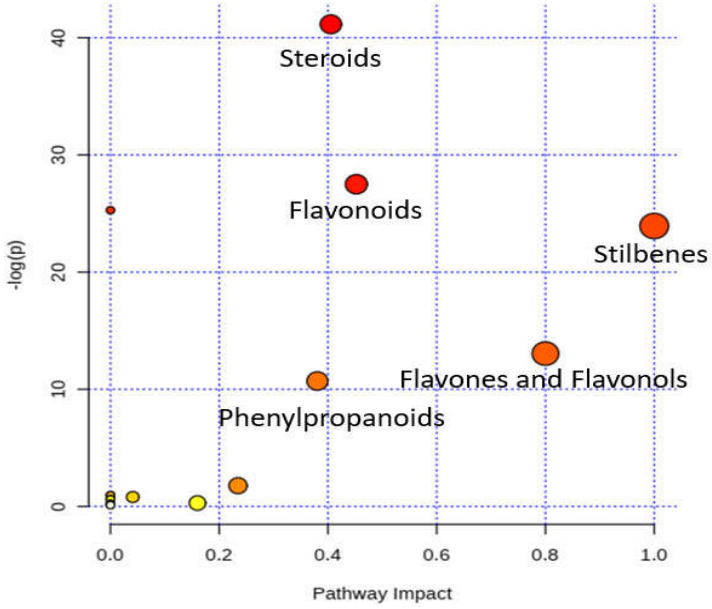

Figure 25. Pathway analysis of the constituents from the stems of *C. trifoliata*

Quantification of stilbene derivatives in *Vitis* stems showed that the most abundant stilbenes are trans-ε-viniferin, resveratrol, cis-resveratrol, and piceid, and their accumulation is higher in the lignified organs such as stems [200]. The finding of stilbenes as the metabolites with high impact in the extracts from the stems of *C. trifoliata* is also consistent with the isolation of stilbene derivatives from the stems of *C. quadrangularis*, *C. repens* and *C. sycioides*. As previously suggested, the metabolic profiling of a medicinal plant by GC-MS, and LC-MS, is useful to infer its bioactivity [83]. Accordingly, bioactivity against cancer cells can be inferred from the metabolic profile of *C. trifoliata* that was high in sterols, stilbenes and flavonoids [201-203]. The results of the biological evaluation of the extracts are presented in detail in the next section.

5.1.7. Biological evaluation of the extracts

5.1.7.1. Antibacterial activity.

Increasing antibiotic resistance encourages the search for novel compounds and affordable treatments to effectively treat bacterial infections. In this regard, medicinal plants from the genus *Cissus* had shown antibacterial activities [118, 119, 204]. Furthermore, the ethnomedical uses of *C. trifoliata* include the treatment of infections, thus, the extracts from the stems were evaluated against a panel of bacteria that represent the most common type of drug-resistant strains in the clinical setting [23] (Table 16).

No antibacterial activity was observed against strains from the ATCC or clinical isolates at the highest concentration employed (500 µg/ml). Previous studies of the antibacterial activity of extracts from the stems of *C. quadrangularis* report MIC values between 0.93 mg/ml to 6.25 mg/ml against *P. aeruginosa, S. aureus* and *E. coli* [118]. However, according to the National Committee for Clinical Laboratory Standards, the concentration of the extracts evaluated should not exceed the range of 1 mg/ml.

Furthermore, a MIC ≥ 30 µg/ml is considered negative for antibacterial activity [38], thus, the extracts from the stems of *C. trifoliata* were considered inactive for the inhibition of bacterial growth. We cannot discard that *C. trifoliata* possess activity against other microorganisms. Perhaps, infections managed successfully with *C. trifoliata* include dermatophytes, originated from bacteria and fungi. We speculate this based on the fact that the bacteria evaluated in the present study include pathogens of the respiratory and gastrointestinal tracts. Additionally, mycosis is common in places were *C. trifoliata* is still traditionally used [91, 205] and the metabolic profile predicts good antifungal properties [206].

Table 16. MIC of the extracts (μg/ml) of *C. trifoliata* stems and levofloxacin against bacteria

Bacteria	Hexane	$CHCl_3$-MeOH	Aqueous	Levofloxacin
S. aureus (ATCC, 29213)	≥ 500	≥ 500	≥ 500	3.12
S. epidermidis (ATCC,14990)	≥ 500	≥ 500	≥ 500	3.12
E. faecium (ATCC, 2127)	≥ 500	≥ 500	≥ 500	3.12
E. coli (ATCC, 25922)	≥ 500	≥ 500	≥ 500	3.12
P. aeruginosa (ATCC, 27853)	≥ 500	≥ 500	≥ 500	3.12
K. pneumoniae (ATCC, 19606)	≥ 500	≥ 500	≥ 500	3.12
A. baumanni (ATCC, 13883)	≥ 500	≥ 500	≥ 500	3.12
Methicillin-resistant *S.aureus* (14-2095)	≥ 500	≥ 500	≥ 500	12.5
Linezolid-resistant *S. epidermidis* (14-583)	≥ 500	≥ 500	≥ 500	6.25
Vancomycin-resistant *E. faecium* (10-984)	≥ 500	≥ 500	≥ 500	12.5
Beta lactamic-resistant *E.coli* (14-2081)	≥ 500	≥ 500	≥ 500	25.0
Carbapenem-resistant *P. aeruginosa* (13-1391)	≥ 500	≥ 500	≥ 500	12.5
Oxacillin-resistant *K. pneumoniae* (17-1692)	≥ 500	≥ 500	≥ 500	6.25
Beta lactamic-resistant *K. pneumoniae* (14-3335)	≥ 500	≥ 500	≥ 500	50.0
Carbapenem-resistant *A. baumannii* (12-666)	≥ 500	≥ 500	≥ 500	12.5

Thus, *C. trifoliata* could exhibit good responses against infection originated from dermatophytes. It is worthy to mention that the production of stilbenes in Vitaceae increases when plants suffer from fungal infections and they exhibited good activity against dermatophytes [198]. Thus, extracts from *C. trifoliata* could possess strong antifungal activities and should be considered for evaluation in further studies.

5.1.7.2 Cytotoxic activity

Results from the MTS assay showed that the hexane extract was the most active against the tested cancer cell lines. According to the NCI guidelines, an active crude extract must inhibit the 50% of cell proliferation (IC_{50}) at a concentration of 30 µg/ml after the exposure time of 72 h to be considered cytotoxic [36]. Therefore, the hexane extract from the stems of *C. trifoliata* was active against HepG2, Hep3b, and MCF7 cells and the aqueous extract against MCF7 cells (Table 17). Previously, the extracts from the stems of other plants from the genus *Cissus* have been evaluated against cancer cells. In the next section, this information is compared with the results from *C. trifoliata*.

Table 17. MTS assay IC_{50} (µg/ml) of the extracts from the stems of *C. trifoliata*

Cancer cell lines	Hexane	$CHCl_3$-MeOH	Aqueous	Taxol
HepG2	26±2*	80±8	79±5	64.0×10^{-3}
Hep3b	24±2*	81±4	81±7	33.0×10^{-3}
HeLa	35±3	82±4	90±8	5.12×10^{-3}
A549	51±4	85±3	94±9	5.12×10^{-3}
PC3	62±3	61±3	58±4	4.27×10^{-3}
MCF7	30±3*	78±5	30±2*	79.4×10^{-3}
*active according to NCI guidelines ($IC_{50} \leq 30$ µg/ml)				

For example, the hexane extract from *C. quadrangularis* was inactive (IC_{50} of 200 µg/ml) against KB (keratin-forming tumor cell line HeLa) and A431 (epidermoid carcinoma) by MTT assay [124]. Regarding polar extracts, the acetonic extract from *C. quadrangularis* showed an IC_{50} of 43 µg/ml against HepG2 [207], whereas the ethanolic and ethyl acetate

extracts from *C. sicyoides* showed an IC_{50} of 50 µg/ml and 43 µg/ml against NCI-H292 and HepG2 respectively [127]. The methanolic extract of *C. debilis* displays an IC_{50} of 50 µg/ml against CaCo-2 cells [125]. Thus, previous results suggested that hexane and the aqueous extracts from *C. trifoliata* were more active than other *Cissus* plants. However, we cannot conclude that considering the variability in the results from the evaluation of cytotoxicity *in vitro*, such as the cellular phenotypes, the cell passages and the techniques used for the IC_{50} determination [208]. In conclusion, the cytotoxic activity of the extracts provides evidence of the anti-tumor effects of *C. trifoliata* and encourages the realization of a bioassay-guided study to identify the bioactive compounds according to the recommendations of the NCI for plants that show promising anticancer effects [36]. Despite the hexane and the aqueous extract showed more activity against cancer cells, the $CHCl_3$-MeOH was used in the bioassay guided study. One of the reasons obeyed to the small quantity that remains after the hexane extract column-fractionation for the isolation of the solids. Additionally, the high activity of the hexane extract might be related to the presence of plant sterols and triterpenes and their cytotoxicity and the mechanism of action in the cancer cell lines assayed is well described (discussed in the next section). In the case of the aqueous extract, their fractions were inactive against cancer cells (data not showed). The aqueous extract showed signs of decomposition and is reported its susceptibility of contamination and degradation [197]. Thus, further studies were performed with the $CHCl_3$-MeOH extract. The next section provides a revision of the current literature of the antiproliferative effects of the bioactive molecules identified by the chemical analysis of the active extracts since they might contribute with their anti-tumor mechanisms against the liver and breast cancer cells.

5.1.8. Cytotoxic compounds identified in the stems of *C. trifoliata*.

The overrepresentation of biosynthetic pathways of sterols, stilbenes, and flavonoids in the metabolomic profile of the stems of *C. trifoliata* might play a major role in their effects against HepG2, Hep3b, and MCF7 cells. The plant sterols campesterol, stigmasterol, and β-sitosterol have been previously evaluated against those cancer cell lines. For example, β-sitosterol showed cytotoxic activity against MCF7 (IC_{50} 250 µg/ml) [209] and Hep3B (IC_{50} 25 µg/ml). β-Sitosterol increases caspase-8 activity [210] and affect sphingolipid metabolism, causing apoptosis and cell growth inhibition in a dose-dependent manner [157]. Stigmasterol also showed cytotoxic activities against MCF7 (IC_{50} 9.2 µg/ml) [209] and Hep3B cells (IC_{50} 30 µM) [211]. Both sterols modulate the estrogen receptor (ER), thus inhibiting the proliferation of MCF7 (ER-positive) [212]. Pentacyclic triterpenes also exhibit potent anticancer activities; for example, lupeol showed cytotoxicity activity against MCF7 (IC_{50} 32 µg/ml), and HepG2 (IC_{50} 48 µg/ml) [213]. Lupeol induces apoptosis through mitochondrial cell death pathway and cell cycle arrest by inhibition of cyclin-dependent kinases (CDKs), and bcl-2 [214], and suppression of STAT3 in parallel with the inhibition of the proteins cyclin D1, Bcl-2, the B-cell lymphoma extra-large protein (BclxL), the antiapoptotic protein survivin, the VEGF and the metalloprotease 9 [215]. The bioactivity of the aqueous extract might be related to its polyphenol content. Piceatannol, quercetin, and kaempferol may account for most of the effects in MCF7 cells. Piceatannol induces antiproliferative effects at IC_{50} of 30 µg/ml [216] and competes with the estradiol for binding the ER [217]. Kaempferol is a flavonol, and its biological activities against cancer cells include disruption of the cell cycle process, angiogenesis and inflammation. Kaempferol decreased the cell viability in MCF7 cells cultured with 50-100 µM. The mechanism of action is also the modulation of the ER signaling acting as an anti-estrogen. The effect on cell cycle progression was

accompanied by a reduction of the protein expression of cyclin D1 and E, and increased p21 expression [218]. Quercetin is a flavonol whose intake is associated with a reduced risk of mortality from chronic diseases including cancer. In MCF7 cells treated with 50 μM/ml reduces 50% in viability and proliferation was accompanied by changes in the expression of the proapoptotic protein caspase-3 [219]. Quercetin showed estrogen receptor antagonism [220], thus, the combination of polyphenols with antiestrogenic activities might account for the higher susceptibility of the breast cancer cells MCF7.

Current knowledge of the anticancer bioactivities of the phytocompounds identified in the cytotoxic extracts partially explained the ethnomedical uses of *C. trifoliata* as an antitumor agent. However, a bioassay-guided study would indicate more precisely the bioactive secondary metabolites that accounts for most of the antiproliferative effects against cancer cells. In the next section, these results are presented in detail.

5.2. Bioassay-guided study *C. trifoliata* stems

The screening of the cytotoxic activity and the chemical content of the complete extracts demonstrated potential anticancer effects of the extracts from *C. trifoliata*. Following a bioassay-guided study, the $CHCl_3$-MeOH extract was subjected to fractionation by column chromatography and biological evaluation by WST-1 to test the activity of the fractions against cancer cells. The $CHCl_3$-MeOH extract was the most abundant (23g), and according to the mixture of solvents employed during the extraction it may possess a wider range of secondary metabolites [197]. The fractions of the extract were tested against the cell lines MCF7 and PC3 that showed higher sensitivity (the lowest IC_{50} when exposed to the complete extract). The column fractionation of the $CHCl_3$-MeOH extract yields 210

fractions pooled in 14 according to their TLC behavior (A to N). Fractions A to E were not included in the WST-1 assay, they were reminiscent of the fractions obtained in the hexane extract and were composed mainly of waxes (mixtures of alkanes, fatty acids, and fatty alcohols).

Table 18. Results of cell viability expressed as a percentage of control mean viable cells (± standard deviation). Cancer cell lines were treated with three different concentrations of the fractions of the $CHCl_3$-MeOH extract from the stems of *C. trifoliata* and with taxol.

PC3 cells			
Treatment	100 µg/ml	50 µg/ml	25 µg/ml
F1	20.52 ± 0.57*	49.21 ± 9.64	156.79 ± 9.71
F2	17.79 ± 1.55*	133.19 ± 10.04	158.36 ± 3.87
F3	68.85 ± 5.73	150.72 ± 3.17	147.49 ± 5.49
F4	96.26 ± 7.86	136.39 ± 8.81	108.22 ± 12.02
F5	139.40 ± 4.12	145.19 ± 6.85	141.93 ± 3.21
F6	139.31 ± 5.10	145.65 ± 4.20	143.24 ± 3.18
F7	122.95 ± 7.31	128.42 ± 6.09	143.24 ± 3.18
F8	83.42 ± 11.46	88.45 ± 6.29	108.91 ± 8.25
F9	99.95 ± 0.58	118.89 ± 5.18	114.64 ± 5.59
Taxol	40.15 ± 7.58	62.95 ± 10.43	70.32 ± 1.19
MCF cells			
F1	6.50 ± 2.70*	27.67 ± 9.49	74.45 ± 9.49
F2	10.29 ± 0.13*	89.07 ± 9.44	104.71 ± 2.12
F3	89.11 ± 6.17	95.88 ± 3.05	96.57 ± 6.19
F4	100.79 ± 1.16	105.20 ± 7.55	100.24 ± 4.78
F5	101.74 ± 7.64	105.82 ± 4.96	105.73 ± 2.39
F6	96.80 ± 3.44	104.41 ± 4.78	102.72 ± 2.84
F7	97.74 ± 4.15	102.61 ± 1.77	102.06 ± 1.46
F8	114.87 ± 2.47	103.98 ± 4.48	106.32 ± 8.52
F9	93.99 ± 1.51	100.76 ± 5.62	102.17 ± 3.41
Taxol	62.25 ± 3.06	67.68 ± 4.50	68.58 ± 0.78
* Asterisks indicate significant differences in the analysis (ANOVA-LSD test, values of $p < 0.05$			

The anti-proliferative activity of the fractions F1 to F9 was studied by WST1 (for details of fraction polarity see table 4). Cancer cells were treated with doses of 100, 50 and 25 µg/ml for 48 hours. The resulting data were expressed as the percentage value of the cell growth respect to the control. Then, results were subjected to ANOVA-LSD test. Fractions F1 and

F2 showed a significative reduction ($p > 0.05$) in the cell viability of both cancer cell lines at the concentration of 100 µg/ml (Table 18). Therefore, the chemical composition of both fractions was analyzed by LC-MS to identify the compounds accountable for the antiproliferative activity of *C. trifoliata* against cancer cells.

5.2.1. Chemical analysis of the active fractions by UPLC-QTOF-MS

The fraction F1 of the $CHCl_3$-MeOH extract was characterized by UPLC-QTOF-MS analysis using the negative mode. The figure 26 shows the chromatogram of the fraction F1.

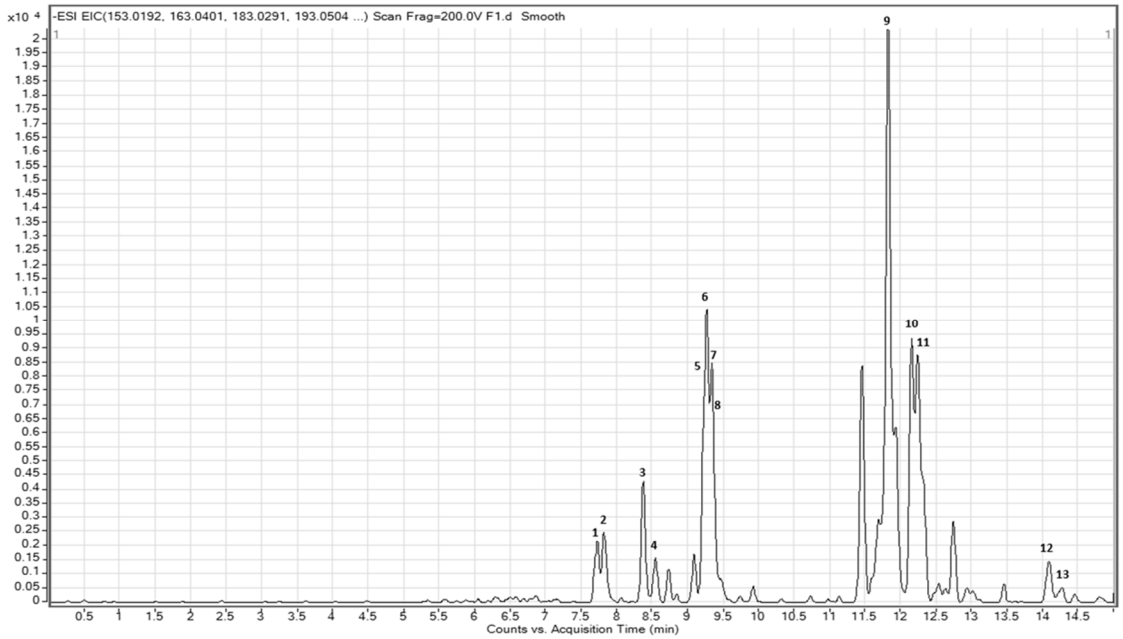

Figure 26. Chromatogram of F1 from the $CHCl_3$-MeOH stem extract of *C. trifoliata* by UPLC-QTOF-MS

The tentatively identified compounds include simple phenolics, fatty acids, terpenes, flavonoids and stilbenes. The table 19 summarized them along with the retention time, the experimental m/z and the molecular formula. The phenolic compounds tentatively identified include the trans-p-coumaric acid and isoferulic acid. The polyphenolic

compounds include the flavonoids dihydrokaempferol, apigenin, kaempferol, chrysoeriol and naringenin, and the stilbene resveratrol. Regarding the terpenes, the hydroxyursolic acid, ursolic acid and betulic acid were identified along with the palmitic and stearic fatty acids. Fraction 2 showed similar TLC behavior and polarity, thus UPLC-QTOF-MS analysis were performed under the same conditions.

Table 19. UPLC-QTOF-MS analysis of F1 from the $CHCl_3$-MeOH extract from the stems of *C. trifoliata*

Peak	RT (min)	Experimental m/z $[M-H]^-$	Molecular formula	Tentatively identified compound
1	6.785	163.0401	$C_9H_8O_3$	Trans-p-coumaric acid
2	7.908	193.0504	$C_{10}H_{10}O_4$	Isoferulic acid
3	8.541	287.0569	$C_{15}H_{12}O_6$	Dihydrokaempferol
4	8.567	227.0716	$C_{14}H_{12}O_3$	Resveratrol
5	9.103	269.0434	$C_{15}H_{10}O_5$	Apigenin
6	9.243	285.0404	$C_{15}H_{10}O_6$	Kaempferol
7	9.345	299.0561	$C_{16}H_{12}O_6$	Chrysoeriol
8	9.479	271.0612	$C_{15}H_{12}O_5$	Naringenin
9	11.699	471.3475	$C_{30}H_{48}O_4$	2-alpha hydroxyursolic acid
10	13.994	455.3515	$C_{30}H_{48}O_3$	Ursolic acid
11	14.071	455.3422	$C_{30}H_{48}O_3$	Betulinic acid
12	14.401	253.2161	$C_{16}H_{28}O_2$	Hexadecadienoic acid
13	14.582	279.2348	$C_{16}H_{32}O_2$	Octadecadienoic acid

The results of the analysis showed similar bioactive content and chromatogram of the fraction F2 (Figure 27). The phytocompounds tentatively identified include simple phenolics, flavonoids, stilbenes and terpenes. The phenolic compounds include the protocatechuic acid, the methylgallate, the isoferulic acid and the trans-p-coumaric acid. The flavonoids include the dihydrokaempferol, apigenin, kaempferol, and quercetin, whereas the only stilbene identified was the piceatannol glucoside.

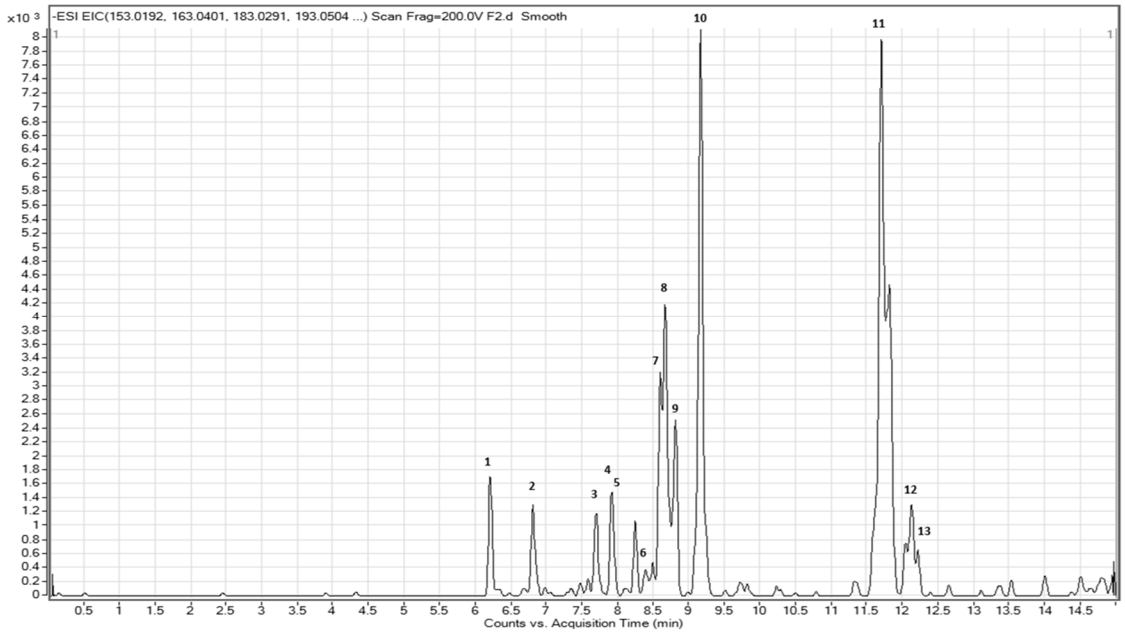

Figure 27. Chromatogram of F2 from the $CHCl_3$-MeOH stem extract of *C. trifoliata* by UPLC-QTOF-MS

Regarding the terpenes, the hydroxyursolic acid, ursolic acid and betulic acid were also present in F2. The table 20 summarizes them along with the retention time, the experimental m/z and the molecular formula.

Table 20. UPLC-QTOF-MS analysis of F2 from the $CHCl_3$-MeOH extract from the stems of *C. trifoliata*

Peak	RT (min)	Experimental m/z $[M-H]^-$	Molecular formula	Tentatively identified compound
1	6.234	153.0192	$C_7H_6O_4$	Protocatechuic acid
2	6.836	183.0291	$C_8H_7O_5$	Methylgallate
3	6.785	163.0401	$C_9H_8O_3$	Trans-p-coumaric acid
4	7.751	431.1013	$C_{21}H_{20}O_{10}$	Apigenin glucoside
5	7.908	193.0504	$C_{10}H_{10}O_4$	Isoferulic acid
6	8.487	405.1198	$C_{20}H_{22}O_9$	Piceatannol glucoside
7	8.741	287.0569	$C_{15}H_{12}O_6$	Dihydrokaempferol
8	8.859	301.0367	$C_{15}H_{10}O_7$	Quercetin
9	9.103	269.0434	$C_{15}H_{10}O_5$	Apigenin
10	9.243	285.0404	$C_{15}H_{10}O_6$	Kaempferol
11	11.699	471.3475	$C_{30}H_{48}O_4$	2-alpha hydroxyursolic acid
12	13.994	455.3515	$C_{30}H_{48}O_3$	Ursolic acid
13	14.071	455.3422	$C_{30}H_{48}O_3$	Betulinic acid

According with the chemical analysis by LC-MS both active fractions share similar composition. The most significative difference was the lack of fatty acid content in fraction F2 compared with F1, that may be explained based on their differences in polarity. However, bioactive fractions share the content of flavonoids, stilbenes, simple phenolics and terpenes. Thus, the antiproliferative activity against cancer cells can be inferred based on the bioactive content. A bioassay guided isolation from the stems of *V. vinifera* founded related results. They identified oleanolic acid, resveratrol, ε-viniferin, and daucosterol as the compounds responsible for the antiproliferative properties of the most active fractions [221].

The pentacyclic triterpenes tend to be more active than polyphenols at low concentration [222]. They are highly active against almost all cancer cell lines tested with an IC_{50} value lower than 15 µg/ml [209, 223, 224]. Additionally, the betulic, ursolic, oleanolic and hydroxyursolic acids are commonly found as the most active compounds in studies of the bioassay-guided isolation of antiproliferative constituents from plant extracts [225, 226]. Betulinic acid exhibits cytotoxic activity against all cancer cell lines tested including PC3 and MCF-7 at IC_{50} value of 10 µg/ml. Furthermore, *in vivo* it decreases angiogenesis, proliferation and invasion [227]. Ursolic acid decreased the proliferation of cancer cells including the MCF7 by 80% at doses of 10 µM [224]. It exerts its action through the mitochondrial pathway [228], inhibits phosphorylation of JAK2 (Janus kinase 2) and STAT3 downregulated Bcl-xl. The oleanolic acid showed significant inhibition on MCF7 with IC_{50} of 15 µmol/l by reducing the expression of Bcl-2, Bcl-xL, and survivin. The oleanolic acid inhibits survival and proliferation of all the models of prostate cancer cells including the PC3 (15 µmol/l) by inhibition of the cancer pathway PI3k/Akt1 [229]. The 2α-hydroxyursolic

acid also shows growth inhibitory activity against tumor cell lines [223]. In breast cancer cells, the 2α-hydroxyursolic acid inhibits the cell proliferation by the modulation of the p38/MAPK pathway [230]. The phenolic acids, coumaric and isoferulic have been tested against PC3 and MC7 cells and showed potential as chemopreventive agents. Coumaric acids showed apoptotic effects against MCF7 cells (IC_{50} 40 mM) [231] and PC-3 cells (IC_{50} 30 mM). Their mechanism of action includes downregulation of CDKs and increased expression of p53 and ATM [232]. Flavonoids and stilbenes were also founded in the bioactive fractions F1 and F2 of *C. trifoliata* stems. Their antitumor and cytotoxic activities have been previously reviewed (section 5.1.7).

The bioactive fractions result in a mixture of anticancer compounds that may act in synergy to inhibit cancer cell proliferation. The extracts and the most active fractions were rich in triterpenes, sterols, phenolic compounds with known cytotoxic, antiproliferative and anti-estrogen activities. Altogether the metabolic profile and the observed antiproliferative activity could partially explain the traditional use of *C. trifoliata* as antitumor agent. Medicinal plants are often administered as a complete extract, composed of a complex mixture of phytocompounds. However, in natural product chemistry is tradition to reduce the complexity of plant extracts by isolating the most active compound. Then, the active constituents are subjected to evaluation of the molecular mechanisms and some of them will be used for drug development [233]. Since most of the identified triterpenes and flavonoids in the cytotoxic fractions are widely distributed in plants [234], we opt to evaluate the bioactivity and mechanism of action of stilbenes. Resveratrol derivatives exhibit a narrow distribution and Vitaceae plants have been characterized by their content [198]. Additionally, stilbenes have been isolated from the stems of other *Cissus* plants [133] and

the biosynthetic pathway of stilbenes characterized the metabolite profile of *C. trifoliata* stems. Given the results, we considered that some of the antitumoral properties of *C. trifoliata* may relate to its high content of stilbenes. Therefore, the stilbene profile of the most active fraction (F1) of *C. trifoliata* was analyzed by a targeted metabolomic approach. This method has been previously useful in the study of grape metabolomics with UPLC-QTOF-MS technology and is called suspect screening analysis [235]. This protocol uses the molecular formula and the isotopic pattern of stilbenes to extract them from the total ion chromatogram. The result is showed in figure 28. The extracted ion chromatogram (EIC) of the fraction F1 contained the stilbenes resveratrol, resveratrol glucoside, piceatannol, resveratrol methyl ether, piceatannol glucoside, ε-viniferin, δ-viniferin, pallidol, and caraphenol B.

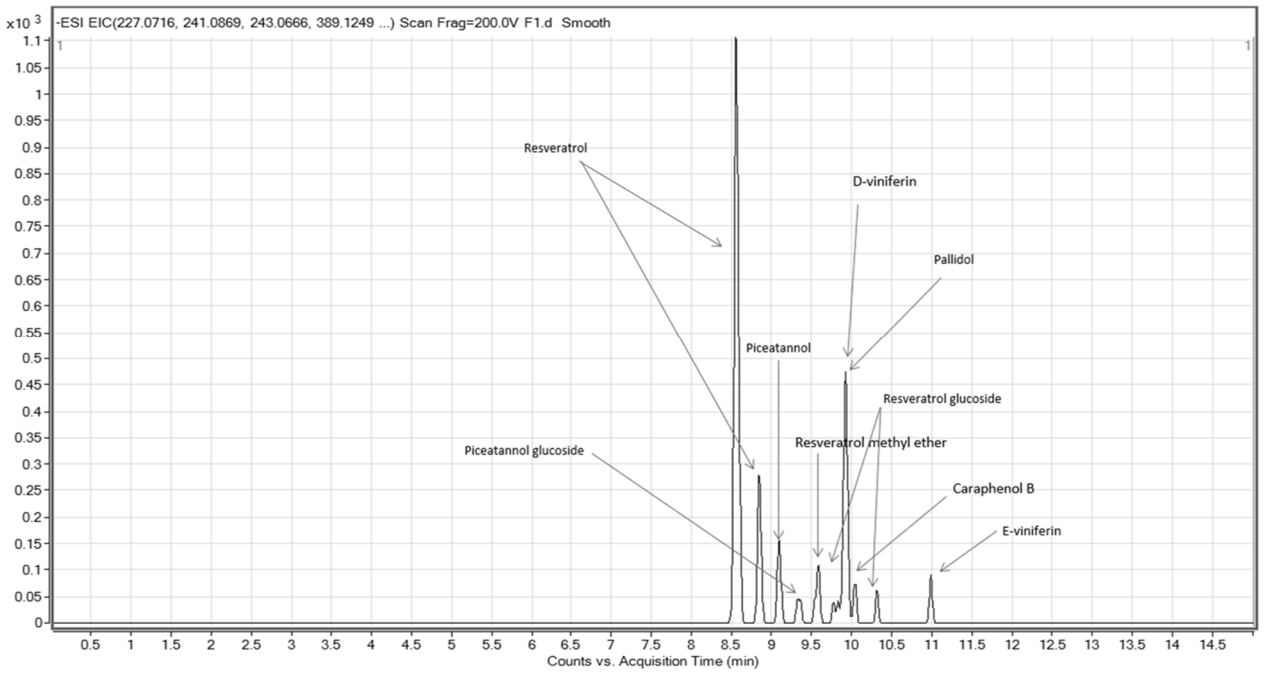

Figure 28. Extract-ion chromatogram of stilbene derivatives in fraction F1

5.3. Determination of the IC_{50} of stilbenes

The antitumor activity of the most abundant stilbene in the active fraction F1, was examined in the cancer cells MCF and PC3. Resveratrol and its glucoside (piceid) were purchased as pure compounds from Sigma Aldrich. Cells were treated with 100, 50, 25, 12.5 and 6.5 µg/ml for 24 hours and their effects on cell growth were evaluated by WST-1 (Table 21). In the MCF7 cells, resveratrol caused marked growth inhibition, with an IC_{50} value of 211 µM. Cells showed more resistance to piceid, thus the mechanism of action was assessed for resveratrol. The criteria for selecting the PC3 cells over the model of breast cancer was the well-characterized effects of resveratrol in MCF7 by several studies that include microarrays [236]. In contrast, at present no reports of the effects of resveratrol by microarrays have been published in PC3 cells.

Table 21. IC_{50} (µM) of stilbenes against the cancer cell lines.

Cancer	Resveratrol		Piceid	
cell line	Calculated	Reference	Calculated	Reference
PC3	232	15 [237]	387	72 *[238]
MCF7	211	80 [236]	593	103 [239]
* The IC_{50} included as reference was performed in CaCo cells, no reports in PC3.				

Regarding the elevated IC_{50} for stilbenes of our results in comparison with literature, we attributed most of the resistance to the process of subculture. One of the most common phenomena observed as the responsible of the increased tolerance of cell lines is the loss of markers of differentiation that occur along with the increased number of passages. Cell lines can experience alterations in morphology, response to stimuli, growth rate and sensibility to compounds. To avoid passage-dependent effects and increase the reproducibility of the results is recommended to start with well know characterized cell lines and test them genetically and morphologically as the passages increases [240]. The

reproducibility of the IC_{50} of stilbenes does not represent an issue in the present study. Rather, one of the objectives was the identification of a novel mechanism of action of one of the compounds present in the active extracts from the stems of *C. trifoliata*. In this regard, the exposition to sublethal doses of phytocompounds (IC_{30} or IC_{25}) has been successfully employed for the identification of new anticancer mechanism of action of well-known anticancer compounds [156]. Thus, gene expression changes of PC3 cells exposed to resveratrol (IC_{25}) were determined by microarrays to explore a potential novel mechanism of action of resveratrol against prostate cancer cells.

5.4. Mechanism of action of resveratrol in PC3 cells.

5.4.1 Resveratrol influences gene expression in human prostate cancer cells

The gene expression profile of a cell determines its phenotype, function, and response to the environment. The technique of DNA microarrays has a high performance and efficiency to measure the simultaneous expression of all the genes of the genome of an organism [241]. Microarrays can be used to study the mechanism of drug action by examining the effect of gene expressions [242]. Thus, microarrays have been previously used for the identification of the mechanisms of action of phytocompounds [243, 244]. To identify the genes modulated by resveratrol, cDNA microarray hybridization analysis using the entire human genome was carried out. PC3 cells, a human prostate cancer cell line, were treated with resveratrol for 24 h at IC_{25} and the RNA was isolated. Figure 29 illustrates the transcriptional changes according to the fold change of gene expression. The genes considered for the functional analysis were those with a z-score of ± 2 SD. The PC3 cells exposed to resveratrol undergone significative transcriptional changes (2-fold) in 847 genes (Fig 29, B).

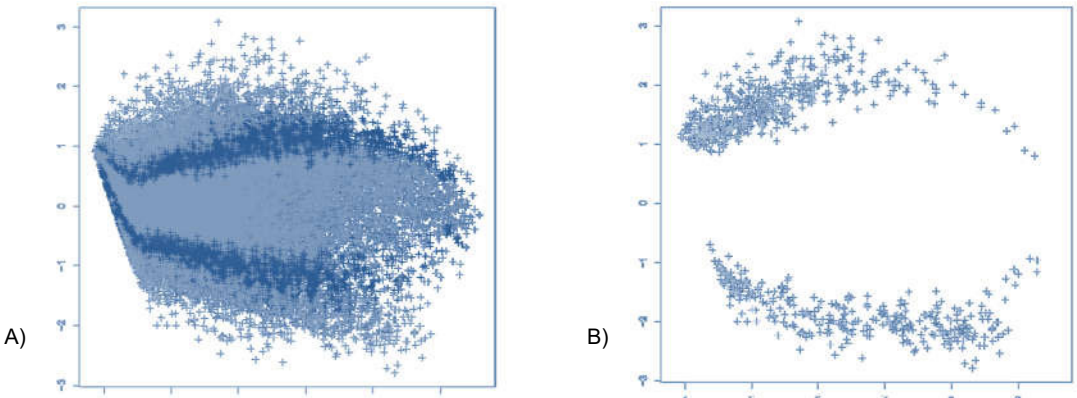

Figure 29. Z- score of microarrays. A) Z-score of all genes; B) Z-score ± 2 SD. In total 848 genes were affected.

Resveratrol upregulated 526 genes and downmodulated 322. The full gene identifiers of the upregulated and downregulated genes are listed in tables 24 and 25 of the supplementary material. The table 22 showed the results of the genes upregulated.

Table 22. Functional Annotation Chart of upregulated genes.

Category	Term	Count	%	*p*-value	Bonferroni
UP_KEYWORDS	Transcription regulation	53	20.8	3.10E-05	8.70E-03
UP_KEYWORDS	Nucleus	93	36.5	7.50E-05	2.10E-02
GOTERM_BP_DIRECT	Transcription RNA polymerase II	22	8.6	7.20E-06	9.90E-03
UP_KEYWORDS	DNA-binding	43	16.9	6.60E-04	1.70E-01
UP_KEYWORDS	Phosphoprotein	127	49.8	1.00E-03	2.50E-01
UP_KEYWORDS	Alternative splicing	154	60.4	2.30E-03	4.80E-01
UP_KEYWORDS	Hydrolase	30	11.8	3.80E-02	1.00E+00
UP_KEYWORDS	Ubl conjugation	30	11.8	4.70E-02	1.00E+00
UP_KEYWORDS	ATP-binding	25	9.8	5.90E-02	1.00E+00
UP_KEYWORDS	Differentiation	14	5.5	6.90E-02	1.00E+00
INTERPRO	Homeodomain-like	12	4.7	4.50E-03	9.20E-01
GOTERM_MF_DIRECT	Ubiquitin protein ligase binding	10	3.9	1.80E-02	1.00E+00
GOTERM_CC_DIRECT	Mitochondrial inner membrane	12	4.7	3.50E-02	1.00E+00
GOTERM_BP_DIRECT	Cell differentiation	11	4.3	1.00E-01	1.00E+00
Functional annotation data derived from DAVID algorithm. Table derived from the functional annotation chart that shows all cellular functions associated with the number of genes affected by the treatment by resveratrol. The upregulated genes are showed. *p* value of 0.05 was considered significative.					

The gene list was analyzed with the functional classification tool available in the bioinformatic software DAVID. The most significant changes were observed in the process associated with transcription, nuclear proteins, DNA-binding process, splicing, hydrolase and ubiquitin activities, ATP binding, cell differentiation, homeobox proteins, and mitochondrial membrane. The downregulated genes belong with process related to components and signaling of the cell membrane, cytoplasm and transport proteins, endoplasmic reticulum components and process, and the g-protein coupled receptor signaling pathways (Table 23). Overall, the microarrays indicate that resveratrol induces transcriptional responses in PC3 cells that impact their differentiation, stemness, metabolism, apoptosis, and metastatic potential.

Table 23. Functional Annotation Chart of downregulated genes.

Category	Term	Count	%	*p*-value	Bonferroni
UP_KEYWORDS	Membrane	71	49.1	1.70E-03	3.10E-01
UP_KEYWORDS	Phosphoprotein	69	47.6	4.80E-02	1.00E+00
GOTERM_CCDIRECT	Integral component of membrane	51	35.2	2.00E-02	9.70E-01
GOTERM_CCDIRECT	Plasma membrane	44	30.3	9.60E-03	8.10E-01
UP_SEQ_FEATURE	Cytoplasmic	39	26.9	3.70E-03	8.60E-01
UP_KEYWORDS	Cell membrane	32	22.1	3.10E-02	1.00E+00
UP_KEYWORDS	Transport	27	18.6	1.20E-03	2.30E-01
UP_KEYWORDS	Receptor	22	15.2	5.30E-03	6.80E-01
UP_KEYWORDS	Transducer	15	10.3	4.30E-03	6.00E-01
GOTERM_CCDIRECT	Endoplasmic reticulum membrane	15	10.3	5.10E-03	5.80E-01
GOTERM_BPDIRECT	G-protein coupled receptor pathway	15	10.3	6.50E-03	9.90E-01
UP_KEYWORDS	Endoplasmic reticulum	14	9.7	3.70E-02	1.00E+00
UP_KEYWORDS	Ubl conjugation pathway	11	7.6	2.10E-02	9.90E-01

Functional annotation data derived from DAVID algorithm. Table derived from the functional annotation chart that shows all cellular functions associated with the number of genes affected by the treatment by resveratrol. The downregulated genes are showed. *p* value of 0.05 was considered significative.

In the next section the functional significance of the most important genes that were modulated is discussed, and how they interact and impact the cellular process and pathways that the functional analysis indicated.

5.4.2. Resveratrol influences cell differentiation

Resveratrol upregulated the expression of 44 genes that codify transcription factors and 6 epigenetic modifiers. Is have been shown that transcription factors are key players in orchestrating cell decisions, such as cell cycle, cell differentiation, cellular inflammation, apoptosis or autophagy [245]. We found that resveratrol induced the expression of the homeobox genes, including the H6 family homeobox 2 (HMX2), homeobox A3 (Hox-A3), homeobox D12 (Hox D12), msh homeobox 2 (MSX-2), PBX/knotted homeobox 1 (PKNOX1), and lim homeobox 8 (LHX8). Many of these proteins have reported deregulated in cancer, but their role in carcinogenesis remains unknown. In general, homeobox genes that are upregulated in cancer are normally expressed during development or in undifferentiated cells [246]. In our experiment, it seems that the upregulation of Homeobox proteins is associated with antitumor effects of resveratrol by induction of cell differentiation and reduction of cell proliferation. In line with this hypothesis, we found high expression of other transcription factors involved with cellular differentiation and developmental pathways. For example, we also found upregulated the POU class 4 homeobox 2 (POU4F2) which is a transcription factor involved in the developmental process that activates the differentiation of cells. This protein is also involved in carcinogenesis, but their role is not well understood [247]. The T-box 1 protein (TBX1) is also a transcription factor involved in development that acts as a negative regulator of tumor cell growth [248].

The protein Cbp/p300-interacting trans activator 4 (CITED4) function as an inhibitor of hypoxia-induced factor 1 (HIF1A) and prevents their interaction with CREB binding protein (CREBBP). The functional consequences of this overexpression also seem to be related to the differentiation of cells and the prevention of tumor growth and angiogenesis [249].

Also, resveratrol induced the expression of the genes Kruppel-like Factor 14 (KLF14) and Ikaros is a DNA-binding zinc finger protein (IKZF1) also involved in differentiation. The KLF14 gene induces epigenetic reprogramming during cell differentiation. Thus, the overexpression of KLF14 also suggests cell differentiation via chromatin remodeling [250]. Furthermore, IKZF1 regulates gene expression and chromatin remodeling with important tumor suppressor properties [251]. The chromatin remodeling is possible by the activation of chromatin remodeling proteins. The antitumor effects of resveratrol have been associated with its influence in epigenetics [252]. We found upregulation of jumonji domain containing 2B (JMJD2B), the methyltransferase mixed-lineage leukemia protein 3 (MLL3), and the histone lysine N-methyltranferase (SETD3). These enzymes regulate transcription by altering the epigenetic marks on histones but the pathologic roles in cancer remain to be elucidated [253]. Likewise, the mitochondrial NAD-dependent protein deacylase sirtuin-5 (SIRT5) and the bifunctional heparan sulfate N-deacetylase/N-sulfotransferase (NDST2), were upregulated by resveratrol. It is well documented that SIRT5 is upregulated by resveratrol and that their activation protects cells from oncogenic transformation [254]. On the other hand, resveratrol downregulates a histone-lysine N-methyltransferase (SETD1B) that showed to promote cell proliferation, migration, and invasion of cancer cell lines. Furthermore, the overexpression in carcinomas is associated with an unfavorable prognosis. Thus, downmodulation of the activities of SETD1B in the generation of trimethylated histone H3 at Lys4 is consistent with the anti-cancer activities of resveratrol [255]. Resveratrol also induces high expression of the eukaryotic translation initiation factor 4H (eIF4H), an activator of the RNA helicase eIF4A, which is overexpressed in carcinomas although the exact role of eIF4H in tumorigenesis and the molecular mechanisms involved are unknown [256].

5.4.3. Resveratrol impair cancer stemness

In line with the findings of induction of differentiation, resveratrol impairs biomarkers of pluripotency. We found that resveratrol downmodulates the homeobox protein Nanog (NANOG). This transcription factor maintains pluripotency in embryonic stem cells and cancer stem cells. The activity of Nanog is associated with many different types of cancer. It is considered an oncogene and its high expression correlates with poor survival, therapeutic resistance, relapse, and metastasis. Its upregulation enhances tumorigenicity both *in vivo* and *in vitro* whereas their repression inhibits tumor initiation [257]. Thus, its downregulation is consistent with the upregulation of transcription factors related to cell differentiation. Recent evidence demonstrated that resveratrol inhibits Nanog, affecting the self-renewal capacity of pancreatic cancer stem cells reducing tumor growth and development in mice. Furthermore, the pancreatic cancer cells showed a lower capacity of invasion, migration, and resistance to chemotherapy and radiation [258].

Furthermore, resveratrol also represses the expression of the recombining binding protein suppressor of hairless (RBPSUH), a transcriptional regulator of Notch signaling. This signaling pathway is involved in cell-cell communication and regulates cell-fate determination during embryonic development. The Notch signaling regulates Nanog and the insulin-like growth factor 1 (IGF1-R), and helps in maintain stemness by preventing cellular differentiation [259]. In line with the induction of differentiation by resveratrol, it showed downregulation of the transcription factor (THRAP3). This protein is involved in the ability of prostate cancer cells to grow in an androgen-independent manner [260]. Therefore, this finding suggests that PC3 cells become less aggressive when exposed to resveratrol.

5.4.4. Resveratrol reduces metastatic potential

Consistent with the previous assumption, resveratrol induces the upregulation of tight junction proteins and cell adhesion molecules. We found overexpression of the tight junction protein ZO-2 (TJP2), gap junction alpha-1 protein (GJA1), the tight junction partitioning defective 6 homolog gamma Gap (PARD6G), the gap junction alpha-10 protein (NP115991), and the unconventional myosin-VIIb (MYO7B). Among the cell adhesion molecules syndecan-2 cell adhesion molecule (SDC2), the high-affinity immunoglobulin gamma Fc receptor (FCGR1A) and necdin (NDN). These proteins control cellular proliferation and differentiation and during cancer progression and metastasis are frequently deleted. Furthermore, induction of their expression *in vitro* promotes the abrogation of the metastatic potential of the cell lines [261].

5.4.5. Resveratrol reprogram cell metabolism

Resveratrol affects genes involved in cell metabolism and the process of autophagia on PC3 cells. The mitochondrial activity, and the electron transport chain were highly affected. Resveratrol downregulated ATPases, GTPases, DNA, and RNA polymerases, kinases, transferases, and n-methyltransferases. The metabolic pathways affected are involved with the metabolism of glucose, fatty acids, amino acids, ATP, NADPH, and cytochromes. We found downmodulation of 40 genes related to metabolism, including the mitochondrial cytochromes CYB561D2, the NAD(P) transhydrogenase (NNT), the NADPH P450 reductase (POR), and the c oxidase subunit 1 (MT-CO1). The lipid metabolism was affected as showed by the downregulation of the palmitoyltransferase specific of HRas (ZDHHC9) and the palmitoyltransferase (ZDHHC20), the fatty-acid amide hydrolase (FAAH2), the very-long-chain 3-hydroxyacyl-CoA dehydratase (PTPLA)

and the long-chain fatty acid transport protein 1 ligase (SLC27A1) and the acyl-coenzyme A thioesterase 11 (ACOT11). Furthermore, the tricarboxylate mitochondrial transport protein (SLC25A1), the sarcosine mitochondrial dehydrogenase (SARDH) and the creatine kinase M-type (CKM) were also affected. Taken together these changes in expression indicate disruption of cancer cell metabolism by resveratrol, particularly affecting mitochondrial functions. Recently, resveratrol has been to be shown to inhibit the mitochondrial electron transport chain proteins, NADH/ubiquinone oxidoreductase complex-1, F0-F1 ATPase, and cytochrome P450 isoenzymes such as CYP1A1, and quinone reductase-2 (QR-2) [262], which is consistent with our results. Furthermore, it has been proved that resveratrol suppresses the fermentative glycolysis in normoxia of tumors (Warburg effect). This high glycolytic phenotype results from the conjunction of uncontrolled growth signaling, deregulated c-Myc and HIF-1 activity leading to induction of glycolytic enzymes and inhibition of mitochondrial pyruvate oxidation [263]. Resveratrol targets the pyruvate dehydrogenase complex in cancer cells and PI3K signaling pathway. Resveratrol also downregulate the glucose transporter GLUT1, phosphofructokinase, the hexokinase 2, the phosphoglycerate mutase, the glucose 6 phosphate dehydrogenase, the transketolase and the pyruvate kinase 2 [264]. Thus, resveratrol seems to normalize the metabolism and the altered mitochondria functions deregulated in cancer [265].

5.4.6. Resveratrol abrogates cancer pathways

Resveratrol was able to downmodulate key components of pathways involved in carcinogenesis such as the TGF-β, Notch, HIF-1α, PI3K/Akt and insulin/IGF-1 signaling. Several findings indicate that exists a cross-talk among the major signaling pathways involved in carcinogenesis [266]. Our results support the integrated nature of the molecular

networks involved in cellular differentiation, growth, and metabolism. Resveratrol was able to affect those processes at the transcriptional level, but also showed changes in the cancer pathways. For example, the gene glucagon-like peptide 1 receptor (GLP1R) was downregulated on PC3 exposed to resveratrol. GLP-1 receptors are expressed in most cancer cells and upon activation exert proliferation via activation of PI3K and MAPK kinases [267]. We found downmodulation of the phosphatidylinositol 3-kinase regulatory subunit beta (PIK3R2) which is considered an oncogene and is highly amplified in neoplasia. Additionally, resveratrol downmodulated the phospholipase C gamma (PLCG1), a member of the family of phosphoinositide specific PLC that converts phosphatidylinositol 4,5-bisphosphate into second messengers 1,2-diacylglycerol (DAG) and inositol 1,4,5-trisphosphate (IP3), thereby initiating and propagating proliferation.

Resveratrol also increases the expression of negative regulators of proliferation. The insulin-like growth factor-binding protein 6 (IGFBP6) possess anticancer effects; its expression inhibits cell proliferation in PC-3 cells. IGFBP-6 blocks the IGF-II in a dose-dependent manner [268] These genes are major components of the insulin/IGF-1 signaling which is frequently deregulated in cancer [269]. We found upregulation of the protein called mothers against decapentaplegic homolog 7 (Smad7). This protein prevents TGF-β-associated Smad signaling. Smad7 abrogates tumorigenesis in late stage cancers mainly through family E3 ubiquitin ligases [270]. We found that another mechanism by which resveratrol abrogates TGF-β pathway is by the downregulation of the receptor of TGF-β, the bone morphogenetic protein receptor type-2 (BMPR2). The downregulation of the TGF-β pathway by resveratrol might implicate the inactivation of angiogenesis, the epithelial-mesenchymal transition (EMT) and the CSC properties of the PC3 cells [271]. It

has been reported that sirtuins inactivates hypoxia-inducible factor (HIF)-1α, and inhibits β-catenin and cyclins [272]. SIRT5 was upregulated by resveratrol. It normally resides in the mitochondrial matrix and catalyzes the removal of negatively charged lysine acyl modifications; succinyl, malonyl, and glutaryl groups. SIRT5 acts as a regulator of cellular homeostasis. SIRT5 regulates protein substrates involved in glycolysis, the TCA cycle, fatty acid oxidation, electron transport chain, ketone body formation, nitrogenous waste management, and ROS detoxification. Furthermore, SIRT5 is involved in tumor suppressor mechanisms and also explains the metabolic changes observed with resveratrol exposition [273].

5.4.7. Resveratrol sensitizes to apoptosis

The downregulation of the MDM4 gene suggests the induction of apoptosis by the reactivation of the p53 pathway. The protein p53 is the most frequently inactivated gene in human cancers, is mutated in more than half of human tumors. In response to various extra and intracellular stresses p53 functions as a transcriptional factor and transactivates a set of genes engaged in multiple cellular processes such as cell-cycle arrest, cellular senescence, energy metabolism, and apoptosis. p53 signaling is inactivated by high levels of p53 inhibitors, such as Mdm4. The upregulation of Mdm4 serves as an alternate means of inactivating the p53 pathway [274]. Thus, resveratrol seems to reactivate p53 pathway by suppressing MDM4 gene. Furthermore, we also found the upregulation of the apoptosis-inducing factor 1 (AIFM1). This mitochondrial protein indicates apoptosis and its overexpression in cancer cell lines is related to apoptosis mediated by caspase 3 [275]. To our knowledge, this is the first report of the study of the effects of resveratrol on PC3 cells by microarrays.

Previously the LNCaP cells; another *in vitro* model of prostate cancer was studied by DNA microarrays. Upon exposition at 150 μM of resveratrol in DMSO (0.01%) for 24 h they analyzed the expression change (>2.0-fold) among 42,000 genes. They found that resveratrol inhibits 50% of cell growth by affecting 1656 genes. They found 37 genes upregulated and 63 downregulated related to stress, lipid metabolism, protein trafficking, androgen responsiveness and cell proliferation. The most affected genes were related to proliferation such as the p53-induced protein sestrin (PA26), the tumor susceptibility gene (TSG101), P300/CBP-associated factor (PCAF) and the histone deacetylase 3 (HDAC3). The proapoptotic genes induced were the transcription factor JunD (JUND), the phospholipase A2 (PLA2), p53 (TP53), the murine double minute 2 (MDM2), the programmed cell death 4 (PDCD4) and the serine/threonine kinase 17a (STK17A). They conclude that resveratrol elicits gene expression changes with anticancer activities in prostate cancer cells by regulation of the androgen axis and cell cycle [244]. It is important to clarify that the LNCaP is a cell line derived from a metastatic lymph node lesion of human prostate cancer which is AR-positive, thus exhibits androgen-sensitive growth. In contrast, PC3 cells are human prostate cancer cells derived from bone metastasis of grade IV prostate cancer. Thus, PC3 are useful in investigating biochemical changes in advanced prostate cancer cells, such as the mechanism of resistance to androgen ablation. PC3 have high metastatic potential compared to LNCaP cells, which have low metastatic potential. Thus, a direct comparison is not straightforward, and PC3 cells represent an advanced stage of the disease with more aggressive traits and a less differentiated phenotype [276].

CHAPTER VI

6. CONCLUSIONS

The metabolomic profile of *Cissus trifoliata* (L.) L was analyzed by the hyphenated techniques of GC-MS and LC-MS. The use of accurate mass spectrometry and spectral data led to the identification of *C. trifoliata* stems as a high producer of anticancer compounds of the class of terpenes, sterols, flavonoids, and stilbenes. The MTS and WST-1 antiproliferative assays with the cancer cells A549, HepG2, Hep3B, HeLa, MCF7, and PC3 provide insight on the antitumor activity of the plant. The hexane and aqueous extract showed high cytotoxic activity, and their bioactive triterpenes, sterols, and polyphenols suggested synergistic antiproliferative and antiestrogenic effects against the HepG2, Hep3B, and MCF7 cells. The combination of column chromatography, LC-MS, and WST-1 led to the identification of the fraction with the most anticancer properties in the $CHCl_3$-MeOH extract. The bioassay-guided study showed that the content of the fraction F1 includes the antitumor compounds 2-alpha hydroxyursolic acid, ursolic acid, betulinic acid, dihydrokaempferol, apigenin, kaempferol, chrysoeriol, naringenin, and resveratrol. The identification of resveratrol in the most active fraction encourages its selection for the evaluation of its mechanism of action. The findings of the microarray study indicated novel mechanisms of action of resveratrol against the proliferation of prostate cancer cells that include the downregulation of the transcription factor Nanog. Therefore, is suggested that resveratrol impairs the cancer stem cell characteristics of PC3 cells by induction of differentiation and the loss of malignancy. According to our results, the metabolic profile of *Cissus trifoliata* is enriched in anticancer compounds associated with its antiproliferative effects against cancer cells, and the molecular mechanism of an active constituent provides a better understanding of this medicinal plant used in the management of tumors.

CHAPTER VII

7. PERSPECTIVES

The metabolic profiling of *C. trifoliata* by advanced chromatography-spectrometry technology represented an effective tool to detect and identify its bioactive content and to understand its traditional use. Nonetheless, since comparison with databases was used for compound identification, the characterization at a higher level of confidence would require the inclusion of authentic standards.

The microarray analysis suggested many anticancer properties of resveratrol including novel mechanisms of action against PC3 cells. The investigation of the mechanism underlying the inhibition of the pluripotency maintaining factors altogether with biological assays for the evaluation of cancer stem properties, migration, and invasion would provide additional evidence to support the findings.

Proponents of the medicinal use of natural mixtures often claim that complete extracts are more effective than purified compounds due to the synergy that efficiently addresses the problematic of tumor resistance. *Cissus trifoliata* is traditionally used as an aqueous extract. The understanding of how the complex mixture of compounds acts in concert to achieve the biological effect would require the application of advanced analytical and molecular techniques. Additionally, the use of a murine model of tumorigenesis is required to provide a more comprehensive characterization of the systemic antitumor properties of *C. trifoliata.*

CHAPTER VIII

8. REFERENCES

1. Stewart, B.; Wild, C. P., World cancer report 2014. 2014.
2. Bosetti, C.; Rodriguez, T.; Chatenoud, L.; Bertuccio, P.; Levi, F.; Negri, E.; La Vecchia, C., Trends in cancer mortality in Mexico, 1981-2007. *European Journal of Cancer Prevention* 2011, 20 (5), 355-63.
3. Hanahan, D.; Weinberg, R. A., Hallmarks of cancer: the next generation. *Cell* 2011, 144 (5), 646-674.
4. Mansoori, B.; Mohammadi, A.; Davudian, S.; Shirjang, S.; Baradaran, B., The Different Mechanisms of Cancer Drug Resistance: A Brief Review. *Advanced pharmaceutical bulletin* 2017, 7 (3), 339.
5. Morgan, G.; Ward, R.; Barton, M., The contribution of cytotoxic chemotherapy to 5-year survival in adult malignancies. *Clinical oncology* 2004, 16 (8), 549-560.
6. Boffetta, P.; Kaldor, J. M., Secondary malignancies following cancer chemotherapy. *Acta Oncologica* 1994, 33 (6), 591-598.
7. Cutler, D. M., Are we finally winning the war on cancer? *The Journal of Economic Perspectives* 2008, 22 (4), 3-26.
8. Manders, D. B.; Kehoe, S. M.; Miller, D. S.; Lea, J. S.; Richardson, D. L., Third-line Salvage Chemotherapy for Recurrent Carcinoma of the Cervix is Associated With Minimal Response Rate and High Toxicity. *American journal of clinical oncology* 2017.
9. Choi, C.-H., ABC transporters as multidrug resistance mechanisms and the development of chemosensitizers for their reversal. *Cancer cell international* 2005, 5 (1), 30.
10. Meijer, C.; Mulder, N. H.; Timmer-Bosscha, H.; Sluiter, W. J.; Meersma, G. J.; de Vries, E. G., Relationship of cellular glutathione to the cytotoxicity and resistance of seven platinum compounds. *Cancer research* 1992, 52 (24), 6885-6889.
11. Malet-Martino, M.; Martino, R., Clinical studies of three oral prodrugs of 5-fluorouracil (capecitabine, UFT, S-1): a review. *The oncologist* 2002, 7 (4), 288-323.
12. Palmberg, C.; Koivisto, P.; Hyylinen, E.; Isola, J.; Visakorpi, T.; Kallioniemi, O.-P.; Tammela, T., Androgen receptor gene amplification in a recurrent prostate cancer after monotherapy with the nonsteroidal potent antiandrogen Casodex (bicalutamide) with a subsequent favorable response to maximal androgen blockade. *European urology* 1997, 31, 216-219.
13. Shaw, A. T.; Yeap, B. Y.; Solomon, B. J.; Riely, G. J.; Gainor, J.; Engelman, J. A.; Shapiro, G. I.; Costa, D. B.; Ou, S.-H. I.; Butaney, M., Effect of crizotinib on overall survival in patients with advanced non-small-cell lung cancer harbouring ALK gene rearrangement: a retrospective analysis. *The lancet oncology* 2011, 12 (11), 1004-1012.
14. Fan, S.; El-Deiry, W. S.; Bae, I.; Freeman, J.; Jondle, D.; Bhatia, K.; Fornace, A. J.; Magrath, I.; Kohn, K. W.; O'Connor, P. M., p53 gene mutations are associated with decreased sensitivity of human lymphoma cells to DNA damaging agents. *Cancer research* 1994, 54 (22), 5824-5830.
15. Kirschner, K.; Melton, D. W., Multiple roles of the ERCC1-XPF endonuclease in DNA repair and resistance to anticancer drugs. *Anticancer research* 2010, 30 (9), 3223-3232.
16. Shore, G. C.; Viallet, J., Modulating the bcl-2 family of apoptosis suppressors for potential therapeutic benefit in cancer. *ASH Education Program Book* 2005, 2005 (1), 226-230.

17. Wang, C.-Y.; Guttridge, D. C.; Mayo, M. W.; Baldwin, A. S., NF-κB induces expression of the Bcl-2 homologue A1/Bfl-1 to preferentially suppress chemotherapy-induced apoptosis. *Molecular and cellular biology* 1999, 19 (9), 5923-5929.

18. Holohan, C.; Van Schaeybroeck, S.; Longley, D. B.; Johnston, P. G., Cancer drug resistance: an evolving paradigm. *Nature Reviews Cancer* 2013, 13 (10), 714-726.

19. Fauci, A. S.; Touchette, N. A.; Folkers, G. K., Emerging infectious diseases: a 10-year perspective from the National Institute of Allergy and Infectious Diseases. *International Journal of Risk & Safety in Medicine* 2005, 17 (3, 4), 157-167.

20. Organization, W. H.; Organization, W. H., The top 10 causes of death. 2012. 2015.

21. Pop-Vicas, A.; Opal, S. M., The clinical impact of multidrug-resistant gram-negative bacilli in the management of septic shock. *Virulence* 2014, 5 (1), 206-212.

22. Arias-Flores, R.; Rosado-Quiab, U.; Vargas-Valerio, A.; Grajales-Muñiz, C., Los microorganismos causantes de infecciones nosocomiales en el Instituto Mexicano del Seguro Social. *Revista Médica del Instituto Mexicano del Seguro Social* 2016, 54 (1), 20-24.

23. Amabile-Cuevas, C., Antibiotic resistance in Mexico: a brief overview of the current status and its causes. *The Journal of Infection in Developing Countries* 2010, 4 (03), 126-131.

24. Arredondo-García, J. L.; Amábile-Cuevas, C. F., High resistance prevalence towards ampicillin, co-trimoxazole and ciprofloxacin, among uropathogenic Escherichia coli isolates in Mexico City. *The Journal of Infection in Developing Countries* 2008, 2 (05), 350-353.

25. Munita, J. M.; Arias, C. A., Mechanisms of antibiotic resistance. *Microbiology spectrum* 2016, 4 (2).

26. Davies, J.; Davies, D., Origins and evolution of antibiotic resistance. *Microbiology and molecular biology reviews* 2010, 74 (3), 417-433.

27. Aldred, K. J.; Kerns, R. J.; Osheroff, N., Mechanism of quinolone action and resistance. *Biochemistry* 2014, 53 (10), 1565-1574.

28. Martín, J. F.; Ullán, R. V.; García-Estrada, C., Regulation and compartmentalization of β-lactam biosynthesis. *Microbial biotechnology* 2010, 3 (3), 285-299.

29. Gudiol, C.; Carratalà, J., Antibiotic resistance in cancer patients. *Expert review of anti-infective therapy* 2014, 12 (8), 1003-1016.

30. Teillant, A.; Gandra, S.; Barter, D.; Morgan, D. J.; Laxminarayan, R., Potential burden of antibiotic resistance on surgery and cancer chemotherapy antibiotic prophylaxis in the USA: a literature review and modelling study. *The Lancet infectious diseases* 2015, 15 (12), 1429-1437.

31. Rausher, M. D., Co-evolution and plant resistance to natural enemies. Nature 2001, 411 (6839), 857.

32. González-Lamothe, R.; Mitchell, G.; Gattuso, M.; Diarra, M. S.; Malouin, F.; Bouarab, K., Plant antimicrobial agents and their effects on plant and human pathogens. *International Journal of Molecular Sciences* 2009, 10 (8), 3400-3419.

33. Balunas, M. J.; Kinghorn, A. D., Drug discovery from medicinal plants. *Life sciences* 2005, 78 (5), 431-441.

34. Newman, D. J.; Cragg, G. M.; Snader, K. M., The influence of natural products upon drug discovery. *Natural product reports* 2000, 17 (3), 215-234.

35. Oberlies, N. H.; Kroll, D. J., Camptothecin and taxol: historic achievements in natural products research. *Journal of natural products* 2004, 67 (2), 129-135.

36. Grever, M. R.; Schepartz, S. A.; Chabner, B. A. In The National Cancer Institute: cancer drug discovery and development program, *Seminars in oncology*, Elsevier: 1992; pp 622-638.

37. Patridge, E.; Gareiss, P.; Kinch, M. S.; Hoyer, D., An analysis of FDA-approved drugs: natural products and their derivatives. *Drug discovery today* 2016, 21 (2), 204-207.

38. Balouiri, M.; Sadiki, M.; Ibnsouda, S. K., Methods for in vitro evaluating antimicrobial activity: A review. *Journal of Pharmaceutical Analysis* 2016, 6 (2), 71-79.

39. Bussmann, R.; Malca-García, G.; Glenn, A.; Sharon, D.; Chait, G.; Díaz, D.; Pourmand, K.; Jonat, B.; Somogy, S.; Guardado, G., Minimum inhibitory concentrations of medicinal plants used in Northern Peru as antibacterial remedies. *Journal of ethnopharmacology* 2010, 132 (1), 101-108.

40. Cavalieri, S. J.; Harbeck, R.; McCarter, Y.; Ortez, J.; Rankin, I.; Soutter, R.; Sharp, S.; Spiegel, C., *Manual de pruebas de susceptibilidad antimicrobiana*. Seattle: University of Washington 2005.

41. Gibbons, S., Plants as a source of bacterial resistance modulators and anti-infective agents. *Phytochemistry Reviews* 2005, 4 (1), 63-78.

42. Garg, A. K.; Buchholz, T. A.; Aggarwal, B. B., Chemosensitization and radiosensitization of tumors by plant polyphenols. *Antioxidants & redox signaling* 2005, 7 (11-12), 1630-1647.

43. Shiota, S.; Shimizu, M.; Mizushima, T.; Ito, H.; Hatano, T.; Yoshida, T.; Tsuchiya, T., Marked reduction in the minimum inhibitory concentration (MIC) of β-lactams in methicillin-resistant Staphylococcus aureus produced by epicatechin gallate, an ingredient of green tea (Camellia sinensis). *Biological and Pharmaceutical Bulletin* 1999, 22 (12), 1388-1390.

44. Smith, E. C.; Kaatz, G. W.; Seo, S. M.; Wareham, N.; Williamson, E. M.; Gibbons, S., The phenolic diterpene totarol inhibits multidrug efflux pump activity in Staphylococcus aureus. *Antimicrobial agents and chemotherapy* 2007, 51 (12), 4480-4483.

45. Stermitz, F. R.; Lorenz, P.; Tawara, J. N.; Zenewicz, L. A.; Lewis, K., Synergy in a medicinal plant: antimicrobial action of berberine potentiated by 5′-methoxyhydnocarpin, a multidrug pump inhibitor. *Proceedings of the National Academy of Sciences* 2000, 97 (4), 1433-1437.

46. Falcão-Silva, V. S.; Silva, D. A.; Souza, M. d. F. V.; Siqueira-Junior, J. P., Modulation of drug resistance in Staphylococcus aureus by a kaempferol glycoside from Herissantia tiubae (Malvaceae). *Phytotherapy Research* 2009, 23 (10), 1367-1370.

47. Park, J.-H.; Oh, E.-J.; Choi, Y. H.; Kang, C.-D.; Kang, H. S.; Kim, D.-K.; Kang, K. I.; Yoo, M.-A., Synergistic effects of dexamethasone and genistein on the expression of Cdk inhibitor p21WAF1/CIP1 in human hepatocellular and colorectal carcinoma cells. *International journal of oncology* 2001, 18 (5), 997-1002.

48. Gupta, S. C.; Kannappan, R.; Reuter, S.; Kim, J. H.; Aggarwal, B. B., Chemosensitization of tumors by resveratrol. *Annals of the New York Academy of Sciences* 2011, 1215 (1), 150-160.

49. Hour, T. C.; Chen, J.; Huang, C. Y.; Guan, J. Y.; Lu, S. H.; Pu, Y. S., Curcumin enhances cytotoxicity of chemotherapeutic agents in prostate cancer cells by inducing p21WAF1/CIP1 and C/EBPβ expressions and suppressing NF-κB activation. *The prostate* 2002, 51 (3), 211-218.

50. Drees, M.; Dengler, W. A.; Roth, T.; Labonte, H.; Mayo, J.; Malspeis, L.; Grever, M.; Sausville, E. A.; Fiebig, H. H., Flavopiridol (L86-8275): selective antitumor activity in vitro and activity in vivo for prostate carcinoma cells. *Clinical Cancer Research* 1997, 3 (2), 273-279.

51. Limtrakul, P.; Khantamat, O.; Pintha, K., Inhibition of P-glycoprotein function and expression by kaempferol and quercetin. *Journal of chemotherapy* 2005, 17 (1), 86-95.

52. Zhang, Y., Cancers with Stem-Like Attractors and “Loss Of Differentiation” Novel Hallmark: Does the “Cyto-Education” with Stem Cell Therapy Help?. Curr Synthetic Sys Biol 2013, 2:2. *Current Synthetic and Systems Biology* 2014, 4 (130), 6.

53. Gocek, E.; Studzinski, G. P., Vitamin D and differentiation in cancer. *Critical reviews in clinical laboratory sciences* 2009, 46 (4), 190-209.
54. Warrell Jr, R. P.; Frankel, S. R.; Miller Jr, W. H.; Scheinberg, D. A.; Itri, L. M.; Hittelman, W. N.; Vyas, R.; Andreeff, M.; Tafuri, A.; Jakubowski, A., Differentiation therapy of acute promyelocytic leukemia with tretinoin (all-trans-retinoic acid). *New England Journal of Medicine* 1991, 324 (20), 1385-1393.
55. Tallman, M. S.; Andersen, J. W.; Schiffer, C. A.; Appelbaum, F. R.; Feusner, J. H.; Woods, W. G.; Ogden, A.; Weinstein, H.; Shepherd, L.; Willman, C., All-trans retinoic acid in acute promyelocytic leukemia: long-term outcome and prognostic factor analysis from the North American Intergroup protocol: Presented in part at the 39th meeting of the American Society of Hematology, New Orleans, LA, December 1999. *Blood* 2002, 100 (13), 4298-4302.
56. Finn, G. J.; Creaven, B. S.; Egan, D. A., Daphnetin induced differentiation of human renal carcinoma cells and its mediation by p38 mitogen-activated protein kinase. *Biochemical pharmacology* 2004, 67 (9), 1779-1788.
57. Riveiro, M. E.; Shayo, C.; Monczor, F.; Fernández, N.; Baldi, A.; De Kimpe, N.; Rossi, J.; Debenedetti, S.; Davio, C., Induction of cell differentiation in human leukemia U-937 cells by 5-oxygenated-6, 7-methylenedioxycoumarins from Pterocaulon polystachyum. *Cancer letters* 2004, 210 (2), 179-188.
58. Agarwal, C.; Sharma, Y.; Zhao, J.; Agarwal, R., A polyphenolic fraction from grape seeds causes irreversible growth inhibition of breast carcinoma MDA-MB468 cells by inhibiting mitogen-activated protein kinases activation and inducing G1 arrest and differentiation. *Clinical Cancer Research* 2000, 6 (7), 2921-2930.
59. Qin, Y.; Li, Z.; Chen, Y.; Hui, H.; Sun, Y.; Yang, H.; Lu, N.; Guo, Q., III-10, a newly synthesized flavonoid, induced differentiation of human U937 leukemia cells via PKCδ activation. *European Journal of Pharmaceutical Sciences* 2012, 45 (5), 648-656.
60. Verpoorte, R.; Choi, Y.; Mustafa, N.; Kim, H., Metabolomics: back to basics. *Phytochemistry Reviews* 2008, 7 (3), 525-537.
61. Fernie, A. R., The future of metabolic phytochemistry: larger numbers of metabolites, higher resolution, greater understanding. *Phytochemistry* 2007, 68 (22-24), 2861-2880.
62. Sumner, L. W.; Mendes, P.; Dixon, R. A., Plant metabolomics: large-scale phytochemistry in the functional genomics era. *Phytochemistry* 2003, 62 (6), 817-836.
63. Matuszewski, B.; Constanzer, M.; Chavez-Eng, C., Strategies for the assessment of matrix effect in quantitative bioanalytical methods based on HPLC− MS/MS. *Analytical chemistry* 2003, 75 (13), 3019-3030.
64. Dettmer, K.; Aronov, P. A.; Hammock, B. D., Mass spectrometry-based metabolomics. *Mass spectrometry reviews* 2007, 26 (1), 51-78.
65. Lisec, J.; Schauer, N.; Kopka, J.; Willmitzer, L.; Fernie, A. R., Gas chromatography mass spectrometry–based metabolite profiling in plants. *Nature protocols* 2006, 1 (1), 387.
66. De Vos, R. C.; Moco, S.; Lommen, A.; Keurentjes, J. J.; Bino, R. J.; Hall, R. D., Untargeted large-scale plant metabolomics using liquid chromatography coupled to mass spectrometry. *Nature protocols* 2007, 2 (4), 778.
67. Grata, E.; Boccard, J.; Guillarme, D.; Glauser, G.; Carrupt, P.-A.; Farmer, E. E.; Wolfender, J.-L.; Rudaz, S., UPLC–TOF-MS for plant metabolomics: a sequential approach for wound marker analysis in Arabidopsis thaliana. *Journal of Chromatography* 2008, 871 (2), 261-270.
68. Weickhardt, C.; Moritz, F.; Grotemeyer, J., Time-of-flight mass spectrometry: State-of the-art in chemical analysis and molecular science. *Mass spectrometry reviews* 1996, 15 (3), 139-162.
69. Dunn, W. B.; Ellis, D. I., Metabolomics: current analytical platforms and methodologies. *Trends in Analytical Chemistry* 2005, 24 (4), 285-294.

70. Sumner, L. W.; Amberg, A.; Barrett, D.; Beale, M. H.; Beger, R.; Daykin, C. A.; Fan, T. W.-M.; Fiehn, O.; Goodacre, R.; Griffin, J. L., Proposed minimum reporting standards for chemical analysis. *Metabolomics* 2007, 3 (3), 211-221.

71. Brown, M.; Dunn, W. B.; Dobson, P.; Patel, Y.; Winder, C.; Francis-McIntyre, S.; Begley, P.; Carroll, K.; Broadhurst, D.; Tseng, A., Mass spectrometry tools and metabolite-specific databases for molecular identification in metabolomics. *Analyst* 2009, 134 (7), 1322-1332.

72. Smith, C. A.; O'Maille, G.; Want, E. J.; Qin, C.; Trauger, S. A.; Brandon, T. R.; Custodio, D. E.; Abagyan, R.; Siuzdak, G., METLIN: a metabolite mass spectral database. *Therapeutic drug monitoring* 2005, 27 (6), 747-751.

73. Sawada, Y.; Nakabayashi, R.; Yamada, Y.; Suzuki, M.; Sato, M.; Sakata, A.; Akiyama, K.; Sakurai, T.; Matsuda, F.; Aoki, T., RIKEN tandem mass spectral database (ReSpect) for phytochemicals: a plant-specific MS/MS-based data resource and database. *Phytochemistry* 2012, 82, 38-45.

74. Wishart, D. S.; Tzur, D.; Knox, C.; Eisner, R.; Guo, A. C.; Young, N.; Cheng, D.; Jewell, K.; Arndt, D.; Sawhney, S., HMDB: the human metabolome database. *Nucleic acids research* 2007, 35, D521-D526.

75. Giacomoni, F.; da Silva, A. L. B.; Bronze, M.; Gladine, C.; Hollman, P.; Kopec, R.; Yanwen, D. L.; Micheau, P.; dos Santos, M. C. N.; Pavot, B. In PhytoHub, an online platform to gather expert knowledge on polyphenols and other dietary phytochemicals. *International Conference on Polyphenols and Health*, 2017; p np.

76. Fahy, E.; Sud, M.; Cotter, D.; Subramaniam, S., LIPID MAPS online tools for lipid research. *Nucleic acids research* 2007, 35 (2), W606-W612.

77. Liland, K. H., Multivariate methods in metabolomics–from pre-processing to dimension reduction and statistical analysis. *Trends in Analytical Chemistry* 2011, 30 (6), 827-841.

78. Xia, J.; Sinelnikov, I. V.; Han, B.; Wishart, D. S., MetaboAnalyst 3.0 - making metabolomics more meaningful. *Nucleic acids research* 2015, 43 (W1), W251-W257.

79. Jorge, T. F., Caldana, C.; Schmidt, R., van Dongen, J. T., Thomas-Oates, J., António, C., Mass spectrometry-based plant metabolomics: Metabolite responses to abiotic stress. *Mass Spectrometry Reviews* 2016, 35 (5), 620-649.

80. Schwikkard, S. L.; Mulholland., Useful methods for targeted plant selection in the discovery of potential new drug candidates. *Journal Planta medica* 2014, 80 (14), 1154-1160.

81. Malviya, N.; Malviya, Bioassay guided fractionation-an emerging technique influence the isolation, identification and characterization of lead phytomolecules. *International Journal of Hospital Pharmacy* 2017, 2 (5), 1-6.

82. Graziani, V.; Scognamiglio, M.; Belli, V.; Esposito, A.; D'Abrosca, B.; Chambery, A.; Russo, R.; Panella, M.; Russo, A.; Ciardiello, Metabolomic approach for a rapid identification of natural products with cytotoxic activity against human colorectal cancer cells. *Molecular cancer therapeutics* 2018, 8 (1), 5309.

83. Farag, M. A.; Weigend, M.; Luebert, F.; Brokamp, G.; Wessjohann, Phytochemical, phylogenetic, and anti-inflammatory evaluation of 43 Urtica accessions (stinging nettle) based on UPLC–Q-TOF-MS metabolomic profiles. J *Food chemistry* 2013, 96, 170-183.

84. Farag, M. A.; Gad, H. A.; Heiss, A. G.; Wessjohann, Metabolomics driven analysis of six Nigella species seeds via UPLC-qTOF-MS and GC–MS coupled to chemometrics. *Journal Food chemistry* 2014, 151, 333-342.

85. Wen, J.; Lu, L. M.; Nie, Z. L.; Liu, X. Q.; Zhang, N.; Ickert-Bond, S.; Gerrath, J.; Manchester, S. R.; Boggan, J.; Chen, Z., A new phylogenetic tribal classification of the grape family (Vitaceae). *Journal of Systematics and Evolution* 2018.

86. Standley, P. C., Trees and shrubs of Mexico. Smithsonian Institution: *US Government* 1967; Vol. 1.

87. Adams, N. F.; Collinson, M. E.; Smith, S. Y.; Bamford, M. K.; Forest, F.; Malakasi, P.; Marone, F.; Sykes, D., X-rays and virtual taphonomy resolve the first Cissus (Vitaceae) macrofossils from Africa as early-diverging members of the genus. *American Journal of Botany* 2016, 103 (9), 1657-1677.

88. Rodrigues, J. G.; Lombardi, J. A.; Lovato, M. B., Phylogeny of Cissus (Vitaceae) focusing on South American species. *Taxon* 2014, 63 (2), 287-298.

89. McCartney, P., SEINet: metadata-mediated access to distributed ecological data. LTER. *DataBits Spring* 2003, 1.

90. Heinrich, M.; Ankli, A.; Frei, B.; Weimann, C.; Sticher, O., Medicinal plants in Mexico: Healers' consensus and cultural importance. *Social Science & Medicine* 1998, 47 (11), 1859-1871.

91. de las Mercedes Rodríguez, L., Etnobotánica maya: Algunas plantas de uso medicinal en estomatología. *Revista ADM* 2015, 72 (1).

92. Mendieta, R. M.; Rodríguez, A. Plantas medicinales del estado de Yucatán; *Boletín de la Sociedad Botánica de México* 1981, vol. 43, p. 94-95.

93. Estrada-Castillón, E.; Soto-Mata, B. E.; Garza-López, M.; Villarreal-Quintanilla, J. Á.; Jiménez-Pérez, J.; Pando-Moreno, M.; Sánchez-Salas, J.; Scott-Morales, L.; Cotera-Correa, M., Medicinal plants in the southern region of the State of Nuevo León, México. *Journal of ethnobiology and ethnomedicine* 2012, 8 (1), 45.

94. Perez, R.; Pérez, S.; Perez, C.; Zavala, M. J. F., Anti-inflammatory activity of Cissus trifoliata. *Fitoterapia* 1993, 64, 103-107.

95. Banu, J., Medicinal properties of plants from the genus Cissus: A review. *Journal of Medicinal Plants Research* 2012, 6 (16), 3080-3086.

96. Lassak, E.; McCarthy, T., Australian Medicinal Plants. *Reed Books*, : Victoria, Australia, 1997; p 230.

97. Pepato, M. T.; Baviera, A. M.; Vendramini, R. C.; Da Silva Perez, M. d. P.; Kettelhut, I. d. C.; Brunetti, I. L., Cissus sicyoides (princess vine) in the long-term treatment of streptozotocin-diabetic rats. *Biotechnology and Applied Biochemistry* 2003, 37 (1), 15-20.

98. de Sousa Lino, C.; de Paiva Sales, T.; Alexandre, F. S. O.; Ferreira, J. M.; de Sousa, D. F.; Gomes, P. B.; do Amaral, J. F.; Maia, F. D.; Silveira, E. R.; de Queiroz, M. G. R., Antioxidant activity of a Cissus verticillata fraction and tyramine, its bioactive constituent, on alloxan-induced diabetic rats. *Open Pharmacology Journal* 2008, 2, 63-69.

99. Olaoye S, B.; Ibrahim A, O.; Zhiqiang, L., Chemical compositions and radical scavenging potentials of essential oils from Tragia benthamii (BAKER) and Cissus aralioides (WELW). *Journal of Biologically Active Products from Nature* 2016, 6 (1), 59-64.

100. Otshudi, A. L.; Foriers, A.; Vercruysse, A.; Van Zeebroeck, A.; Lauwers, S., In vitro antimicrobial activity of six medicinal plants traditionally used for the treatment of dysentery and diarrhoea in Democratic Republic of Congo (DRC). *Phytomedicine* 2000, 7 (2), 167-172.

101. Yang, L.; Wang, F.; Liu, M., A study of an endothelin antagonist from a Chinese anti-snake venom medicinal herb. *Journal of Cardiovascular Pharmacology* 1998, 31, S249-S250.

102. Li, Y.-j.; Xu, C.-t.; Lin, D.-d.; Qin, J.-k.; Ye, G.-j.; Deng, Q.-h., Anti-inflammatory polyphenol constituents derived from Cissus pteroclada Hayata. *Bioorganic & Medicinal Chemistry Letters* 2016, 26 (15), 3425-3428.

103. Wang, Y.-H.; Zhang, Z.-K.; He, H.-P.; Wang, J.-S.; Zhou, H.; Ding, M.; Hao, X.-J., Stilbene C-glucosides from Cissus repens. *Journal of Asian Natural Products Research* 2007, 9 (7), 631-636.

104. Mishra, G.; Srivastava, S.; Nagori, B., Pharmacological and therapeutic activity of Cissus quadrangularis: an overview. *International journal of pharmtech research* 2010, 2 (2), 1298-1310.

105. Abubakar, M.; Musa, A.; Ahmed, A.; Hussaini, I., The perception and practice of traditional medicine in the treatment of cancers and inflammations by the Hausa and Fulani tribes of Northern Nigeria. *Journal of Ethnopharmacology* 2007, 111 (3), 625-629.

106. Ahmadu, A.; Onanuga, A.; Aquino, R., Flavonoid glycosides from the leaves of Cissus ibuensis hook (vitaceae). *African Journal of Traditional, Complementary and Alternative Medicines* 2010, 7 (3).

107. Lockett, C.; Christopher, C.; Grivetti, C., Energy and micronutrient composition of dietary and medicinal wild plants consumed during drought. Study of rural Fulani, Northeastern Nigeria. *International Journal of Food Sciences and Nutrition* 2000, 51 (3), 195-208.

108. Adebayo, J.; Krettli, A., Potential antimalarials from Nigerian plants: a review. *Journal of ethnopharmacology* 2011, 133 (2), 289-302.

109. Soladoye, M.; Chukwuma, E., Quantitative phytochemical profile of the leaves of Cissus populnea Guill. & Perr.(Vitaceae)-an important medicinal plant in central Nigeria. *Archives of Applied Science Research* 2012, 4 (1), 200-206.

110. Loraine, S.; Mendoza-Espinoza, J. A., Las plantas medicinales en la lucha contra el cáncer, relevancia para México. *Revista Mexicana de Ciencias Farmacéuticas* 2010, 41 (4), 18-27.

111. Mahonge, C.; Nsenga, J.; Mtengeti, E.; Mattee, A., Utilization of medicinal plants by Waluguru people in East Uluguru Mountains Tanzania. *African Journal of Traditional, Complementary and Alternative Medicines* 2006, 3 (4), 121-134.

112. Lans, C. A., Ethnomedicines used in Trinidad and Tobago for urinary problems and diabetes mellitus. *Journal of ethnobiology and ethnomedicine* 2006, 2 (1), 45.

113. Lans, C., Ethnomedicines used in Trinidad and Tobago for urinary problems and diabetes mellitus. *Journal of Ethnobiology and Ethnomedicine* 2006, 2 (1), 45.

114. Lee, K. H.; Lee, S. W.; Lee, S. H.; Li, W.; Lee, S., Rat Lens Aldose Reductase Inhibitory Activities of Cissus assamica var. pilosissima and Syzygium oblatum. *Natural Product Sciences* 2013, 19 (4), 275-280.

115. Lekshmi, R.; Rajesh, R.; Mini, S., Ethyl acetate fraction of Cissus quadrangularis stem ameliorates hyperglycaemia-mediated oxidative stress and suppresses inflammatory response in nicotinamide/streptozotocin induced type 2 diabetic rats. *Phytomedicine* 2015, 22 (10), 952-960.

116. Pathomwichaiwat, T.; Ochareon, P.; Soonthornchareonnon, N.; Ali, Z.; Khan, I. A.; Prathanturarug, S., Alkaline phosphatase activity-guided isolation of active compounds and new dammarane-type triterpenes from Cissus quadrangularis hexane extract. *Journal of ethnopharmacology* 2015, 160, 52-60.

117. Suhashini, R.; Chandra, J., Study of antibacterial potential and phytochemical constituents of three sided Cissus quadrangularis. *Journal of Chemical and Pharmaceutical Research* 2015, 7 (4), 1466-1469.

118. Kashikar, N.; George, I., Antibacterial activity of Cissus quadrangularis Linn. *Indian journal of pharmaceutical sciences* 2006, 68 (2).

119. Moyo, B.; Mukanganyama, S., Antibacterial Effects of Cissus welwitschii and Triumfetta welwitschii Extracts against Escherichia coli and Bacillus cereus. *International journal of bacteriology* 2015, 2015.

120. Vijayalakshmi, G.; Aysha, O.; Valli, S., Antibacterial and phytochemical analysis of cissus quadrangularis on selected uti pathogens and molecular characterization for phylogenetic analysis of klebsiella pneumoniae. *World Journal Of Pharmacy And Pharmaceutical Sciences* 2015, 4 (11), 1702-1713.

121. Selvan, A. T.; Yezdhani, R.; Subramanian, N. S.; Devi, M. R.; Prasad, B. S. G.; Kumar, S.; Parimala, S., Antimicrobial activity of methanolic extract of cissus pallida. *International Journal Of Pharmacognosy* 2014, 1 (9), 592-595.

122. Subramani, V.; Kamaraji, M.; Ramachandran, B.; Jerome, J., Screening of phytochemical constituents, trace metals and antimicrobial efficiency of Cissus vitiginea. *International Journal of Phytopharmacy* 2014, 4, 96-8.
123. Alzoreky, N.; Nakahara, K., Antibacterial activity of extracts from some edible plants commonly consumed in Asia. *International journal of food microbiology* 2003, 80 (3), 223-230.
124. Bhujade, A.; Gupta, G.; Talmale, S.; Das, S.; Patil, M., Induction of apoptosis in A431 skin cancer cells by Cissus quadrangularis Linn stem extract by altering Bax–Bcl-2 ratio, release of cytochrome c from mitochondria and PARP cleavage. *Food & function* 2013, 4 (2), 338-346.
125. Sáenz, M.; Garcia, M.; Quilez, A.; Ahumada, M., Cytotoxic activity of Agave intermixta L.(Agavaceae) and Cissus sicyoides L.(Vitaceae). *Phytotherapy Research* 2000, 14 (7), 552-554.
126. Lucena, F. R.; Almeida, E. R.; Aguiar, J. S.; Silva, T. G.; Souza, V. M.; Nascimento, S. C., Cytotoxic, antitumor and leukocyte migration activities of resveratrol and sitosterol present in the hidroalcoholic extract of Cissus sicyoides L., Vitaceae, leaves. *Revista Brasileira de Farmacognosia* 2010, 20 (5), 729-733.
127. Line-Edwige, M.; Raymond, F. G.; François, E.; Edouard, N., Antiproliferative effect of alcoholic extracts of some Gabonese medicinal plants on human colonic cancer cells. *African Journal of Traditional, Complementary and Alternative Medicines* 2009, 6 (2).
128. Vasconcelos, T. H. C. d.; Modesto-Filho, J.; Diniz, M. d. F. F. M.; Santos, H. B.; Aguiar, F. B. d.; Moreira, P. V. L., Acute pre-clinical toxicological study with the hydroalcoholic extract of the leaves of Cissus sicyoides L.(Vitaceae). *Revista Brasileira de Farmacognosia* 2007, 17 (4), 583-591.
129. Kothari, S. C.; Shivarudraiah, P.; Venkataramaiah, S. B.; Koppolu, K. P.; Gavara, S.; Jairam, R.; Krishna, S.; Chandrappa, R. K.; Soni, M. G., Safety assessment of Cissus quadrangularis extract (CQR-300): Subchronic toxicity and mutagenicity studies. *Food and chemical toxicology* 2011, 49 (12), 3343-3357.
130. Vijayalakshmi, A.; Kumar, P.; Sakthi Priyadarsini, S.; Meenaxshi, C., In Vitro Antioxidant and Anticancer Activity of Flavonoid Fraction from the Aerial Parts of Cissus quadrangularis Linn. against Human Breast Carcinoma Cell Lines. *Journal of Chemistry* 2013, 2013.
131. Jainu, M.; Mohan, K. V.; Devi, C. S., Protective effect of Cissus quadrangularis on neutrophil mediated tissue injury induced by aspirin in rats. *Journal of ethnopharmacology* 2006, 104 (3), 302-305.
132. Bhujade, A. M.; Talmale, S.; Kumar, N.; Gupta, G.; Reddanna, P.; Das, S. K.; Patil, M., Evaluation of Cissus quadrangularis extracts as an inhibitor of COX, 5-LOX, and proinflammatory mediators. *Journal of Ethnopharmacology* 2012, 141 (3), 989-996.
133. Adesanya, S. A.; Nia, R.; Martin, M.-T.; Boukamcha, N.; Montagnac, A.; Païs, M., Stilbene derivatives from Cissus quadrangularis. *Journal of Natural Products* 1999, 62 (12), 1694-1695.
134. Choi, E. J.; Ahn, W. S., Kaempferol induced the apoptosis via cell cycle arrest in human breast cancer MDA-MB-453 cells. *Nutrition research and practice* 2008, 2 (4), 322-325.
135. Jaganathan, S. K.; Supriyanto, E., Antiproliferative and molecular mechanism of eugenol-induced apoptosis in cancer cells. *Molecules* 2012, 17 (6), 6290-6304.
136. Walsh, S. E.; Maillard, J. Y.; Russell, A.; Catrenich, C.; Charbonneau, D.; Bartolo, R., Activity and mechanisms of action of selected biocidal agents on Gram-positive and-negative bacteria. *Journal of applied microbiology* 2003, 94 (2), 240-247.
137. Vanella, L.; Barbagallo, I.; Acquaviva, R.; Di Giacomo, C.; Cardile, V.; G Abraham, N.; Sorrenti, V., Ellagic acid: Cytodifferentiating and antiproliferative effects in human prostatic cancer cell lines. *Current pharmaceutical design* 2013, 19 (15), 2728-2736.

138. Abuelsaad, A. S.; Mohamed, I.; Allam, G.; Al-Solumani, A. A., Antimicrobial and immunomodulating activities of hesperidin and ellagic acid against diarrheic Aeromonas hydrophila in a murine model. *Life sciences* 2013, 93 (20), 714-722.

139. Mokoka, T. A.; McGaw, L. J.; Mdee, L. K.; Bagla, V. P.; Iwalewa, E. O.; Eloff, J. N., Antimicrobial activity and cytotoxicity of triterpenes isolated from leaves of Maytenus undata (Celastraceae). *BMC complementary and alternative medicine* 2013, 13 (1), 111.

140. Bhardwaj, A.; Sethi, G.; Vadhan-Raj, S.; Bueso-Ramos, C.; Takada, Y.; Gaur, U.; Nair, A. S.; Shishodia, S.; Aggarwal, B. B., Resveratrol inhibits proliferation, induces apoptosis, and overcomes chemoresistance through down-regulation of STAT3 and nuclear factor-κB–regulated antiapoptotic and cell survival gene products in human multiple myeloma cells. *Blood* 2007, 109 (6), 2293-2302.

141. Liu, Y.; Tang, Z.-G.; Lin, Y.; Qu, X.-G.; Lv, W.; Wang, G.-B.; Li, C.-L., Effects of quercetin on proliferation and migration of human glioblastoma U251 cells. *Biomedicine & Pharmacotherapy* 2017, 92, 33-38.

142. Zeng, J.; Liu, X.; Li, X.; Zheng, Y.; Liu, B.; Xiao, Y., Daucosterol Inhibits the Proliferation, Migration, and Invasion of Hepatocellular Carcinoma Cells via Wnt/β-Catenin Signaling. *Molecules* 2017, 22 (6), 862.

143. Prasad, S.; Yadav, V. R.; Sung, B.; Gupta, S. C.; Tyagi, A. K.; Aggarwal, B. B., Ursolic acid inhibits the growth of human pancreatic cancer and enhances the antitumor potential of gemcitabine in an orthotopic mouse model through suppression of the inflammatory microenvironment. *Oncotarget* 2016, 7 (11), 13182.

144. Saleh, N.; Zwiefak, A.; Mordarski, M.; Pulverer, G., Antibacterial activity of selected tropones and tropolones. Zentralblatt für Bakteriologie, Mikrobiologie und Hygiene. *Series a Medical Microbiology, Infectious Diseases, Virology, Parasitology* 1988, 270 (1-2), 160-170.

145. Puupponen-Pimiä, R.; Nohynek, L.; Meier, C.; Kähkönen, M.; Heinonen, M.; Hopia, A.; Oksman-Caldentey, K. M., Antimicrobial properties of phenolic compounds from berries. *Journal of applied microbiology* 2001, 90 (4), 494-507.

146. Keawsa-ard, S.; Natakankitkul, S.; Liawruangrath, S.; Teerawutgulrag, A.; Trisuwan, K.; Charoenying, P.; Pyne, S. G.; Liawruangrath, B., Anticancer and antibacterial activities of the isolated compounds from Solanum spirale Roxb. leaves. *Chiang Mai Journal of Science* 2012, 39 (3), 445-454.

147. Xie, Y.; Deng, P.; Zhang, Y.; Yu, W., Studies on the chemical constituents from Cissus assamica. *Journal of Chinese Medicinal Materials* 2009, 32 (2), 210-213.

148. Pan, G.; Li, W.; Luo, P.; Qin, J.; Su, G., Study on steroidal and triterpenoid constituents from Cissus pteroclada. *Journal of Chinese medicinal materials* 2013, 36 (8), 1274-1277.

149. Jain, V.; Thakur, A.; Hingorani, L.; Laddha, K., Lipid constituents from Cissus quadrangularis leaves. *Pharmacognosy Research* 2009, 1 (4), 231.

150. Xu, F.; Matsuda, H.; Hata, H.; Sugawara, K.; Nakamura, S.; Yoshikawa, M., Structures of new flavonoids and benzofuran-type stilbene and degranulation inhibitors of rat basophilic leukemia cells from the Brazilian herbal medicine Cissus sicyoides. *Chemical and Pharmaceutical Bulletin* 2009, 57 (10), 1089-1095.

151. Rao, G. V.; Annamalai, T.; Mukhopadahyay, T.; Machavolu, S.; Lakshmi, M., Chemical constituents and melanin promotion activity of Cissus quadrangularis Linn. *Research Journal of Chemical Sciences* 2011, 1 (0), 25-29.

152. Musa, A. M.; Tajuddeen, N.; Idris, A. Y.; Rafindadi, A. Y.; Abdullahi, M. I.; Aliyu, A. B.; Abdullahi, M. S.; Ibrahim, M. A., A new Antimicrobial Prenylated Benzo-lactone from the Rhizome of Cissus cornifolia. *Pharmacognosy research* 2015, 7 (4), 363.

153. Zgoda, J.; Porter, J., A convenient microdilution method for screening natural products against bacteria and fungi. *Pharmaceutical Biology* 2001, 39 (3), 221-225.

154. Murray, P.; Baron, E.; Pfaller, M.; Tenover, F.; Myolken, National Committee for Clinical Laboratory Standards. Antibacterial Susceptibility Tests: Dilution and Disk Diffusion Methods. *J Manual of Clinical Microbiology* 1999, 1526-1543.

155. Basu, A.; Saito, K.; Meyer, K.; Ray, R. B.; Friedman, S. L.; Chang, Y.-H.; Ray, R., Stellate cell apoptosis by a soluble mediator from immortalized human hepatocytes. *Apoptosis* 2006, 11 (8), 1391.

156. Souza, R. P.; Bonfim-Mendonça, P. d. S.; Gimenes, F.; Ratti, B. A.; Kaplum, V.; Bruschi, M. L.; Nakamura, C. V.; Silva, S. O.; Maria-Engler, S. S.; Consolaro, M. E., Oxidative stress triggered by Apigenin induces apoptosis in a comprehensive panel of human cervical cancer-derived cell lines. *Oxidative medicine and cellular longevity* 2017, 2017.

157. Awad, A. B.; Barta, S. L.; Fink, C. S.; Bradford, P. G., β-Sitosterol enhances tamoxifen effectiveness on breast cancer cells by affecting ceramide metabolism. *Molecular nutrition & food research* 2008, 52 (4), 419-426.

158. Cookson, D. J.; Smith, B. E., Determination of structural characteristics of saturates from diesel and kerosine fuels by carbon-13 nuclear magnetic resonance spectrometry. *Analytical Chemistry* 1985, 57 (4), 864-871.

159. Tessmann, D.; Dianese, J, Hentriacontane: a leaf hydrocarbon from Syzygium jambos with stimulatory effects on the germination of urediniospores of Puccinia psidii. *Fitopatologia Brasileira* 2002, 27 (5), 538-542.

160. Tayade, A. B.; Dhar, P.; Kumar, J.; Sharma, M.; Chauhan, R. S.; Chaurasia, O. P.; Srivastava, O., Chemometric profile of root extracts of Rhodiola imbricata Edgew. with hyphenated gas chromatography mass spectrometric technique. *J PLoS One* 2013, 8 (1).

161. Siddiqui, B. S.; Ali, S. T.; Rajput, M. T.; Gulzar, T.; Rasheed, M.; Mehmood, GC-based analysis of insecticidal constituents of the flowers of Azadirachta indica A. Juss. *Journal Natural Product Research* 2009, 23 (3), 271-283.

162. Aggarwal, B.; Ali, M.; Singh, V.; Singla, R. K., Isolation and Characterization of Phytoconstituents from the Stems of Ichnocarpus frutescens. *Chinese Journal of Natural Medicines* 2010, 8 (6), 401-404.

163. Biswas, S. M.; Chakraborty, Shedded Artocarpus leaves-good plant sources of natural squalene with potent antioxidant and antimicrobial activity-alternative to marine animals. *Journal of Natural Pharmacy*, 2013, 4 (1), 21-27.

164. Khan, R.; Khanam, Z.; Khan, Isolation and characterization of n-octacosanoic acid from Viburnum foetens: a novel antibiofilm agent against Streptococcus Mutans. *J Medicinal Chemistry Research* 2012, 21 (7), 1411-1417.

165. Babu, A.; Anand, D.; Saravanan, Phytochemical Analysis of Ficus arnottiana (Miq.) Miq. Leaf Extract Using GC-MS Analysis. *International Journal of Pharmacognosy and Phytochemical Research* 2017, 9, 775-779.

166. Stein, S.; Linstrom, P.; Mirokhin, Y.; Tchekhovskoi, D.; Yang, NIST Mass Spectral Search Program (Version 2.0 f). 2008.

167. Chaturvedula. Prakash, I., Isolation of Stigmasterol and β-Sitosterol from the dichloromethane extract of Rubus suavissimus. *International Journal of Pharmacy and Pharmaceutical Sciences* 2012.

168. Sheng, Y.; Chen, Isolation and identification of an isomer of β-sitosterol by HPLC and GC-MS. *Health* 2009, 1 (3), 203-206.

169. Gololo, S. S.; Shai, L. J.; Sethoga, L.; Agyei, N.; Bassey, K. E.; Mogale, Isolation of a mixture of Phytosterol compounds from the n-Hexane extract of Jatropha lagarinthoides (Sond) collected from Zebediela sub-region in Limpopo province, South Africa. *Journal Chemical Pharmaceutical Sciences* 2016, 9 (4), 3084-3087.

170. Nyemb, J. N.; Magnibou, L. M.; Talla, E.; Tchinda, A. T.; Tchuenguem, R. T.; Henoumont, C.; Laurent, S.; Mbafor, Lipids constituents from gardenia aqualla stapf & hutch. *Open Chemistr* 2018, 16 (1), 371-376.

171. Gniwotta, F.; Vogg, G.; Gartmann, V.; Carver, T. L.; Riederer, M.; Jetter, What do microbes encounter at the plant surface? Chemical composition of pea leaf cuticular waxes. *Plant Physiology* 2005, 139 (1), 519-530.

172. Hannoufa, A.; McNevin, J.; Lemieux, B. J. Epicuticular waxes of eceriferum mutants of Arabidopsis thaliana. *Journal of Phytochemistry* 1993, 33 (4), 851-855.
173. Kunst, L.; Samuels, A., Biosynthesis and secretion of plant cuticular wax. *Progress in lipid research* 2003, 42 (1), 51-80.
174. Gupta, M. M.; Verma, R. K., Lipid constituents of Cissus quadrangularis. *Phytochemistry* 1991, 30 (3), 875-878.
175. Heredia-Guerrero, J. A.; Benítez, J. J.; Domínguez, E.; Bayer, I. S.; Cingolani, R.; Athanassiou, A.; Heredia, A., Infrared and Raman spectroscopic features of plant cuticles: a review. *Frontiers in plant science* 2014, 5, 305.
176. Vishnuthari., N.; Sripathi., S. K., GC-MS Analysis of Hexane Extract of Stems and Roots of the Ethnomedicinal Plant Cissus quadrangularis Linn. *Journal of Chemical, Biological and Physical Sciences* 2015, 5 (4), 3954-3963.
177. Rosy, B. A.; Rosakutty, P., GC-MS analysis of methanol wild plant and callus extracts from three Cissus species, Family Vitaceae. *Journal of chemical and pharmaceutical research* 2012, 4 (7), 3420-3426.
178. Chipiti, T.; Ibrahim, M. A.; Koorbanally, N. A.; Islam, M. S., In vitro antioxidant activity and GC-MS analysis of the ethanol and aqueous extracts of Cissus cornifolia (Baker) Splanch (Vitaceae) parts. *Acta Poloniae Pharmaceutica Drug Research* 2015, 72 (1), 119-127.
179. Lara, I.; Belge, B.; Goulao, L. F., A focus on the biosynthesis and composition of cuticle in fruits. *Journal of agricultural and food chemistry* 2015, 63 (16), 4005-4019.
180. Zhukov, A., Palmitic acid and its role in the structure and functions of plant cell membranes. *Russian journal of plant physiology* 2015, 62 (5), 706-713.
181. Gunstone, F. D.; Harwood, J. L.; Dijkstra, A. J., The lipid handbook with CD-ROM. *CRC press* 2007.
182. Chanda, S.; Baravalia, Y.; Nagani, K., Spectral analysis of methanol extract of Cissus quadrangularis L. stem and its fractions. *Journal of Pharmacognosy and Phytochemistry* 2013, 2 (4).
183. Heldt, H., Plant biochemistry. *Elsevier Academic Press*. XXIV: 2005.
184. Koonce, S. D.; Brown, J., A study of the alcohols of carnauba wax. *Journal of the American Oil Chemists' Society* 1944, 21 (8), 231-234.
185. Wal, P.; Wal, A.; Sharma, G.; Rai, A., Biological activities of lupeol. *Systematic Reviews in Pharmacy* 2011, 2 (2), 96.
186. Sheikh, S.; Siddiqui, S.; Dhasmana, A., Cissus quadrangularis Linn. Stem ethanolic extract liberates reactive oxygen species and induces mitochondria mediated apoptosis in KB cells. *Pharmacognosy magazine* 2015, 11 (Suppl 3), S365.
187. Griebel, T.; Zeier, J., A role for β-sitosterol to stigmasterol conversion in plant–pathogen interactions. *The plant journal* 2010, 63 (2), 254-268.
188. Jing, X.; Grebenok, R. J.; Behmer, S. T., Plant sterols and host plant suitability for generalist and specialist caterpillars. *Journal of insect physiology* 2012, 58 (2), 235-244.
189. Choubey, S.; Varughese, L. R.; Kumar, V.; Beniwal, Medicinal importance of gallic acid and its ester derivatives: a patent review. *Pharmaceutical patent analyst* 2015, 4 (4), 305-315.
190. Al-Said, M.; Khalifa, A.; Al-Azizi, M., Flavonoids from Cissus digitata. *International journal of pharmacognosy* 1991, 29 (4), 281-283.
191. Vijayalakshmi, A.; Kumar, P.; Sakthi Priyadarsini, S.; Meenaxshi, C., In vitro antioxidant and anticancer activity of flavonoid fraction from the aerial parts of Cissus quadrangularis linn against human breast carcinoma cell lines. *Journal of Chemistry* 2013, 2013.

192. Toledo, M.; Reyes, F.; Iaderoza, F.; Francis, F.; Draettao, S., Anthocyanins from anil trepador Cissus sicyoides. *Journal of Food Science* 1983, 48.

193. Tröndle, D.; Schröder, S.; Kassemeyer, H. H.; Kiefer, C.; Koch, M. A.; Nick, P., Molecular phylogeny of the genus Vitis (Vitaceae) based on plastid markers. *American Journal of Botany* 2010, 97 (7), 1168-1178.

194. Billet, K.; Houillé, B.; de Bernonville, T. D.; Besseau, S.; Oudin, A.; Courdavault, V.; Delanoue, G.; Guérin, L.; Clastre, M.; Giglioli-Guivarc'h, N., Field-based metabolomics of vitis vinifera l. Stems provides new insights for genotype discrimination and polyphenol metabolism structuring. *Frontiers in plant science* 2018, 9.

195. Kiselev, K. V.; Aleynova, O. A.; Grigorchuk, V. P.; Dubrovina, A. S., Stilbene accumulation and expression of stilbene biosynthesis pathway genes in wild grapevine Vitis amurensis Rupr. *Planta* 2017, 245 (1), 151-159.

196. Halket, J. M.; Waterman, D.; Przyborowska, A. M.; Patel, R. K.; Fraser, P. D.; Bramley, Chemical derivatization and mass spectral libraries in metabolic profiling by GC/MS and LC/MS/MS. *Journal of Experimental Botany* 2004, 56 (410), 219-243.

197. Pandey, A.; Tripathi, S., Concept of standardization, extraction and pre phytochemical screening strategies for herbal drug. *Journal of Pharmacognosy and Phytochemistry* 2014, 2 (5).

198. Morales, M.; Ros, B.; Pedreno, M., Plant stilbenes: recent advances in their chemistry and biology. *Advances in plant physiology*. Volume 3 2000, 39-70.

199. Jeandet, P.; Douillet-Breuil, A.-C.; Bessis, R.; Debord, S.; Sbaghi, M.; Adrian, M., Phytoalexins from the Vitaceae: biosynthesis, phytoalexin gene expression in transgenic plants, antifungal activity, and metabolism. *Journal of Agricultural and food chemistry* 2002, 50 (10), 2731-2741.

200. Dercks, W.; Creasy, L.; Luczka-Bayles, C., Stilbene phytoalexins and disease resistance in Vitis. *Marcel Dekker* New York: 1995.

201. Grattan, B., Plant sterols as anticancer nutrients: evidence for their role in breast cancer. *Journal of Nutrients* 2013, 5 (2), 359-387.

202. De Filippis, B.; Ammazzalorso, A.; Fantacuzzi, M.; Giampietro, L.; Maccallini, C.; Amoroso, R. Anticancer activity of stilbene-based derivatives. *Journal of Chemical and Medicinal Chemistry* 2017, 12 (8), 558-570.

203. Kanadaswami, C.; Lee, L.T.; Lee, P.P.; Hwang, J.J.; Ke, F.C.; Huang, Y.T.; Lee, M.T. The antitumor activities of flavonoids. *In vivo* 2005, 19 (5), 895-909.

204. Beltrame, F. L.; Pessini, G. L.; Doro, D. L.; Dias Filho, B. P.; Bazotte, R. B.; Cortez, D. A. G., Evaluation of the antidiabetic and antibacterial activity of Cissus sicyoides. *Brazilian Archives of Biology and Technology* 2002, 45 (1), 21-25.

205. Alejandro, M.; Alberto, M.; Gama Campillo, L. M.; Mariaca Méndez, R., El uso de las plantas medicinales en las comunidades Maya-Chontales de Nacajuca, Tabasco, México. *Polibotánica* 2010, (29), 213-262.

206. Chan, M., Antimicrobial effect of resveratrol on dermatophytes and bacterial pathogens of the skin. *Biochemical Pharmacology* 2002, 63 (2), 99-104.

207. Opoku, A.; Geheeb-Keller, M.; Lin, J.; Terblanche, S.; Hutchings, A.; Chuturgoon, A.; Pillay, D., Preliminary screening of some traditional Zulu medicinal plants for antineoplastic activities versus the HepG2 cell line. *Phytotherapy Research* 2000, 14 (7), 534-537.

208. Wang, P.; Henning, S. M.; Heber, D. Limitations of MTT and MTS-based assays for measurement of antiproliferative activity of green tea polyphenols. *Plos one* 2010, 5 (4).

209. Tahsin, T.; Wansi, J. D.; Al-Groshi, A.; Evans, A.; Nahar, L.; Martin, C.; Sarker, S. D., Cytotoxic Properties of the Stem Bark of Citrus reticulata Blanco (Rutaceae). *Phytotherapy Research* 2017, 31 (8), 1215-1219.

210. Awad, A.; Chinnam, M.; Fink, C.; Bradford, P., β-Sitosterol activates Fas signaling in human breast cancer cells. *Phytomedicine* 2007, 14 (11), 747-754.
211. Chen, Y.-C.; Lee, H.-Z.; Chen, H.-C.; Wen, C.-L.; Kuo, Y.-H.; Wang, G.-J., Anti-inflammatory components from the root of Solanum erianthum. *International journal of molecular sciences* 2013, 14 (6), 12581-12592.
212. Ju, Y. H.; Clausen, L. M.; Allred, K. F.; Almada, A. L.; Helferich, W. G., β-sitosterol, β-sitosterol glucoside, and a mixture of β-sitosterol and β-sitosterol glucoside modulate the growth of estrogen-responsive breast cancer cells in vitro and in ovariectomized athymic mice. *The Journal of nutrition* 2004, 134 (5), 1145-1151.
213. He, Y.; Liu, F.; Zhang, L.; Wu, Y.; Hu, B.; Zhang, Y.; Li, Y.; Liu, H., Growth inhibition and apoptosis induced by lupeol, a dietary triterpene, in human hepatocellular carcinoma cells. *Biological and Pharmaceutical Bulletin* 2011, 34 (4), 517-522.
214. Prasad, S.; Nigam, N.; Kalra, N.; Shukla, Y., Regulation of signaling pathways involved in lupeol induced inhibition of proliferation and induction of apoptosis in human prostate cancer cells. *Molecular carcinogenesis* 2008, 47 (12), 916-924.
215. Siveen, K.; Nguyen, A.; Lee, J.; Li, F.; Singh, S.; Kumar, A. P.; Low, G.; Jha, S.; Tergaonkar, V.; Ahn, K., Negative regulation of signal transducer and activator of transcription-3 signalling cascade by lupeol inhibits growth and induces apoptosis in hepatocellular carcinoma cells. *British journal of cancer* 2014, 111 (7), 1327.
216. Zhang, Y.; Gu, Y.; Xie, J.; Hu, Y. Anti-tumor effect of piceatannol through induction of cell apoptosis via up-regulation of microRNA-125b expression on pancreatic cancer. *International Journal of Clinical and Experimental Medicine* 2017, 10 (10), 14495-14502.
217. Maggiolini, M.; Recchia, A.; Bonofiglio, D.; Catalano, S.; Vivacqua, A.; Carpino, A.; Rago, V.; Rossi, R.; Ando, S. J. The red wine phenolics piceatannol and myricetin act as agonists for estrogen receptor α in human breast cancer cells. *Journal of Molecular Endocrinology* 2005, 35 (2), 269-281.
218. Kim, S. H.; Hwang, K. A.; Choi, K. C., Treatment with kaempferol suppresses breast cancer cell growth caused by estrogen and triclosan in cellular and xenograft breast cancer models. *The Journal of nutritional biochemistry* 2016, 28, 70-82.
219. Khorsandi, L.; Orazizadeh, M.; Niazvand, F.; Abbaspour, M.; Mansouri, E.; Khodadadi, A., Quercetin induces apoptosis and necroptosis in MCF-7 breast cancer cells. *Bratislavske lekarske listy* 2017, 118 (2), 123-128.
220. Ranganathan, S.; Halagowder, D.; Sivasithambaram, N. D., Quercetin suppresses twist to induce apoptosis in MCF-7 breast cancer cells. *PloS one* 2015, 10 (10), e0141370.
221. Amico, V.; Barresi, V.; Chillemi, R.; Tringali, C., Bioassay-Guided Isolation of Antiproliferative Compounds from Grape (Vitis vinifera) Stems. *Natural Product Communications* 2008, 4 (1), 27-34.
222. Hao, J.; Liu, J.; Wen, X.; Sun, H., Synthesis and cytotoxicity evaluation of oleanolic acid derivatives. *Bioorganic & medicinal chemistry letters* 2013, 23 (7), 2074-2077.
223. Kim, Y.-K.; Yoon, S. K.; Ryu, S. Cytotoxic triterpenes from stem bark of Physocarpus intermedius. *Planta Medica* 2000, 66 (05), 485-486.
224. Mishra, T.; Arya, R. K.; Meena, S.; Joshi, P.; Pal, M.; Meena, B.; Upreti, D.; Rana, T.; Datta, D., Isolation, characterization and anticancer potential of cytotoxic triterpenes from Betula utilis bark. *PloS one* 2016, 11 (7), e0159430.
225. Pisha, E.; Chai, H.; Lee, I.-S.; Chagwedera, T. E.; Farnsworth, N. R.; Cordell, G. A.; Beecher, C. W.; Fong, H. H.; Kinghorn, A. D.; Brown, D. Discovery of betulinic acid as a selective inhibitor of human melanoma that functions by induction of apoptosis. *Nature Medicine* 1995, 1 (10), 1046.

226. Kang, H. R.; Eom, H. J.; Lee, S. R.; Choi, S. U.; Kang, K. S.; Lee, K. R. Bioassay-guided isolation of antiproliferative triterpenoids from Euonymus alatus twigs. *Natural Products Communications* 2015, 10 (11).

227. Damle, A. A.; Pawar, Y. P.; Narkar, A. A., Anticancer activity of betulinic acid on MCF-7 tumors in nude mice. *Indian Journal of Experimental Biology* 2013.

228. Kassi, E.; Papoutsi, Z.; Pratsinis, H.; Aligiannis, N.; Manoussakis, M.; Moutsatsou, P., Ursolic acid, a naturally occurring triterpenoid, demonstrates anticancer activity on human prostate cancer cells. *Journal of cancer research and clinical oncology* 2007, 133 (7), 493-500.

229. Li, X.; Song, Y.; Zhang, P.; Zhu, H.; Chen, L.; Xiao, Y.; Xing, Y. J. T. B., Oleanolic acid inhibits cell survival and proliferation of prostate cancer cells in vitro and in vivo through the PI3K/Akt pathway. *Journal of Tumor Biology* 2016, 37 (6), 7599-7613.

230. Jiang, X.; Li, T.; Liu, R. 2α-Hydroxyursolic acid inhibited cell proliferation and induced apoptosis in MDA-MB-231 human breast cancer cells through the p38/MAPK signal transduction pathway. *Journal of Agricultural and Food Chemistry* 2016, 64 (8), 1806-1816.

231. Kolahi, M.; Tabandeh, M. R.; Saremy, S.; Hosseini, S. A.; Hashemitabar, M. The Study of Apoptotic Effect of p-Coumaric Acid on Breast Cancer Cells MCF-7. *Journal of Shahid Sadoughi University of Medical Sciences and Health Services* 2016, 24 (3), 211-221.

232. Eroğlu, C.; Seçme, M.; Bağcı, G.; Dodurga, Y. Assessment of the anticancer mechanism of ferulic acid via cell cycle and apoptotic pathways in human prostate cancer cell lines. *Tumor Biology* 2015, 36 (12), 9437-9446.

233. Caesar, L. K.; Cech, N. Synergy and antagonism in natural product extracts: when 1+ 1 does not equal 2. *Natural Product Reports* 2019.

234. Wishart, D. S.; Feunang, Y. D.; Marcu, A.; Guo, A. C.; Liang, K.; Vázquez-Fresno, R.; Sajed, T.; Johnson, D.; Li, C.; Karu, N. HMDB 4.0: the human metabolome database for 2018. *Nucleic Acids Research* 2017, 46 (D1), D608-D617.

235. Flamini, R.; De Rosso, M.; De Marchi, F.; Dalla Vedova, A.; Panighel, A.; Gardiman, M.; Maoz, I.; Bavaresco, L. An innovative approach to grape metabolomics: stilbene profiling by suspect screening analysis. *Metabolomics* 2013, 9 (6), 1243-1253.

236. Du, C.; Dong, M.-H.; Ren, Y.-J.; Jin, L.; Xu, C. Design, synthesis and antibreast cancer MCF-7 cells biological evaluation of heterocyclic analogs of resveratrol. *Journal of Asian Natural Product Research* 2017, 19 (9), 890-902.

237. Kai, L.; Levenson, A. Combination of resveratrol and antiandrogen flutamide has synergistic effect on androgen receptor inhibition in prostate cancer cells. *Anticancer research* 2011, 31 (10), 3323-3330.

238. De Maria, S.; Scognamiglio, I.; Lombardi, A.; Amodio, N.; Caraglia, M.; Cartenì, M.; Ravagnan, G.; Stiuso, P. Polydatin, a natural precursor of resveratrol, induces cell cycle arrest and differentiation of human colorectal Caco-2 cell. *Journal of Translational Medicine* 2013, 11 (1), 264.

239. Zhang, T.; Zhu, X.; Wu, H.; Jiang, K.; Zhao, G.; Shaukat, A.; Deng, G.; Qiu, C. Targeting the ROS/PI3K/AKT/HIF-1α/HK2 axis of breast cancer cells: Combined administration of Polydatin and 2-Deoxy-d-glucose. *Journal of Cellular and Molecular Medicine* 2019, 23 (5), 3711-3723.

240. Esquenet, M.; Swinnen, J. V.; Heyns, W.; Verhoeven, G. LNCaP prostatic adenocarcinoma cells derived from low and high passage numbers display divergent responses not only to androgens but also to retinoids. *Journal of Steroid Biochemistry and Molecular Biology* 1997, 62 (5-6), 391-399.

241. Chavan, P.; Joshi, K.; Patwardhan, B., DNA microarrays in herbal drug research. *Evidence-Based Complementary and Alternative Medicine* 2006, 3 (4), 447-457.

242. Wang, S.; Cheng, Q., Microarray analysis in drug discovery and clinical applications. *In Bioinformatics and Drug Discovery*, Springer: 2006; pp 49-65.

243. Jeoung, D.; Oh, S.J.; Lee, S.; Baek, M.; Lee, Y.H.; Baek, N.I.; Kim, H.Y. Microarray analysis of piceatannol-induced changes in gene expression in human gastric cancer cells. *Biotechnology Letters volume* 2002, 24 (6), 463-467.

244. Jones, S. B.; DePrimo, S. E.; Whitfield, M. L.; Brooks, J. Resveratrol-induced gene expression profiles in human prostate cancer cells. *Cancer Epidemiology Biomarkers Prevention*. 2005 Mar; 14(3): 596-604.

245. Zaret, K. S.; Mango, S. E. Pioneer transcription factors, chromatin dynamics, and cell fate control. *Current opinion in genetics and development* 2016, 37, 76-81.

246. Abate-Shen, C. Deregulated homeobox gene expression in cancer: cause or consequence? *Nature Reviews Cance*r 2002, 2 (10), 777.

247. Dennis, J. H.; Budhram-Mahadeo, V.; Latchman, D. The Brn-3b POU family transcription factor regulates the cellular growth, proliferation, and anchorage dependence of MCF7 human breast cancer cells. *Oncogene* 2001, 20 (36), 4961.

248. Trempus, C. S.; Wei, S. J.; Humble, M. M.; Dang, H.; Bortner, C. D.; Sifre, M. I.; Kissling, G. E.; Sunman, J. A.; Akiyama, S. K.; Roberts, J. A novel role for the T-box transcription factor Tbx1 as a negative regulator of tumor cell growth in mice. *Molecular Carcinogenesis* 2011, 50 (12), 981-991.

249. Wu, D.; Zhang, R.; Zhao, R.; Chen, G.; Cai, Y. A novel function of novobiocin: disrupting the interaction of HIF 1α and p300/CBP through direct binding to the HIF1α C-terminal activation domain. *Plos One* 2013, 8 (5), e62014.

250. Sarmento, O. F.; Svingen, P. A.; Xiong, Y.; Xavier, R. J.; McGovern, D.; Smyrk, T. C.; Papadakis, K. A.; Urrutia, R. A.; Faubion, W. A novel role for Kruppel-like Factor 14 (KLF14) in T-regulatory cell differentiation. *Cellular and molecular gastroenterology and hepatology*. 2015, 1 (2), 188-202. e4.

251. Payne, K. J.; Dovat, S. Ikaros and tumor suppression in acute lymphoblastic leukemia. *Critical reviews in oncogenesis* 2011, 16 (1-2).

252. Fernandes, G. F. S.; Silva, G. D. B.; Pavan, A. R.; Chiba, D. E.; Chin, C. M.; Dos Santos, J. Epigenetic regulatory mechanisms induced by resveratrol. *Nutrients* 2017, 9 (11), 1201.

253. Toyokawa, G.; Cho, H.S.; Iwai, Y.; Yoshimatsu, M.; Takawa, M.; Hayami, S.; Maejima, K.; Shimizu, N.; Tanaka, H.; Tsunoda, T. The histone demethylase JMJD2B plays an essential role in human carcinogenesis through positive regulation of cyclin-dependent kinase 6. *Cancer prevention research* 2011, 4 (12), 2051-2061.

254. Yu, H.; Pan, W.; Huang, H.; Chen, J.; Sun, B.; Yang, L.; Zhu, P. J. Screening Analysis of Sirtuins Family Expression on Anti-Inflammation of Resveratrol in Endothelial Cells. *Medical science monitor* 2019, 25, 4137.

255. Chen, D.; Li, T.; Wang, C.; Lei, G.; Wang, R.; Wang, Z.; Yu, L.; Yan, J.; Zhang, P.; Wang, X. High-level SETD1B gene expression is associated with unfavorable prognosis in hepatocellular carcinoma. *Molecular medicine reports* 2019, 19 (3), 1587-1594.

256. Vaysse, C.; Philippe, C.; Martineau, Y.; Quelen, C.; Hieblot, C.; Renaud, C.; Nicaise, Y.; Desquesnes, A.; Pannese, M.; Filleron, T. Key contribution of eIF4H-mediated translational control in tumor promotion. *Oncotarget* 2015, 6 (37), 39924.

257. Gong, S.; Li, Q.; Jeter, C. R.; Fan, Q.; Tang, D. G.; Liu, B. Regulation of NANOG in cancer cells. *Molecular Carcinogenesis* 2015, 54 (9), 679-687.

258. Shankar, S.; Nall, D.; Tang, S.N.; Meeker, D.; Passarini, J.; Sharma, J.; Srivastava, R. Resveratrol inhibits pancreatic cancer stem cell characteristics in human and KrasG12D transgenic mice by inhibiting pluripotency maintaining factors and epithelial-mesenchymal transition. *Plos One* 2011, 6 (1).

259. Capaccione, K. M.; Pine, S. The Notch signaling pathway as a mediator of tumor survival. *Carcinogenesis* 2013, 34 (7), 1420-1430.

260. Ino, Y.; Arakawa, N.; Ishiguro, H.; Uemura, H.; Kubota, Y.; Hirano, H.; Toda, T. Phosphoproteome analysis demonstrates the potential role of THRAP3 phosphorylation in androgen-independent prostate cancer cell growth. *Proteomics* 2016, 16 (7), 1069-1078.

261. Runkle, E., Mu, D. Tight junction proteins: from barrier to tumorigenesis. *Cancer letters* 2013, 337 (1), 41-48.

262. Sareen, D.; Van Ginkel, P. R.; Takach, J. C.; Mohiuddin, A.; Darjatmoko, S. R.; Albert, D. M.; Polans, A. Mitochondria as the primary target of resveratrol-induced apoptosis in human retinoblastoma cells. *Investigative Ophthalmology & Visual Science* 2006, 47 (9), 3708-3716.

263. de Padua, M. C.; Delodi, G.; Vučetić, M.; Durivault, J.; Vial, V.; Bayer, P.; Noleto, G. R.; Mazure, N. M.; Ždralević, M.; Pouysségur, J. Disrupting glucose-6-phosphate isomerase fully suppresses the "Warburg effect" and activates OXPHOS with minimal impact on tumor growth except in hypoxia. *Oncotarget* 2017, 8 (50), 87623.

264. Saunier, E.; Antonio, S.; Regazzetti, A.; Auzeil, N.; Laprévote, O.; Shay, J. W.; Coumoul, X.; Barouki, R.; Benelli, C.; Huc, L. Resveratrol reverses the Warburg effect by targeting the pyruvate dehydrogenase complex in colon cancer cells. *Scientific Reports* 2017, 7 (1), 6945.

265. Lytovchenko, O.; Kunji, E. R. Expression and putative role of mitochondrial transport proteins in cancer. *Biochimica et biophysica acta. Bioenergetics* 2017, 1858 (8), 641-654.

266. Rahman, M. S.; Akhtar, N.; Jamil, H. M.; Banik, R. S.; Asaduzzaman, S. TGF-β/BMP signaling and other molecular events: regulation of osteoblastogenesis and bone formation. *Bone Research* 2015, 3, 15005.

267. Körner, M.; Stöckli, M.; Waser, B.; Reubi, J. GLP-1 receptor expression in human tumors and human normal tissues: potential for in vivo targeting. *Journal of Nuclear Medicine* 2007, 48 (5), 736-743.

268. Koike, H.; Ito, K.; Takezawa, Y.; Oyama, T.; Yamanaka, H.; Suzuki, K. Insulin-like growth factor binding protein-6 inhibits prostate cancer cell proliferation: implication for anticancer effect of diethylstilbestrol in hormone refractory prostate cancer. *British Journal of Cancer* 2005, 92 (8), 1538.

269. Belfiore, A.; Malaguarnera, R. The insulin receptor: a new target for cancer therapy. *Frontiers in endocrinology* 2011, 2, 93.

270. Stolfi, C.; Marafini, I.; De Simone, V.; Pallone, F.; Monteleone, G. J. The dual role of Smad7 in the control of cancer growth and metastasis. *International journal of molecular sciences*. 2013, 14 (12), 23774-23790.

271. Bach, D. H; Park, H. J.; Lee, S. The dual role of bone morphogenetic proteins in cancer. *Molecular therapy oncolytics*. 2018, 8, 1-13.

272. Chao, S.C.; Chen, Y.J.; Huang, K.H.; Kuo, K.L.; Yang, T.H.; Huang, K.Y.; Wang, C.C.; Tang, C.H.; Yang, R.S.; Liu, S.H. Induction of sirtuin-1 signaling by resveratrol induces human chondrosarcoma cell apoptosis and exhibits antitumor activity. *Scientific Reports* 2017, 7 (1), 3180.

273. Kumar, S.; Lombard, D. B. Functions of the sirtuin deacylase SIRT5 in normal physiology and pathobiology. *Critical reviews in biochemistry and molecular biology* 2018, 53 (3), 311-334.

274. Li, Q.; Lozano, G. J., Molecular pathways: targeting Mdm2 and Mdm4 in cancer therapy. *Clinical Cancer Research* 2013, 19 (1), 34-41.

275. Liu, D.; Liu, M.; Wang, W.; Pang, L.; Wang, Z.; Yuan, C.; Liu, K. Overexpression of apoptosis-inducing factor mitochondrion-associated 1 (AIFM1) induces apoptosis by promoting the transcription of caspase3 and DRAM in hepatoma cells. *Biochemical and biophysical research communications* 2018, 498 (3), 453-457.

276. Liu, A. Y. Differential expression of cell surface molecules in prostate cancer cells. *Cancer Research* 2000, 60 (13), 3429-3434.

Supplementary Contents

Table 24. Functional annotation of upregulated genes by resveratrol (IC_{25}) on PC3 cells (part 1)

No	Gene ID	Gene Name	Biological function
1	SNX12	Sorting nexin-12	
2	AHNAK	Neuroblast differentiation-associated protein AHNAK	
3	ABCA12	ATP-binding cassette sub-family A member 12	ATP-binding cassette (ABC) transporter
4	NP001025045	Rab15 effector protein	
5	CAV3	Caveolin-3	G-protein modulator
6	ERCC6	DNA excision repair protein ERCC-6	
7	HMX2	Homeobox protein HMX2	transcription factor
8	C7orf26	Uncharacterized protein C7orf26	
9	GABPB2	GA-binding protein subunit beta-1	
10	ALG1	beta-mannosyltransferase	glycosyltransferase
11	MAFA	Transcription factor MafA	basic leucine zipper transcription factor
12	NP001073958	Glyoxalase domain-containing protein 5	
13	KITLG	Kit ligand	
14	ACSS2	Acetyl-coenzyme A synthetase, cytoplasmic	
15	IKZF1	DNA-binding protein Ikaros	KRAB box transcription factor
16	DCHS2	Protocadherin-23	
17	ZNF524	Zinc finger protein 524	transcription factor
18	PCDH18	Protocadherin-18	
19	EFHC2	EF-hand domain-containing family member C2	
20	HOXD12	Homeobox protein Hox-D12	transcription factor
21	OGT	UDP-N-acetylglucosamine	N-acetylglucosaminyltransferase
22	MON1A	Vacuolar fusion protein MON1 homolog A	
23	KRBA2	KRAB-A domain-containing protein 2	
24	MTHFD2	Bifunctional methylenetetrahydrofolate	dehydrogenase, mitochondrial
25	RBX1	E3 ubiquitin-protein ligase RBX1	ubiquitin-protein ligase
26	IZUMO1	Izumo sperm-egg fusion protein 1	
27	UTP20	Small subunit processome component 20 homolog	
28	FAM124B	Protein FAM124B	
29	UBADC1	Ubiquitin-associated domain-containing protein 1	
30	VAMP4	Vesicle-associated membrane protein 4	
31	ATP5H	ATP synthase subunit d, mitochondrial	ATP synthase
32	MLL3	Histone-lysine N-methyltransferase 2C	epigenetic modifier
33	KDELR3	ER lumen protein-retaining receptor 3	membrane trafficking regulatory protein
34	SERPINC1	Antithrombin-III	serine protease inhibitor
35	NP_056274	Atlastin-3	heterotrimeric G-protein
36	CTSZ	Cathepsin Z	cysteine protease
37	ATXN1	Ataxin-1	
38	MARCH7	E3 ubiquitin-protein ligase MARCH7	
39	LAGE3	EKC/KEOPS complex subunit LAGE3	
40	CITED4	Cbp/p300-interacting transactivator 4	transcription cofactor

Table 24. Functional annotation of upregulated genes by resveratrol (IC_{25}) on PC3 cells (part 2)

No	Gene ID	Gene Name	Biological function
41	NUSAP1	Nucleolar and spindle-associated protein 1	
42	SIRT5	NAD-dependent protein, sirtuin-5, mitochondrial	chromatin deacylase
43	CENTD3	Arf-GAP with Rho-GAP domain	PH domain-containing protein 3
44	GJA1	Gap junction alpha-1 protein	gap junction
45	ARSJ	Arylsulfatase J	
46	DNM1L	Dynamin-1-like protein	hydrolase
47	GABRA3	Gamma-aminobutyric acid receptor subunit alpha-3	GABA receptor
48	CASP8AP2	CASP8-associated protein 2	transcription cofactor
49	RYK	Tyrosine-protein kinase RYK	tyrosine kinase
50	IRX5	Iroquois-class homeodomain protein IRX-5	homeodomain transcription factor
51	ZNF750	Zinc finger protein 750	transcription factor
52	TBX1	T-box transcription factor TBX1	Rel homology transcription factor
53	ATP10D	Probable phospholipid-transporting ATPase VD	cation transporter
54	VNN3	Vascular non-inflammatory molecule 3	hydrolase
55	C12orf46	Endoplasmic reticulum resident protein 27	
56	AGBL3	Cytosolic carboxypeptidase 3	G protein, metalloprotease
57	MCAT	Mitochondrial carnitine	acylcarnitine carrier protein
58	LRRC37A	Leucine-rich repeat-containing protein 37A	extracellular matrix protein
59	MRPS27	28S ribosomal protein S27, mitochondrial	ribosomal protein
60	TAF13	Transcription initiation factor TFIID subunit 13	transcription cofactor
61	SSX2IP	Afadin- and alpha-actinin-binding protein	
62	USP44	Ubiquitin carboxyl-terminal hydrolase 44	cysteine protease
63	KCNK6	Potassium channel subfamily K member 6	channel protein
64	TAF15	TATA-binding protein-associated factor 2N	transcription cofactor
65	MYOCD	Myocardin	
66	MYB	Transcriptional activator Myb	transcription factor
67	MAML3	Mastermind-like protein 3	transcription factor
68	NP001017361	KHDC3-like protein	
69	DIP2A	Disco-interacting protein 2 homolog A	
70	NP001004318	Acid phosphatase type 7	phosphatase
71	KLF14	Transcription factor Sp6	transcription factor
72	EEF1B2	Elongation factor 1-beta	translation elongation factor
73	ACOT4	Acyl-coenzyme A thioesterase 4	thioesterase
74	STK3	Serine/threonine-protein kinase 24	kinase
75	ZNF256	Zinc finger protein 256	transcription factor
76	FAM78A	Protein FAM78A	
77	ACSBG1	Long-chain-fatty-acid-CoA ligase ACSBG1	ligase
78	CYP4A11	Cytochrome P450 4A11	oxygenase
79	MCF2L	Guanine nucleotide exchange factor DBS	signaling molecule
80	FCGR1A	High affinity immunoglobulin gamma Fc receptor I	cell adhesion molecule

Table 24. Functional annotation of upregulated genes by resveratrol (IC_{25}) on PC3 cells (part 3)

No	Gene ID	Gene Name	Biological function
81	DNAH2	Dynein heavy chain 2, axonemal	hydrolase
82	HSPA5	Endoplasmic reticulum chaperone BiP	chaperone
83	LCN2	Neutrophil gelatinase-associated lipocalin	isomerase
84	MARK1	Serine/threonine-protein kinase MARK1	serine/threonine protein kinase
85	PROM1	Prominin-1	membrane traffic protein
86	CALN1	Calcium-binding protein 8	binding protein
87	MAK10	N-alpha-acetyltransferase 35, NatC auxiliary subunit	acetyltransferase
88	MAP2K5	Dual specificity mitogen-activated protein kinase kinase 5	kinase
89	SCG3	Secretogranin-3	
90	DHX32	pre-mRNA-splicing factor ATP-dependent helicase	RNA helicase
91	PDE4DIP	Myomegalin	
92	ITPR3	Inositol 1,4,5-trisphosphate receptor type 3	ligand-gated ion channel
93	OR52K2	Olfactory receptor 52K2	
94	SUSD5	Sushi domain-containing protein 5	
95	CCDC75	G patch domain-containing protein 11	G protein
96	TFAP2C	Transcription factor AP-2 gamma	transcription factor
97	C20orf186	BPI fold-containing family B member 4	
98	REPS2	RalBP1-associated Eps domain-containing protein 2	G-protein modulator
99	PARD6G	Partitioning defective 6 homolog gamma	tight junction
100	NAT8B	Putative N-acetyltransferase 8B	acetyltransferase
101	EIF4H	Eukaryotic translation initiation factor 4H	translation initiation factor
102	PLXNB3	Plexin-B3	
103	ANAPC2	Anaphase-promoting complex subunit 2	
104	UBE1L	Ubiquitin-like modifier-activating enzyme 7	ligase
105	SEMA3F	Semaphorin-3F	membrane-bound signaling molecule
106	THAP6	THAP domain-containing protein 6	
107	RASSF2	Ras association domain-containing protein 2	G-protein modulator
108	DEF6	Differentially expressed in FDCP 6 homolog	nucleic acid binding
109	DMRTC1	Doublesex- and mab-3-related transcription factor C1	
110	TMEM143	Transmembrane protein 143	transmembrane protein
111	GTF2H1	General transcription factor IIH subunit 1	transcription factor
112	RBM41	RNA-binding protein 41	Rna binding protein
113	DPT	Dermatopontin	extracellular matrix protein
114	HMGB3	High mobility group protein B3	HMG box transcription factor
115	ZNF8	Zinc finger protein 8	transcription factor
116	AIFM1	Apoptosis-inducing factor 1, mitochondrial	dehydrogenase
117	ALG1	Alpha-1,3/1,6-mannosyltransferase ALG2	transferase
118	NP115991	Gap junction alpha-10 protein	gap junction
119	DEFB112	Beta-defensin 112	
120	ZNF782	Zinc finger protein 782	KRAB box transcription factor

Table 24. Functional annotation of upregulated genes by resveratrol (IC_{25}) on PC3 cells (part 4)

No	Gene ID	Gene Name	Biological function
121	JMJD2B	Lysine-specific demethylase 4B	zinc finger transcription factor
122	UBE2J1	Ubiquitin-conjugating enzyme E2 J1	
123	MCAT	Malonyl-CoA-acyl carrier protein	transacylase, mitochondrial
124	KLF14	Krueppel-like factor 14	transcription factor
125	PCMT1	Protein-L-isoaspartate(D-aspartate) O-methyltransferase	methyltransferase
126	VPS4B	Vacuolar protein sorting-associated protein 4B	non-motor microtubule binding protein
127	C17orf78	Uncharacterized protein C17orf78	
128	SRGAP2	SLIT-ROBO Rho GTPase-activating protein 2	G-protein modulator
129	C9orf72	Guanine nucleotide exchange C9orf72	
130	CD74	HLA class II histocompatibility antigen gamma chain	protease inhibitor
131	FAM18B	Golgi apparatus membrane protein TVP23 homolog B	
132	KIAA1602	Nck-associated protein 5-like	
133	FBXW11	F-box/WD repeat-containing protein 11	
134	POU4F2	POU domain, class 4, transcription factor 2	transcription factor
135	SPTBN5	Spectrin beta chain, non-erythrocytic 5	
136	GRM1	Metabotropic glutamate receptor 1	G-protein coupled receptor
137	ISCU	Iron-sulfur cluster assembly enzyme ISCU, mitochondrial	
138	GUCA1B	Guanylyl cyclase-activating protein 2	
139	C18orf17	Tetratricopeptide repeat protein 39C	
140	PHF11	PHD finger protein 11	DNA binding protein
141	SUSD2	Sushi domain-containing protein 2	
142	NFAM1	NFAT activation molecule 1	
143	C4orf18	Protein FAM198B	
144	CRTAC1	Cartilage acidic protein 1	
145	GABPB2	GA-binding protein subunit beta-2	
146	TAF15	Transcription initiation factor TFIID subunit 12	transcription factor
147	SDC2	Syndecan-2	cell adhesion molecule
148	C1orf35	SDC2	extracellular matrix glycoprotein
149	MMTAG2	Multiple myeloma tumor-associated protein 2	
150	LHX8	LIM/homeobox protein Lhx8	RNA binding protein
151	CCL17	C-C motif chemokine 17	chemokine
152	MYO7B	Unconventional myosin-VIIb	cell junction protein
153	HOXA3	Homeobox protein Hox-A3	transcription factor
154	TSSK2	Testis-specific serine/threonine-protein kinase 2	serine/threonine protein kinase
155	EFS	Embryonal Fyn-associated substrate	
156	YBX1	Nuclease-sensitive element-binding protein 1	
157	SLC9A10	Sodium/hydrogen exchanger 10	
158	DFFA	DNA fragmentation factor subunit alpha	
159	TJP2	Tight junction protein ZO-2	tight junction
160	PIK3AP1	Phosphoinositide 3-kinase adapter protein 1	

Table 24. Functional annotation of upregulated genes by resveratrol (IC_{25}) on PC3 cells (part 5)

No	Gene ID	Gene Name	Biological function
161	ADRBK2	Beta-adrenergic receptor kinase 2	serine/threonine protein kinase
162	KCNN2	Calcium-activated potassium channel protein 2	voltage-gated potassium channel
163	MAFA	Killer cell lectin-like receptor subfamily G member 1	
164	VPS33A	Vacuolar protein sorting-associated protein 33A	membrane trafficking regulatory protein
165	ZBTB32	Zinc finger and BTB domain-containing protein 32	
166	CCDC107	Coiled-coil domain-containing protein 107	
167	NOB1	RNA-binding protein NOB1	RNA-binding protein
168	SERPIND1	Heparin cofactor 2	serine protease inhibitor
169	NDST2	Bifunctional heparan sulfate N-deacetylase/N-sulfotransferase 2	deacetylase
170	NELFB_	Negative elongation factor B	
171	ELL3	RNA polymerase II elongation factor ELL3	transcription factor
172	SLC17A3	Sodium-dependent phosphate transport protein 4	cation transporter
173	IGFBP6	Insulin-like growth factor-binding protein 6	protease inhibitor
174	XRRA1	X-ray radiation resistance-associated protein 1	
175	NFATC4	Nuclear factor of activated T-cells, cytoplasmic 4	Rel homology transcription factor
176	C14orf179	Intraflagellar transport protein 43 homolog	
177	PDE8B	cAMP-specific 3',5'-cyclic phosphodiesterase 8B	phosphodiesterase
178	SRFBP1	Serum response factor-binding protein 1	
179	MRPL27	39S ribosomal protein L27, mitochondrial	ribosomal protein
180	NUP93	Nuclear pore complex protein Nup93	transporter
181	PSME4	Proteasome activator complex subunit 4	
182	VANGL1	Vang-like protein 1	
183	FAM114A1	Protein NOXP20	
184	PLCB4	1-PI, 4,5-bisphosphate phosphodiesterase beta-4	signaling molecule
185	DEF6	Defensin-6	
186	GABPA	GA-binding protein alpha chain	nucleic acid binding
187	OR5H1	Olfactory receptor 5H1	
188	SMAD7	Mothers against decapentaplegic homolog 7	transcription factor
189	DUSP11	RNA/RNP complex-1-interacting phosphatase	nucleotidyltransferase
190	TRIM7	E3 ubiquitin-protein ligase TRIM7	
191	LCT	Lactase-phlorizin hydrolase	glycosidase
192	NDN	Necdin	cell adhesion molecule
193	C20orf94	Protein SLX4IP	
194	MAP3K1	Mitogen-activated protein kinase kinase kinase 1	kinase
195	KIF23	Kinesin-like protein KIF23	microtubule binding motor protein
196	PHKA2	Phosphorylase b kinase regulatory subunit alpha, liver isoform	kinase activator
197	PHYHIPL	Phytanoyl-CoA hydroxylase-interacting protein-like	
198	TMPRSS3	Transmembrane protease serine 4	serine protease
199	RECQL	ATP-dependent DNA helicase Q1	DNA helicase
200	SLC6A1	Sodium- and chloride-dependent GABA transporter 1	cation transporter

Table 24. Functional annotation of upregulated genes by resveratrol (IC_{25}) on PC3 cells (part 6)

No	Gene ID	Gene Name	Biological function
201	ARRDC2	Arrestin domain-containing protein 2	
202	ACTR3B	Actin-related protein 3B	actin and actin related protein
203	KIAA0562	Centrosomal protein of 104 kDa	
204	MANBA	Beta-mannosidase	galactosidase
205	UBE2U	Ubiquitin-conjugating enzyme E2 U	
206	TLL2	Tolloid-like protein 2	
207	ZNF507	Zinc finger protein 507	KRAB box transcription factor
208	LCN8	Epididymal-specific lipocalin-8	isomerase
209	GPAM	Glycerol-3-phosphate acyltransferase 1, mitochondrial	acyltransferase
210	CCDC113	Coiled-coil domain-containing protein 113	
211	ARMCX3	Armadillo repeat-containing X-linked protein 3	
212	SELK_HUMAN	Selenoprotein K	
213	ANGPTL4	Angiopoietin-related protein 4	signaling molecule
214	ZSCAN5	Zinc finger and SCAN domain-containing protein 5A	transcription factor
215	ZNF740	Zinc finger protein 740	transcription factor
216	SAMSN1	SAM domain-containing protein SAMSN-1	
217	TMPRSS3	Transmembrane protease serine 3	serine protease
218	ASPH	Aspartyl/asparaginyl beta-hydroxylase	hydroxylase
219	RGPD3	RanBP2-like and GRIP domain-containing protein 3	G-protein modulator
220	PPP1R16B	Protein phosphatase 1 regulatory inhibitor subunit 16B	phosphatase modulator
221	NPAS4	Neuronal PAS domain-containing protein 4	basic helix-loop-helix transcription factor
222	FAM11B	Transmembrane protein 185B	transmembrane protein
223	UBQLNL	Ubiquilin-like protein	
224	KLK7	Kallikrein-7	serine protease
225	GLYATL2	GLYATL2	
226	TCFL5	Transcription factor-like 5 protein	
227	ATP6V1C2	V-type proton ATPase subunit C 2	ATP synthase
228	PRAMEF10	PRAME family member 10	
229	IL7R	Interleukin-7 receptor subunit alpha	type I cytokine receptor
230	ZNF662	Zinc finger protein 662	transcription factor
231	NMBR	Neuromedin-B receptor	
232	ZNF544	Zinc finger protein 544	transcription factor
233	ANKRD10	Ankyrin repeat domain-containing protein 10	
234	GPBP1L1	Vasculin-like protein 1	
235	PKDREJ	Polycystic kidney disease and receptor related protein	G-protein modulator
236	SRGAP2	SLIT-ROBO Rho GTPase-activating protein 3	G-protein modulator
237	USF1	Upstream stimulatory factor 1	
238	ADAM8	Disintegrin domain-containing protein 8	metalloprotease
239	MRPL27	39S ribosomal protein L41, mitochondrial	ribosomal protein
240	C9orf58	Allograft inflammatory factor 1-like	annexin

Table 24. Functional annotation of upregulated genes by resveratrol (IC_{25}) on PC3 cells (part 7)

No	Gene ID	Gene Name	Biological function
241	ARRB1	Beta-arrestin-1	enzyme modulator
242	CCDC57	CCDC57	
243	FPR1	fMet-Leu-Phe receptor	G-protein coupled receptor
244	STK3	Serine/threonine-protein kinase 3	kinase
245	SERPINF1	Pigment epithelium-derived factor	serine protease inhibitor
246	LCORL	Ligand-dependent nuclear receptor corepressor	DNA-directed RNA polymerase
247	CRAMP1L	Protein cramped-like	
248	DCP2	m7GpppN-mRNA hydrolase	
249	ADAM29	Disintegrin domain-containing protein 29	metalloprotease
250	ABHD4	Protein ABHD4	
251	BCAS3	Breast carcinoma-amplified sequence 3	
252	PSMD2	26S proteasome non-ATPase regulatory subunit 2	enzyme modulator
253	SPIRE2	Protein spire homolog 2	actin family cytoskeletal protein
254	TTC21B	Tetratricopeptide repeat protein 21B	
255	KRTAP22-1	Keratin-associated protein 22-1	
256	KCNK18	Potassium channel subfamily K member 18	
257	CENPP	Centromere protein P	
258	RPRM	Protein reprimo	
259	PKNOX1	Homeobox protein PKNOX1	transcription factor
260	CC2D1A	Coiled-coil and C2 domain-containing protein 1A	
261	P2RXL1	P2RXL1	
262	C21orf2	Protein C21orf2	
263	PCDHA13	Protocadherin alpha-13	
264	FAM20C	FAM20C	
265	PURG	Purine-rich element-binding protein gamma	transcription factor
266	SPG21	Maspardin	
267	SETD3	Histone-lysine N-methyltransferase setd3	epigenetic modifier
268	TNKS	Tankyrase-1	
269	PGLYRP1	Peptidoglycan recognition protein 1	
270	SNAG1	Sorting nexin-18	
271	USP7	Ubiquitin carboxyl-terminal hydrolase 7	cysteine protease
272	NP060223	Phospholipid phosphatase-related protein type 1	phoshatase
273	BLK	Tyrosine-protein kinase Blk	kinase
274	ANGPT4	Angiopoietin-4	signaling molecule
275	CLPX	ATP-dependent Clp protease	subunit clpX-like, mitochondrial
276	MSX2	Homeobox protein MSX-2	transcription factor
277	MYOM3	Myomesin-3	
278	LHX1	LIM/homeobox protein Lhx1	RNA binding protein
279	C10orf25	Uncharacterized protein C10orf25	
280	NP612412	Myosin regulatory light chain 10	actin family cytoskeletal protein

Table 25. Functional annotation of downregulated genes by resveratrol (IC_{25}) on PC3 cells (part 1)

No	Gene ID	Gene Name	Biological function
1	RANBP2	E3 SUMO-protein ligase RanBP2	
2	C10orf49	Unique cartilage matrix-associated protein	matrix-associated protein
3	OR2AJ1	Olfactory receptor 2AJ1	receptor
4	CYB561D2	Cytochrome b561 domain-containing protein 2	cytochrome
5	RPL18	60S ribosomal protein L18	ribosomal protein
6	CBL	E3 ubiquitin-protein ligase CBL	ligase
7	PARP8	Poly [ADP-ribose] polymerase 8	-
8	FBXO3	F-box only protein 3	-
9	PIK3R2	Phosphatidylinositol 3-kinase regulatory subunit beta	kinase modulator
10	CCNF	Cyclin-F	kinase activator
11	MDM4	Protein Mdm4	chromatin/chromatin-binding protein
12	SFT2D1	Vesicle transport protein SFT2A	-
13	SLC7A14	Probable cationic amino acid transporter	amino acid transporter
14	ARSK	Arylsulfatase K	sulfatase
15	TMCC1	Transmembrane and coiled-coil domains protein 1	-
16	ADAMTSL4	ADAMTS-like protein 4	matrix-associated protein
17	DOT1L	Histone-lysine N-methyltransferase, H3 lysine-79 specific	methyltransferase
18	GALNT3	Polypeptide N-acetylgalactosaminyltransferase 3	glycosyltransferase
19	SMPX	Small muscular protein	-
20	RAB3D	Ras-related protein Rab-3D	-
21	USP19	Ubiquitin carboxyl-terminal hydrolase 19	cysteine protease
22	WDR53	WD repeat-containing protein 53	-
23	NNT	NAD(P) transhydrogenase, mitochondrial	dehydrogenase
24	MPP7	MAGUK p55 subfamily member 7	cell junction protein
25	FCHO2	F-BAR domain only protein 2	-
26	CALD1	Caldesmon	-
27	MS4A3	Membrane-spanning 4-domains subfamily A member 3	receptor
28	WDR7	WD repeat-containing protein 7	-
29	VN1R5	Vomeronasal type-1 receptor 5	-
30	SLC6A6	Sodium- and chloride-dependent taurine transporter	cation transporter
31	ZNRF2	E3 ubiquitin-protein ligase ZNRF2	-
32	RBPSUH	Recombining binding protein suppressor of hairless	nucleic acid binding
33	MT1G	Metallothionein-1G	-
34	BLOC1S2	Biogenesis of lysosome complex 1 subunit 2	-
35	KRTAP9-3	Keratin-associated protein 9-3	-
36	IL10	Interleukin-10	immune system
37	MED12L	Mediator of RNA polymerase II transcription subunit	nucleic acid binding
38	SRPK1	SRSF protein kinase 1	non-receptor serine/threonine protein kinase
39	RMND1	Required for meiotic nuclear division protein 1 homolog	cell cycle
40	PDIA6	Protein disulfide-isomerase A6	-

Table 25. Functional annotation of downregulated genes by resveratrol (IC_{25}) on PC3 cells (part 2)

No	Gene ID	Gene Name	Biological function
41	GABRR2	Gamma-aminobutyric acid receptor subunit rho-2	GABA receptor
42	MAS1	Proto-oncogene Mas	-
43	LRRIQ2	Centrosomal protein of 97 kDa	-
44	ACTN2	Alpha-actinin-2	-
45	NGFRAP1	Protein BEX3	-
46	ATG9A	Autophagy-related protein 9A	autophagy
47	STX19	Syntaxin-19	snare protein
48	DDI2	Protein DDI1 homolog 2	aspartic protease
49	PABPC5	Polyadenylate-binding protein 5	-
50	GAS2L1	GAS2-like protein 1	-
51	TRAF1	TNF receptor-associated factor 1	signaling molecule
52	RTCD1	RNA 3'-terminal phosphate cyclase	RNA binding protein
53	SVOP	Synaptic vesicle 2-related protein	-
54	GPX6	Glutathione peroxidase 6	peroxidase
55	BMPR2	Bone morphogenetic protein receptor type-2	TGF-beta receptor
56	CAMK1	Calcium/calmodulin-dependent protein kinase type 1	serine/threonine protein kinase
57	OR10G4	Olfactory receptor 10G4	receptor
58	SEC11B	Putative signal peptidase complex catalytic subunit	serine protease
59	MUT	Methylmalonyl-CoA mutase, mitochondrial	mutase
60	ZDHHC9	Palmitoyltransferase ZDHHC9	-
61	ZC3H7A	Zinc finger CCCH domain-containing protein 7A	nucleic acid binding
62	C13orf33	Mesenteric estrogen-dependent adipogenesis protein	-
63	SIRPB1	Signal-regulatory protein beta-1	chemokine
64	PNRC1	Proline-rich nuclear receptor coactivator 1	-
65	OBP2A	Odorant-binding protein 2a	isomerase
66	METT5D1	Probable methyltransferase-like protein 15	methyltransferase
67	TRIM64	Tripartite motif-containing protein 64	-
68	RBM34	RNA-binding protein 34	-
69	ATP10B	Probable phospholipid-transporting ATPase VB	cation transporter
70	SLC30A3	Zinc transporter 3	transporter
71	ARCN1	Coatomer subunit delta	vesicle coat protein
72	HTR4	5-hydroxytryptamine receptor 4	G-protein coupled receptor
73	SLC25A1	Tricarboxylate transport protein, mitochondrial	-
74	PTPLA	Very-long-chain (3R)-3-hydroxyacyl-CoA dehydratase 1	-
75	SPAST	Spastin	non-motor microtubule binding protein
76	SARDH	Sarcosine dehydrogenase, mitochondrial	dehydrogenase
77	NXF2	Nuclear RNA export factor 2	RNA binding protein
78	GNPDA1	Glucosamine-6-phosphate isomerase 1	hydrolase
79	C4orf26	Odontogenesis associated phosphoprotein	-
80	KCNK2	Potassium channel subfamily K member 2	-

Table 25. Functional annotation of downregulated genes by resveratrol (IC_{25}) on PC3 cells (part 3)

No	Gene ID	Gene Name	Biological function
81	PTGER3	Prostaglandin E2 receptor EP3 subtype	G-protein coupled receptor
82	ODF2L	Outer dense fiber protein 2-like	-
83	SETD1B	Histone-lysine N-methyltransferase SETD1B	chromatin/chromatin-binding protein
84	SERPINB9	Serpin B9	serine protease inhibitor
85	RAB36	Ras-related protein Rab-36	-
86	CD2BP2	CD2 antigen cytoplasmic tail-binding protein 2	chromatin/chromatin-binding protein
87	CKM	Creatine kinase M-type	amino acid kinase
88	MPP7	Chromatin assembly factor 1 subunit B	chromatin/chromatin-binding protein
89	TBC1D20	TBC1 domain family member 20	-
90	OPA3	Optic atrophy 3 protein	-
91	PNMA5	Paraneoplastic antigen-like protein 5	-
92	NT5DC3	5'-nucleotidase domain-containing protein 3	nucleotide phosphatase
93	SIAH1	E3 ubiquitin-protein ligase SIAH1	-
94	TMEM68	Transmembrane protein 68	-
95	ATP6V0D2	V-type proton ATPase subunit d 2	ATP synthase
96	ZDHHC20	Palmitoyltransferase ZDHHC20	transferase
97	KIAA0310	Protein transport protein Sec16A	transporter
98	NANOG	Homeobox protein NANOG	homeodomain transcription factor
99	FAAH2	Fatty-acid amide hydrolase 2	hydrolase
100	SLC19A3	Thiamine transporter 2	transporter
101	CHMP5	Charged multivesicular body protein 5	transfer/carrier protein
102	USP14	Ubiquitin carboxyl-terminal hydrolase 14	cysteine protease
103	ACE	Angiotensin-converting enzyme	metalloprotease
104	DCLRE1A	DNA cross-link repair 1A protein	-
105	HERC4	Probable E3 ubiquitin-protein ligase HERC4	-
106	FAM114A1	Protein NOXP20	-
107	DUS2L	tRNA-dihydrouridine(20) synthase [NAD(P)+]-like	-
108	SSX6	Putative protein SSX6	nucleic acid binding
109	ZNF667	Zinc finger protein 667	transcription factor
110	LYPD4	Ly6/PLAUR domain-containing protein 4	-
111	THRAP3	Thyroid hormone receptor-associated protein 3	transcription factor
112	OR4C46	Olfactory receptor 4C46	receptor
113	LBH	Protein LBH	-
114	C1orf122	Uncharacterized protein C1orf122	-
115	TAAR1	Trace amine-associated receptor 1	-
116	GPX6	Glutathione peroxidase 7	peroxidase
117	MFSD3	Major facilitator superfamily protein 3	transporter
118	TRPV1	Transient receptor potential cation channel	ion channel
119	OR2AG1	Olfactory receptor 2AG1	receptor
120	FBXL18	F-box/LRR-repeat protein 18	-

Table 25. Functional annotation of downregulated genes by resveratrol (IC_{25}) on PC3 cells (part 4)

No	Gene ID	Gene Name	Biological function
121	OR5M9	Olfactory receptor 5M9	receptor
122	GLP1R	Glucagon-like peptide 1 receptor	receptor
123	OR7G2	Olfactory receptor 7G2	receptor
124	UBE1	Ubiquitin-like modifier-activating enzyme 1	ligase
125	ITGB3BP	Centromere protein R	-
126	PTHR2	Parathyroid hormone 2 receptor	-
127	SLC27A1	Long-chain fatty acid transport protein 1	ligase
128	EDG5	Sphingosine 1-phosphate receptor 2	G-protein coupled receptor
129	NP_001073961	Inactive serine protease 54	annexin
130	INSR	Insulin receptor	receptor
131	FXYD2	Sodium/potassium-transporting ATPase subunit gamma	cation transporter
132	CRABP2	Cellular retinoic acid-binding protein 2	-
133	RASL11B	Ras-like protein family member 11B	-
134	IPO11	Importin-11	small GTPase
135	ST13	Hsc70-interacting protein	-
136	JPH1	Junctophilin-1	-
137	POR	NADPH-cytochrome P450 reductase	cytochrome
138	CLRN1	Clarin-1	-
139	STOML1	Stomatin-like protein 1	cytoskeletal protein
140	S100PBP	S100P-binding protein	-
141	RHBDD1	Rhomboid-related protein 4	serine protease
142	C20orf24	Uncharacterized protein C20orf24	-
143	UBOX5	RING finger protein 37	-
144	PCM1	Pericentriolar material 1 protein	-
145	ZNF136	Zinc finger protein 136	transcription factor
146	CRHR1	Corticotropin-releasing factor receptor 1	-
147	CCDC129	Coiled-coil domain-containing protein 129	-
148	PKIA	cAMP-dependent protein kinase inhibitor alpha	kinase inhibitor
149	ZNF440	Zinc finger protein 440	KRAB box transcription factor
150	TMPO	Lamina-associated polypeptide 2, isoform alpha	peptide hormone
151	ACOT11	Acyl-coenzyme A thioesterase 11	esterase
152	RFPL1	Ret finger protein-like 1	-
153	AGPAT7	Lysophospholipid acyltransferase LPCAT4	acyltransferase
154	CLDN14	Claudin-14	tight junction
155	IL1R1	Interleukin-1 receptor type 1	type I cytokine receptor
156	PLCG1	1-phosphatidylinositol 4,5-bisphosphate phosphodiesterase gamma-1	calcium-binding protein
157	SGOL2	Shugoshin 2	-
158	OR2G3	Olfactory receptor 2G3	receptor
159	CASC2	Protein CASC2, isoform 3	-
160	MT-CO1	Cytochrome c oxidase subunit 1	oxidase

CERTIFICATE OF MANUSCRIPT ACCEPTANCE

International Journal of
Molecular Sciences

Indexed in: PubMed | CITESCORE 4.32 SCOPUS | IMPACT FACTOR 4.183

an Open Access Journal by MDPI

CERTIFICATE OF ACCEPTANCE

Certificate of acceptance for the manuscript (**ijms-704246**) titled:

Metabolic profile and evaluation of the antibacterial and cytotoxic activities of extracts from the stems of Cissus trifoliata

Authored by:

Luis Fernando Méndez-López; Elvira Garza-González; María Yolanda Rios; M. Angeles Ramírez-Cisneros; Laura Alvarez; Leticia González-Maya; Jessica N. Sánchez-Carranza; María del Rayo Camacho-Corona

has been accepted in *Int. J. Mol. Sci.* (ISSN 1422-0067) on 29 January 2020

MDPI Academic Open Access Publishing since 1996

Basel, January 2020

PARTICIPATION IN CONGRESS

Amipronat
Asociación Mexicana de Investigación en Productos Naturales

15ª Reunión Internacional de Investigación en Productos Naturales
Dr. Juan Rogelio Aguirre Rivera

UASLP
Universidad Autónoma de San Luis Potosí

La Asociación Mexicana de Investigación en Productos Naturales, A. C. y la Universidad Autónoma de San Luis Potosí

Otorgan la presente

Constancia

a:

Luis Fernando Mendez Lopez, Elvira Garza González, Yolanda Ríos Gómez, Leticia González Maya, Jessica Sánchez Carranza, María del Rayo Camacho Corona

Por su valiosa participación en la modalidad de cartel con el tema:

Análisis del perfil metabólico de las ramas de *Cissus trifoliata* y determinación de su actividad antibacteriana y citotóxica

Durante la 15ª Reunión Internacional de Investigación en Productos Naturales, 22 al 25 de mayo de 2019 en San Luis Potosí, SLP., México

Dra. Bertha Irene Juárez Flores	Dra. Denisse Atenea de Loera Carrera	Dr. Sergio Rubén Peraza Sánchez
Presidenta del Comité Organizador	Vicepresidenta del Comité Organizador	Presidente de la AMIPRONAT

AUTOBIOGRAPHIC RESUME

Luis Fernando Mendez Lopez

Candidate for the degree of

Doctor in Pharmaceutical Sciences

Thesis: Metabolomic and Bioassay-guided Phytochemical analysis of the Stems of *Cissus trifoliata*, evaluation of their Antibacterial and Cytotoxic activity, and determination of the Mechanism of Action of one active compound.

Area of study: Biomedical Sciences.

Biography: Born in Monterrey, Nuevo Leon, Mexico the 16 of July of 1982, son of Luis Fernando Mendez Borges and Maria Bernardina Lopez Palomo.

Education: Graduated from the School of Biology Sciences of the UANL in 2005 as a Chemist. In 2012 he obtained a Master of Science in Nutrition (Honors) from the School of Public Health and Nutrition, UANL.

Professional Experience: Former Associated Researcher in the Center of Complexity Sciences C3, UNAM, Mexico. Current full-time Associated Professor at the School of Public Health and Nutrition, UANL.